

NASA TECHNICAL NOTE



NASA TN D-7118

NASA TN D-7118

CASE FILE
COPY

EMISSION OF SOUND FROM TURBULENCE
CONVECTED BY A PARALLEL FLOW
IN THE PRESENCE OF SOLID BOUNDARIES

by Marvin E. Goldstein and Burt M. Rosenbaum

Lewis Research Center

Cleveland, Ohio 44135

NATIONAL AERONAUTICS AND SPACE ADMINISTRATION • WASHINGTON, D. C. • FEBRUARY 1973

1. Report No. NASA TN D-7118	2. Government Accession No.	3. Recipient's Catalog No.	
4. Title and Subtitle EMISSION OF SOUND FROM TURBULENCE CONVECTED BY A PARALLEL FLOW IN THE PRESENCE OF SOLID BOUNDARIES		5. Report Date February 1973	
		6. Performing Organization Code	
7. Author(s) Marvin E. Goldstein and Burt M. Rosenbaum		8. Performing Organization Report No. E-6932	
		10. Work Unit No. 501-04	
9. Performing Organization Name and Address Lewis Research Center National Aeronautics and Space Administration Cleveland, Ohio 44135		11. Contract or Grant No.	
		13. Type of Report and Period Covered Technical Note	
12. Sponsoring Agency Name and Address National Aeronautics and Space Administration Washington, D.C. 20546		14. Sponsoring Agency Code	
15. Supplementary Notes			
16. Abstract A theoretical description is given of the sound emitted from an arbitrary point in a parallel or nearly parallel turbulent shear flow confined to a region near solid boundaries. The analysis begins with Lighthill's formulation of aerodynamic noise and assumes that the turbulence is axisymmetric. Specific results are obtained for the sound emitted from an arbitrary point in a turbulent flow within a semi-infinite, open-ended duct.			
17. Key Words (Suggested by Author(s)) Aerodynamic sound Turbulence Augmentor wing		18. Distribution Statement Unclassified - unlimited	
19. Security Classif. (of this report) Unclassified	20. Security Classif. (of this page) Unclassified	21. No. of Pages 91	22. Price* \$3.00

* For sale by the National Technical Information Service, Springfield, Virginia 22151

CONTENTS

	Page
SUMMARY	1
INTRODUCTION	1
FORMULATION	3
TURBULENCE CORRELATION FUNCTIONS	9
EXPANSION FOR LOW EDDY MACH NUMBER - CONVECTIVE AMPLIFICATION	11
LOCALLY HOMOGENEOUS TURBULENCE - VANISHING OF COUPLING TERM	15
REPRESENTATION OF FOURTH-ORDER CORRELATIONS IN TERMS OF SECOND-ORDER CORRELATIONS	16
AXISYMMETRIC TURBULENCE - QUADRUPOLE CORRELATIONS	17
ISOTROPIC TURBULENCE	21
CALCULATION OF FAR-FIELD GREEN'S FUNCTION	22
General Case	22
Two-Dimensional Geometries	25
SUMMARY OF GENERAL EQUATIONS	26
Axisymmetric Turbulence	26
Isotropic Turbulence	27
A PARTICULAR EXAMPLE	29
DISCUSSION	38
Emission of Sound From Monopole Source of Unit Strength	38
Emission of Sound From a Unit Volume of Turbulence Located at a Point Within the Duct and Proposed Experiment	40
Discussion of equations	40
Organization of plots and choice of parameters	41
Discussion of results	43
SUMMARY OF RESULTS	45

APPENDIXES

A - REDUCTION OF SELF-NOISE CORRELATION INTEGRALS	
FOR AXISYMMETRIC TURBULENCE	46
B - REDUCTION OF SHEAR-NOISE CORRELATION INTEGRALS	
FOR AXISYMMETRIC TURBULENCE	50
C - REDUCTION OF SELF-NOISE CORRELATION INTEGRALS	
FOR ISOTROPIC TURBULENCE	52
D - REDUCTION OF SHEAR-NOISE CORRELATION INTEGRALS	
FOR ISOTROPIC TURBULENCE	55
E - SYMBOLS	57
REFERENCES	62

EMISSION OF SOUND FROM TURBULENCE CONVECTED BY A PARALLEL FLOW IN THE PRESENCE OF SOLID BOUNDARIES

by Marvin E. Goldstein and Burt M. Rosenbaum

Lewis Research Center

SUMMARY

A theoretical description is given of the sound emitted from an arbitrary point in a parallel or nearly parallel turbulent shear flow confined to a region near solid boundaries. The analysis begins with Lighthill's formulation of aerodynamic noise and assumes that the turbulence is axisymmetric. It leads to equations which predict the directivity patterns of the spectral density of the intensity of the sound emitted from a unit volume of turbulence located at an arbitrary point within the flow in terms of certain correlation-length scales of the turbulence. In order to apply these equations to predict the sound field emitted from a complete flow, it would be necessary to integrate the results over the flow field. Specific results are obtained for the sound emitted from an arbitrary point in a turbulent flow within a semi-infinite open-ended duct. An experiment which could be used to verify these results is proposed.

INTRODUCTION

Since STOL transport aircraft are intended to operate in densely populated areas, it is necessary to give considerable emphasis to the problem of noise reduction in the development of these aircraft. Most STOL aircraft depend for their performance on lift augmentation devices which involve high-velocity turbulent flows along solid surfaces. It has been found (ref. 1) that the presence of such surfaces can result in a considerable increase in noise production.

In this report we shall attempt to obtain some insight into the effect of solid boundaries on the process of aerodynamic sound generation and at the same time make some progress toward developing techniques for predicting such effects analytically. To this end we shall develop theoretical formulas for predicting the sound emitted from a unit volume of turbulence located at an arbitrary point in a nearly parallel turbulent shear

flow confined to a region near one or more solid boundaries. Typical configurations to which the analysis applies are shown in figures 1(a) and (b). It should be emphasized that the analysis, by itself, only relates the sound field generated by the turbulence at an arbitrary point in the flow to the turbulence correlation length at that point. In order to use this analysis for actually predicting the sound field from a given flow, it is necessary to integrate the formulas over the entire region of turbulence generating this sound. Since the turbulence correlation length appears under the integral sign in this integration, it is necessary to know this correlation length at every point of the flow in order to predict the sound field. However, determining the distribution of this correlation length is in itself a difficult problem, and it will usually be necessary to rely heavily upon experiment for this purpose. Nevertheless, the formulas obtained can be used (even when the distribution of the correlation length is unknown) for studying the effect of the solid boundaries on the sound field from the turbulence located at any individual point within the flow.

The analysis begins with Lighthill's model for the sound emission from turbulent shear flows (ref. 2). The turbulence is assumed to be locally homogeneous and axisymmetric; that is, the statistical properties of the turbulence are independent of rotations about the direction of mean flow. However, they can be different in the direction of mean flow and the directions perpendicular to the mean flow. The analysis is carried through by introducing an appropriate Green's function for an arbitrary geometry and then using the symmetry properties of the turbulence to transform the result into a manageable form. It is then shown how the reciprocity principle can be used to simplify the problem of finding the Green's function for the case where the observer is in the far field. The final result of this analysis is a set of formulas for the spectral density of the far-field intensity of the sound emitted from a unit volume of turbulence located at an arbitrary point in the flow. These formulas can be interpreted as the sound field from a particular sum of statistically independent convected quadrupoles (with certain coupling terms) whose strengths are determined by the statistical properties of the turbulence.

A particular lift augmentation device which is being considered for use in STOL aircraft is the augmentor wing ejector flap shown in figure 2. This flap is fed (blown) through the duct in the wing, as shown in the figure. The high-speed jet issuing from the wing into the flap (at point 1 in fig. 2) is a potentially important source of noise within the flap. The effect of the flap boundaries on the sound emission from this noise source can be important.

Motivated by this problem, we applied the general analysis previously described to predict the noise emitted from a unit volume of turbulence located at an arbitrary point within an open-ended semi-infinite duct. The Green's function needed for the solution to this problem is obtained by transforming the boundary-value problem which deter-

mines this function into one whose solution is known. The turbulence properties which are used in this example are taken from observed results for the mixing region of jets. This is done in order to relate the analysis to the noise emitted from the turbulence in the high-speed jet from the duct in the wing into the flap. It must be emphasized, however, that in order to use this analysis to predict the noise from the jet mixing region in a complete augmentor wing, it is necessary to know the distribution of correlation-length scales within this region and to integrate the results over the entire region of turbulence. In addition, in any real augmentor wing there will be additional noise sources such as the mixing region between the flow leaving the flap and the exterior flow about the wing and the possible noise source due to the flow entering the flap from above the wing. However, the general analysis is also capable of dealing with many of these additional noise sources, provided enough details of the turbulent flow are known. Thus, the present analysis, by itself, certainly does not give a complete solution to the problem of predicting the noise from an augmentor wing jet flap. Nevertheless, it does provide a necessary first step toward this goal. In addition, numerical results are presented for the directivity patterns of the spectral density of the far-field intensity emitted from a unit volume of turbulence located at various points within the duct. These results show how the sound emission processes and the geometric effects of the duct interact. It also shows how the elementary sources of sound, that is, the individual turbulent eddies, contribute to the sound field. An experiment which should permit comparison with the computed results is discussed.

In order to help differentiate which aspects of the sound field are caused by the convected quadrupole nature of the turbulent sound sources and which aspects are geometric effects of the solid boundaries, results are also presented for the sound emission from a simple monopole source located within the duct.

FORMULATION

We shall consider the sound emission from a nearly parallel turbulent shear flow confined to a region near solid boundaries. Typical configurations are shown in figure 1. The mean velocity is taken to be in the y_1 -direction, and it will be assumed that it varies only in the y_2 -direction. We begin with Lighthill's equation (ref. 2) for aerodynamic noise generation

$$\nabla^2 \rho - \frac{1}{c_0^2} \frac{\partial^2 \rho}{\partial t^2} = - \frac{1}{c_0^2} \frac{\partial^2}{\partial y_i \partial y_j} (\rho v_i v_j + p_{ij} - c_0^2 \rho \delta_{ij}) \quad (1)$$

where

$$\nabla^2 \equiv \frac{\partial^2}{\partial y_i \partial y_i}$$

(All symbols are defined in appendix E.) Since aerodynamic noise generation is usually of interest only at very high Reynolds numbers, Lighthill (ref. 2) neglected viscous effects. Following Ffowcs Williams (ref. 3) we shall suppose that viscous effects can also be neglected even when solid boundaries are present. We can therefore set p_{ij} equal to $p\delta_{ij}$. We shall also neglect (ref. 2) the effects of heat conduction so that

$$p - p_0 = c_0^2(\rho - \rho_0)$$

Finally, we suppose that (ref. 2)

$$\rho v_i v_j \approx \rho_0 v_i v_j$$

This assumption amounts to neglecting the direct effects of convection and refraction of the emitted sound by the mean flow and of the scattering of the emitted sound by the turbulence.

When these approximations are introduced into equation (1) we obtain

$$\nabla^2 p - \frac{1}{c_0^2} \frac{\partial^2 p}{\partial t^2} = - \frac{\partial^2 \tau_{ij}}{\partial y_i \partial y_j} \quad (2)$$

where

$$\tau_{ij} \equiv \rho_0 v_i v_j \quad (3)$$

In order to ensure convergence of the integrals to be encountered, we shall suppose that $\tau_{ij} = 0$ for $t > T$, where T is some large time interval which will be put equal to infinity at the end of the analysis.

We shall suppose that the solid boundaries are rigid so that the normal velocity $v_n = v_i n_i$ (where n_i is the i^{th} component of the unit normal directed outward from the turbulent region at the solid boundaries) vanishes at the boundaries. With viscous effects neglected, the equation for the normal component of momentum at the solid boundaries becomes

$$\rho \frac{\partial \mathbf{v}_n}{\partial t} + \rho \mathbf{v}_j n_i \frac{\partial \mathbf{v}_i}{\partial y_j} + n_i \frac{\partial p}{\partial y_i} = 0$$

The first term is zero. The middle term can be shown to be equal to $(\mp \rho v^2/R)$, where R is the radius of curvature of the boundary surface in the direction of the motion and where the negative sign holds when the boundary surface is concave inward along this direction and the positive sign holds when it is convex inward. Thus, we get

$$\hat{n} \cdot \nabla p = \pm \frac{\rho v^2}{R}$$

We shall assume that the surfaces adjacent to the regions of turbulent shear flow are relatively flat; that is, $R \gg h$, where h is a characteristic length representative of the distances between boundary surfaces (see fig. 2). Then $\rho v^2/R \approx 0$ for surfaces adjacent to the flow. We shall also suppose that, at the surfaces outside the regions of turbulent shear flow, the acoustic approximation applies; that is, the terms involving the square of the velocity are negligible. Hence,

$$n_i \frac{\partial p}{\partial y_i} = \hat{n} \cdot \nabla p \approx 0 \quad (\text{on solid boundaries}) \quad (4)$$

that is, the normal derivative of the pressure essentially vanishes at the solid boundaries.

It is convenient to work in terms of the Fourier transforms (with respect to time) of the variables. Hence, we put

$$P = \frac{1}{\sqrt{2\pi}} \int_{-\infty}^{\infty} e^{i\omega t} (p - p_0) dt \quad (5)$$

$$T_{ij} = \frac{1}{\sqrt{2\pi}} \int_{-\infty}^{\infty} e^{i\omega t} \tau_{ij} dt \quad (6)$$

Then equation (2) becomes

$$\nabla^2 P + k^2 P = - \frac{\partial^2 T_{ij}}{\partial y_i \partial y_j} \quad (7)$$

where

$$k \equiv \frac{\omega}{c_0} \quad (8)$$

is the wave number. Then the boundary condition (4) becomes

$$\hat{n} \cdot \nabla P = 0 \quad (\text{on solid boundaries}) \quad (9)$$

The boundary condition at infinity is that P represents an outgoing wave.

The solution to this problem (eq. (7) with boundary condition (9)) can be written in terms of the Green's function G , whose normal derivative vanishes on the solid boundary. Thus,

$$P(\vec{x}) = \int_{\mathcal{V}} G(\vec{x} | \vec{y}) \frac{\partial^2 T_{ij}}{\partial y_i \partial y_j} d\vec{y} \quad (10)$$

where \mathcal{V} denotes the volume outside the solid boundaries

$$\left(\nabla_{\vec{x}}^2 + k^2 \right) G = -\delta(\vec{x} - \vec{y}) \quad (11a)$$

$$\hat{n} \cdot \nabla_{\vec{x}} G = 0 \quad (\text{on solid boundaries}) \quad (11b)$$

where $\nabla_{\vec{x}}^2 \equiv \partial^2 / \partial x_i \partial x_i$ and G represents an outgoing wave at infinity. Differentiating by parts shows that

$$\frac{\partial^2}{\partial y_i \partial y_j} (GT_{ij}) - \frac{\partial}{\partial y_i} \left(T_{ij} \frac{\partial}{\partial y_j} G \right) - \frac{\partial}{\partial y_j} \left(T_{ij} \frac{\partial}{\partial y_i} G \right) = G \frac{\partial^2 T_{ij}}{\partial y_i \partial y_j} - T_{ij} \frac{\partial^2 G}{\partial y_i \partial y_j}$$

Hence, the divergence theorem shows that equation (10) can be written as

$$P(\vec{x}) = \int_{\mathcal{V}} T_{ij} \frac{\partial^2 G}{\partial y_i \partial y_j} d\vec{y} + \int_{\mathcal{S}} n_i \left(\frac{\partial}{\partial y_j} GT_{ij} \right) d\mathcal{S} - \int_{\mathcal{S}} n_i T_{ij} \frac{\partial G}{\partial y_j} d\mathcal{S} - \int_{\mathcal{S}} n_j T_{ij} \frac{\partial G}{\partial y_i} d\mathcal{S} \quad (12)$$

where \mathcal{S} denotes the solid boundaries. But since

$$T_{ij} = \frac{1}{\sqrt{2\pi}} \int_{-\infty}^{\infty} e^{i\omega t} \rho_0 v_i v_j dt$$

the requirement that the normal velocity vanish at the solid boundaries shows that the last two surface integrals on the right side of equation (12) vanish. And since the curvature of the solid surfaces adjacent to the region of turbulence (i.e., where T_{ij} is nonnegligible) vanishes in the flow direction, the rate of change in the normal vector in the direction of flow $(v_j/|\vec{v}|)(\partial/\partial y_j)\vec{n}$ is perpendicular to the flow direction $v/|\vec{v}|$. Hence, it follows that

$$\frac{\vec{v}}{|\vec{v}|} \cdot \left(\frac{v_j}{|\vec{v}|} \frac{\partial}{\partial y_j} \vec{n} \right) = 0$$

so that

$$v_i v_j \frac{\partial}{\partial y_j} n_i = 0$$

and

$$v_j \frac{\partial}{\partial y_j} (v_i n_i) = n_i v_j \frac{\partial}{\partial y_j} v_i$$

Therefore,

$$\begin{aligned} n_i \frac{\partial}{\partial y_j} G T_{ij} &= \frac{1}{\sqrt{2\pi}} \int_{-\infty}^{\infty} e^{i\omega t} \rho_0 \left[n_i v_i \frac{\partial}{\partial y_j} (G v_j) + v_j G \frac{\partial}{\partial y_j} (n_i v_i) \right] dt \\ &= \frac{1}{\sqrt{2\pi}} \int_{-\infty}^{\infty} e^{i\omega t} \left[v_n \frac{\partial (v_j G)}{\partial y_j} + G v_j \frac{\partial}{\partial y_j} v_n \right] dt \end{aligned}$$

But since the second derivative is along the surface and v_n is identically zero on the surface, the remaining surface integral on the right side of equation (12) also vanishes. Hence, equation (12) becomes

$$P(\vec{x}) = \int T_{ij} \frac{\partial^2 G}{\partial y_i \partial y_j} d\vec{y} \quad (13)$$

Although the integral is formally over all space, it need only be carried out over the source region.

The spectral density of the intensity in the far field is

$$I_\omega(\vec{x}) = \frac{|P(\vec{x})|^2}{2T c_o \rho_o}$$

where T is some large period of time such that τ_{ij} can be considered to be zero outside the time interval $(-T, T)$, which is of duration $2T$. At the end of the analysis, the limit will be taken as $T \rightarrow \infty$.

$$I_\omega(\vec{x}) = \frac{1}{c_o \rho_o} \int \int \frac{T_{ij}(\vec{y}') T_{kl}^*(\vec{y}'')}{2T} \frac{\partial^2 G(\vec{x} | \vec{y}')}{\partial y_i' \partial y_j'} \frac{\partial^2 G^*(\vec{x} | \vec{y}'')}{\partial y_i'' \partial y_j''} d\vec{y}' d\vec{y}'' \quad (14)$$

Now upon using the fact that the Fourier transform of a convolution is proportional to the product of the Fourier transforms of its components and the fact that the Fourier transform of $f(-t)$ is the complex conjugate of the Fourier transform of $f(t)$, provided $f(t)$ is real, it follows from equation (6) that

$$\frac{T_{ij}(\vec{y}') T_{kl}^*(\vec{y}'')}{2T} = \frac{\rho_o^2}{2\pi} \int_{-\infty}^{\infty} e^{-i\omega\tau} \overline{v_i' v_j' v_k'' v_l''} d\tau \quad (15)$$

where

$$\overline{v_i' v_j' v_k'' v_l''} \equiv \frac{1}{2T} \int_{-T}^T v_i(\vec{y}', t) v_j(\vec{y}', t) v_k(\vec{y}'', t + \tau) v_l(\vec{y}'', t + \tau) dt \quad (16)$$

is the fourth-order two-point two-time velocity correlation tensor.

TURBULENCE CORRELATION FUNCTIONS

The following development closely parallels that given in reference 4. Since the mean velocity $U(y_2)$ is assumed to be in the y_1 -direction, the velocity v_i can be expressed in the form

$$v_i(\vec{y}, t) = \delta_{i1} U(y_2) + u_i(\vec{y}, t)$$

where u_i is the turbulent (fluctuating) component of the velocity.

Upon introducing this into equation (16) we find that

$$\overline{v_i' v_j' v_k' v_l'} = \rho_{ijkl}^{(0)}(\vec{y}', \vec{\eta}) + \frac{1}{2} \rho_{ijkl}^{(1)}(\vec{y}', \vec{\eta}, \tau) + \frac{1}{2} \rho_{ijkl}^{(2)}[\vec{y}', \vec{\eta}^{(1)}, \tau] \quad (17)$$

where we have put

$$\vec{\eta} \equiv \vec{y}'' - \vec{y}' \equiv -\vec{\eta}^{(1)} \quad (18)$$

$$\rho_{ijkl}^{(0)}(\vec{y}', \vec{\eta}) \equiv U'^2 \delta_{1i} \delta_{1j} \overline{u_k' u_l'} + U''^2 \delta_{1k} \delta_{1l} \overline{u_i' u_j'} + U'^2 U''^2 \delta_{1i} \delta_{1j} \delta_{1k} \delta_{1l} + \overline{u_i' u_j'} \overline{u_k' u_l'}$$

$$\begin{aligned} \rho_{ijkl}^{(1)}(\vec{y}', \vec{\eta}, \tau) \equiv & \overline{u_i' u_j' u_k' u_l'} - \overline{u_i' u_j'} \overline{u_k' u_l'} + 2U'(\delta_{1i} \overline{u_j' u_k' u_l'} + \delta_{1j} \overline{u_i' u_k' u_l'}) \\ & + U'U''(\delta_{1i} \delta_{1k} \overline{u_j' u_l'} + \delta_{1j} \delta_{1l} \overline{u_i' u_k'} + 2\delta_{1j} \delta_{1k} \overline{u_i' u_l'}) \end{aligned} \quad (19)$$

$$\begin{aligned} \rho_{ijkl}^{(2)}[\vec{y}', \vec{\eta}^{(1)}, \tau] \equiv & \overline{u_i' u_j' u_k' u_l'} - \overline{u_i' u_j'} \overline{u_k' u_l'} + 2U''(\delta_{1k} \overline{u_i' u_j' u_l'} + \delta_{1l} \overline{u_i' u_j' u_k'}) \\ & + U'U''(\delta_{1i} \delta_{1k} \overline{u_j' u_l'} + \delta_{1j} \delta_{1l} \overline{u_i' u_k'} + 2\delta_{1i} \delta_{1l} \overline{u_j' u_k'}) \end{aligned} \quad (20)$$

The double primes indicate that the quantities are to be evaluated at $\vec{y}'' = \vec{y}' + \vec{\eta}$ and $t + \tau$, while the primed quantities are evaluated at \vec{y}' and t . Notice that $\rho_{ijkl}^{(0)}(\vec{y}', \vec{\eta})$ is independent of τ . Hence,

$$\frac{1}{2\pi} \int_{-\infty}^{\infty} e^{-i\omega\tau} \rho_{ijkl}^{(0)}(\vec{y}', \vec{\eta}) d\tau = \delta(\omega) \rho_{ijkl}^{(0)}$$

where $\delta(\omega)$ is the delta function.

At zero frequency the inhomogeneous Helmholtz equation (11a) reduces to Poisson's equation. For $|\vec{x}| \gg |\vec{y}|$ (i.e., in the far field), the delta function vanishes, and the Green's function of the resulting Laplace's equation is independent of the source location \vec{y} . Hence,

$$\frac{\partial \mathbf{G}}{\partial y_i} = 0 \quad \text{at } \omega = 0$$

But this implies that

$$\delta(\omega) \frac{\partial \mathbf{G}}{\partial y_i} = 0$$

It therefore follows that, when equation (17) is substituted into equation (15) and the result is substituted into equation (14), the term $\mathcal{R}_{ijkl}^{(0)}(\vec{y}', \vec{\eta})$ makes no contribution to the integral. Hence, upon making this substitution and changing the variables of integration from \vec{y}' and \vec{y}'' to \vec{y}' and $\vec{\eta}$ for the integration over $\mathcal{R}_{ijkl}^{(1)}$ and from \vec{y}' and \vec{y}'' to \vec{y}'' and $\vec{\eta}^{(1)}$ for the integration over $\mathcal{R}_{ijkl}^{(2)}$, we find that

$$\begin{aligned} I_\omega(\vec{x}) = & \frac{\rho_o}{4\pi c_o} \int_{-\infty}^{\infty} \int_{\mathcal{V}^2} \int \frac{\partial^2 G(\vec{x}|\vec{y}')}{\partial y'_i \partial y'_j} \frac{\partial^2 G^*(\vec{x}|\vec{y}' + \vec{\eta})}{\partial y'_k \partial y'_l} \mathcal{R}_{ijkl}^{(1)}(\vec{y}', \vec{\eta}, \tau) e^{-i\omega\tau} d\tau d\vec{y}' d\vec{\eta} \\ & + \frac{\rho_o}{4\pi c_o} \int_{-\infty}^{\infty} \int_{\mathcal{V}^2} \int \frac{\partial^2 G[\vec{x}|\vec{y}'' + \vec{\eta}^{(1)}]}{\partial y''_i \partial y''_j} \frac{\partial^2 G^*(\vec{x}|\vec{y}'')}{\partial y''_k \partial y''_l} \mathcal{R}_{ijkl}^{(2)}[\vec{y}'', \vec{\eta}^{(1)}, \tau] e^{-i\omega\tau} d\tau d\vec{y}'' d\vec{\eta}^{(1)} \end{aligned} \quad (21)$$

where \mathcal{V}^2 denotes the appropriate volume for the double integration over the variables \vec{y}' and $\vec{\eta}$ (which is the same as for the integration over the variables \vec{y}' , $\vec{\eta}^{(1)}$). But since the variables \vec{y}'' and $\vec{\eta}^{(1)}$ in the second integral are variables of integration, we can replace them by \vec{y}' and $\vec{\eta}$, respectively; and since i, j, k , and l are dummy indices, we can interchange the indices i and k and the indices j and l without changing the value of this integral. Thus, the second integral in equation (21) becomes, after changing the variable τ to $-\tau$,

$$\frac{\rho_o}{4\pi c_o} \int_{-\infty}^{\infty} \int_{\mathcal{V}^2} \int \frac{\partial^2 G^*(\vec{x}|\vec{y}')}{\partial y'_i \partial y'_j} \frac{\partial^2 G(\vec{x}|\vec{y}' + \vec{\eta})}{\partial y'_k \partial y'_l} \mathcal{R}_{ijkl}^{(2)}(\vec{y}', \vec{\eta}, -\tau) e^{i\omega\tau} d\tau d\vec{\eta} d\vec{y}' \quad (22)$$

Now, if it is assumed that the turbulence is stationary in time, the correlations must be invariant under a translation in time. Hence, we can replace t in $\mathcal{R}_{klij}^{(2)}(\bar{\mathbf{y}}', \bar{\eta}, -\tau)$ by $t + \tau$. It can now be seen that replacing $\bar{\mathbf{y}}''$ by $\bar{\mathbf{y}}'$, $\bar{\eta}^{(1)}$ by $\bar{\eta}$, and τ by $-\tau$ in equation (20) merely interchanges the primed and unprimed quantities. Hence, it follows from equations (19) and (20) that

$$\mathcal{R}_{ijk\ell}^{(1)}(\bar{\mathbf{y}}', \bar{\eta}, \tau) = \mathcal{R}_{klij}^{(2)}(\bar{\mathbf{y}}', \bar{\eta}, -\tau)$$

And upon inserting this into equation (22) we find (since the actual limits of integration on the variables $\bar{\mathbf{y}}''$ and $\bar{\eta}^{(1)}$ are the same as those for $\bar{\mathbf{y}}'$ and $\bar{\eta}^{(0)}$, respectively) that the second term on the right side of equation (21) is the complex conjugate of the first. Hence,

$$I_{\omega}(\bar{\mathbf{x}}) = \frac{\rho_0}{2\pi c_0} \operatorname{Re} \int_{-\infty}^{\infty} \int_{\mathcal{V}^2} \int \frac{\partial^2 G(\bar{\mathbf{x}}|\bar{\mathbf{y}}')}{\partial y_1' \partial y_j'} \frac{\partial^2 G^*(\bar{\mathbf{x}}|\bar{\mathbf{y}}' + \bar{\eta})}{\partial y_k' \partial y_l'} \mathcal{R}_{ijk\ell}^{(1)}(\bar{\mathbf{y}}', \bar{\eta}, \tau) e^{-i\omega\tau} d\tau d\bar{\mathbf{y}}' d\bar{\eta} \quad (23)$$

EXPANSION FOR LOW EDDY MACH NUMBER - CONVECTIVE AMPLIFICATION

We first introduce the new variable

$$\bar{\mathbf{y}} \equiv \left(y_1', \frac{y_2' + y_2''}{2}, \frac{y_3' + y_3''}{2} \right) = \frac{\bar{\mathbf{y}}' + \bar{\mathbf{y}}''}{2} + \hat{\mathbf{i}} \left(\frac{y_1' - y_1''}{2} \right)$$

where $\hat{\mathbf{i}}$ denotes the unit vector in the y_1 -direction. Then

$$\bar{\mathbf{y}}' = \bar{\mathbf{y}} + \frac{1}{2} (\hat{\mathbf{i}} \eta_1 - \bar{\eta})$$

Hence, if in equation (23) we put

$$\mathcal{R}_{ijk\ell}^{(1)}(\bar{\mathbf{y}}', \bar{\eta}, \tau) = \mathcal{R}_{ijk\ell}^+(\bar{\mathbf{y}}, \bar{\eta}, \tau) + \mathcal{R}_{ijk\ell}^c(\bar{\mathbf{y}}', \bar{\eta}, \tau)$$

where

$$\mathcal{R}_{ijk\ell}^+(\vec{y}', \vec{\eta}', \tau) \equiv \overline{u_i' u_j' u_k' u_\ell'} - \overline{u_i' u_j'} \overline{u_k' u_\ell'} + U' U'' (\delta_{1i} \delta_{1k} \overline{u_j' u_\ell'} + \delta_{1j} \delta_{1\ell} \overline{u_i' u_k'} + 2\delta_{1j} \delta_{1k} \overline{u_i' u_\ell'}) \quad (24)$$

$$\mathcal{R}_{ijk\ell}^c(\vec{y}', \vec{\eta}', \tau) \equiv 2U' (\delta_{1i} \overline{u_j' u_k' u_\ell'} + \delta_{1j} \overline{u_i' u_k' u_\ell'})$$

and then change the variables of integration from \vec{y}' and $\vec{\eta}'$ to \vec{y} and $\vec{\eta}$ in performing the integration over $\mathcal{R}_{ijk\ell}^+$, we obtain

$$I_{\omega}(\vec{x}) = \frac{\rho_0}{2\pi c_0} \mathcal{R}e \left[\int_{-\infty}^{\infty} \int_{\mathcal{V}^2} \int \frac{\partial^2 G(\vec{x} | \vec{y} + \frac{1}{2} i\eta_1 - \frac{1}{2} \vec{\eta})}{\partial y_i \partial y_j} \frac{\partial^2 G^*(\vec{x} | \vec{y} + \frac{1}{2} i\eta_1 + \frac{1}{2} i\vec{\eta})}{\partial y_k \partial y_\ell} \times \mathcal{R}_{ijk\ell}^+(\vec{y}, \vec{\eta}, \tau) e^{-i\omega\tau} d\tau d\vec{y} d\vec{\eta} \right. \\ \left. + \int_{-\infty}^{\infty} \int_{\mathcal{V}^2} \int \frac{\partial^2 G(\vec{x} | \vec{y})}{\partial y_i \partial y_j} \frac{\partial^2 G^*(\vec{x} | \vec{y} + \vec{\eta})}{\partial y_k \partial y_\ell} \mathcal{R}_{ijk\ell}^c(\vec{y}, \vec{\eta}, \tau) e^{-i\omega\tau} d\tau d\vec{y} d\vec{\eta} \right] \quad (25)$$

where the integral involving $\mathcal{R}_{ijk\ell}^c$ was obtained simply by changing the name of the dummy variable of integration from \vec{y}' to \vec{y} . Thus,

$$\mathcal{R}_{ijk\ell}^c(\vec{y}, \vec{\eta}, \tau) = 2U(y_2) \left[\overline{\delta_{1i} u_j(\vec{y}, t) u_k(\vec{y} + \vec{\eta}, t + \tau) u_\ell(\vec{y} + \vec{\eta}, t + \tau)} + \overline{\delta_{1j} u_i(\vec{y}, t) u_k(\vec{y} + \vec{\eta}, t + \tau) u_\ell(\vec{y} + \vec{\eta}, t + \tau)} \right] \quad (26)$$

The symbol \mathcal{V}^2 always denotes a given volume of space even though the specific limits for the transformed variables can be different.

If the mean flow were zero, the correlation functions $\mathcal{R}_{ijk\ell}^+(\vec{y}, \vec{\eta}, \tau)$ and $\mathcal{R}_{ijk\ell}^c(\vec{y}, \vec{\eta}, \tau)$ would decay rapidly as functions of $\vec{\eta}$ relative to a characteristic length of the region of flow and the characteristic wavelength associated with the eddy decay time; and it would be possible (as will be seen) to neglect variations in G over the range of $\vec{\eta}$ where $\mathcal{R}_{ijk\ell}^+$ and $\mathcal{R}_{ijk\ell}^c$ are nonzero. However, in the case where there is a mean flow (see ref. 5), the correlations at points along the direction of flow can extend over long distances compared with the wavelength associated with the eddy decay time since the eddies are moving with the flow and their apparent decay time is quite short. In order to allow for this, we introduce a set of coordinates which move with the turbulent eddies. Thus, we introduce the new variable

$$\vec{\xi} \equiv \vec{\eta} - \vec{U}_c(y_2)\tau \quad (27)$$

where \vec{U}_c , which is in the y_1 direction, is the convection velocity of the eddy. The moving-axis correlation functions are now defined by

$$\left. \begin{aligned} R_{ijk\ell}^+(\vec{y}, \vec{\xi}, \tau) &\equiv \mathcal{R}_{ijk\ell}^+(\vec{y}, \vec{\eta}, \tau) \\ R_{ijk\ell}^c(\vec{y}, \vec{\xi}, \tau) &\equiv \mathcal{R}_{ijk\ell}^c(\vec{y}, \vec{\eta}, \tau) \end{aligned} \right\} \quad (28)$$

Then upon introducing the change of variable (27) into equation (25) we get

$$\begin{aligned} I_{\omega}(\vec{x}) = \frac{\rho_o}{2\pi c_o} \rho_e \left[\int_{-\infty}^{\infty} \int_{\mathcal{V}^2} \int \frac{\partial^2 G(\vec{x}|\vec{y} + \frac{1}{2} i\xi_1 - \frac{1}{2} \vec{\xi})}{\partial y_i \partial y_j} \frac{\partial^2 G^*(\vec{x}|\vec{y} + \frac{1}{2} i\xi_1 + \frac{1}{2} \vec{\xi} + \vec{U}_c \tau)}{\partial y_k \partial y_\ell} R_{ijk\ell}^+(\vec{y}, \vec{\xi}, \tau) e^{-i\omega\tau} d\tau d\vec{y} d\vec{\xi} \right. \\ \left. + \int_{-\infty}^{\infty} \int_{\mathcal{V}^2} \int \frac{\partial^2 G(\vec{x}|\vec{y})}{\partial y_i \partial y_j} \frac{\partial^2 G^*(\vec{x}|\vec{y} + \vec{\xi} + \vec{U}_c \tau)}{\partial y_k \partial y_\ell} R_{ijk\ell}^c(\vec{y}, \vec{\xi}, \tau) e^{-i\omega\tau} d\tau d\vec{y} d\vec{\xi} \right] \quad (29) \end{aligned}$$

Now let l denote a typical correlation length (eddy size) of the turbulence, let τ_f denote a typical decay time of the turbulence in the moving frame, and let M_e be the Mach number characteristic of the turbulence. It is shown in reference 6 (see sec. 3, eq. (17)) that

$$\frac{l}{\tau_f c_o} \sim M_e$$

In turbulent shear flows the characteristic turbulent velocity is about $1/10^{\text{th}}$ of the mean flow velocity. Hence, for subsonic flows

$$\frac{l}{\tau_f c_o} = \frac{l}{\lambda_f} \ll 1$$

Thus, the eddy size is very small compared with the wavelength λ_f associated with the eddy decay time. For pipe flows and internal flows in general, the eddy size is very small compared with a typical dimension h of the boundaries (see fig. 1). Hence, we shall suppose that

$$l \ll h$$

The two length scales which appear in the Green's function G (when the observation

point is in the far field) are λ_f and h . Thus, it is expected that the Green's functions $G(\vec{x}|\vec{y} + \frac{1}{2}\hat{i}\xi_1 - \frac{1}{2}\vec{\xi})$, $G^*(\vec{x}|\vec{y} + \vec{\xi} + \vec{U}_c\tau)$, and $G^*(\vec{x}|\vec{y} + \frac{1}{2}\hat{i}\xi_1 + \frac{1}{2}\vec{\xi} + \vec{U}_c\tau)$ will change only slightly when $\vec{\xi}$ varies over the range $0 \leq |\vec{\xi}| \leq l$. But by definition $R_{ijkl}^+(\vec{y}, \vec{\xi}, \tau) \approx 0$ and $R_{ijkl}^c(\vec{y}, \vec{\xi}, \tau) \approx 0$ for $|\vec{\xi}| > l$, so that we can neglect variations in the Green's function insofar as the integration with respect to $\vec{\xi}$ is concerned. In addition, we can carry out the integrations with respect to $\vec{\xi}$ over all space and the integrations with respect to \vec{y} over the volume \mathcal{V} exterior to the solid boundaries. When the approximations are introduced into equation (29), we obtain

$$I_\omega(\vec{x}) = \frac{\rho_0}{2\pi c_0} \Re e \int_{\mathcal{V}} \frac{\partial^2 G(\vec{x}|\vec{y})}{\partial y_i \partial y_j} \int_{-\infty}^{\infty} e^{-i\omega\tau} \frac{\partial^2 G^*(\vec{x}|\vec{y} + \vec{U}_c\tau)}{\partial y_k \partial y_l} \int \left[R_{ijkl}^+(\vec{y}, \vec{\xi}, \tau) + R_{ijkl}^c(\vec{y}, \vec{\xi}, \tau) \right] d\vec{\xi} d\tau d\vec{y} \quad (30)$$

where the omission of a symbol for the limits of integration denotes that the integral is to be carried out over all space.

We let $I_\omega(\vec{x}|\vec{y})$ denote the spectral density of the intensity at the point \vec{x} due to the sound emitted from a unit volume at \vec{y} (ref. 7). Then

$$I_\omega(\vec{x}) = \int_{\mathcal{V}} I_\omega(\vec{x}|\vec{y}) d\vec{y}$$

and it follows from equation (27) that

$$I_\omega(\vec{x}|\vec{y}) = \frac{\rho_0}{2\pi c_0} \Re e G_{ij}(\vec{y}) \int e^{-i\omega\tau} G_{kl}^*(\vec{y} + \vec{U}_c\tau) \int \left[R_{ijkl}^+(\vec{y}, \vec{\xi}, \tau) + R_{ijkl}^c(\vec{y}, \vec{\xi}, \tau) \right] d\vec{\xi} d\tau \quad (31)$$

where

$$G_{ij}(\vec{y}) \equiv \frac{\partial^2 G_\omega(\vec{x}|\vec{y})}{\partial y_i \partial y_j}$$

Now it follows from equations (19) and (28) that

$$\begin{aligned}
\int \left[\tilde{R}_{ijk\ell}^+(\bar{y}, \bar{\xi}, \tau) + \tilde{R}_{ijk\ell}^c(\bar{y}, \bar{\xi}, \tau) \right] d\bar{\xi} &= \int \tilde{R}_{ijk\ell}(\bar{y}, \bar{\xi}, \tau) d\bar{\xi} \\
&+ \int U\left(y_2 - \frac{\xi_2}{2}\right) U\left(y_2 + \frac{\xi_2}{2}\right) \left[\delta_{1i}\delta_{1k}\tilde{R}_{j\ell}(\bar{y}, \bar{\xi}, \tau) + \delta_{1j}\delta_{1\ell}\tilde{R}_{ik}(\bar{y}, \bar{\xi}, \tau) + 2\delta_{1j}\delta_{1k}\tilde{R}_{i\ell}(\bar{y}, \bar{\xi}, \tau) \right] d\bar{\xi} \\
&+ 2U(y_2) \int \left[\delta_{1i}\tilde{R}_{j,k\ell}(\bar{y}, \bar{\xi}, \tau) + \delta_{1j}\tilde{R}_{i,k\ell}(\bar{y}, \bar{\xi}, \tau) \right] d\bar{\xi}
\end{aligned} \tag{32}$$

where

$$\tilde{R}_{ijk\ell}(\bar{y}, \bar{\xi}, \tau) \equiv \overline{u_i' u_j' u_k' u_\ell'} - \overline{u_i' u_j'} \overline{u_k' u_\ell'} \tag{33}$$

$$\tilde{R}_{ij}(\bar{y}, \bar{\xi}, \tau) \equiv \overline{u_i' u_j'} \tag{34}$$

$$\tilde{R}_{i,jk}(\bar{y}, \bar{\xi}, \tau) \equiv \overline{u_i(\bar{y}, t) u_j(\bar{y} + \bar{\eta}, t + \tau) u_k(\bar{y} + \bar{\eta}, t + \tau)} \tag{35}$$

The first two integrals on the right side of equation (32) represent the self noise and the shear noise, respectively (refs. 8 and 9). The last integral in equation (32) represents a coupling between the shear noise and the self noise.

LOCALLY HOMOGENEOUS TURBULENCE - VANISHING OF COUPLING TERM

It is shown in reference 4, under the relatively mild restriction that the turbulence is approximately locally homogeneous and incompressible, that the coupling term between shear noise and self noise in equation (32) vanishes. Hence, after the names of the dummy indices are changed, equation (31) can be written as

$$\begin{aligned}
I_\omega(\vec{x} | \vec{y}) &= \frac{\rho_0}{2\pi c_0} \Re \left[G_{ij}(\vec{y}) \int_{-\infty}^{\infty} e^{-i\omega\tau} G_{k\ell}^*(\vec{y} + \vec{U}_c \tau) \int \tilde{R}_{ijk\ell}(\vec{y}, \bar{\xi}, \tau) d\bar{\xi} d\tau \right] \\
&+ \frac{2\rho_0}{\pi c_0} \Re \left[G_{1j}(\vec{y}) \int_{-\infty}^{\infty} e^{-i\omega\tau} G_{1\ell}^*(\vec{y} + \vec{U}_c \tau) \int U\left(y_2 + \frac{\xi_2}{2}\right) U\left(y_2 - \frac{\xi_2}{2}\right) \tilde{R}_{j\ell}(\vec{y}, \bar{\xi}, \tau) d\bar{\xi} d\tau \right]
\end{aligned} \tag{36}$$

The first term in this equation is the self-noise term and the second is the shear-noise term.

Equation (36) cannot be further simplified without making additional assumptions about the turbulence.

REPRESENTATION OF FOURTH-ORDER CORRELATIONS IN TERMS OF SECOND-ORDER CORRELATIONS

It is argued by Batchelor (ref. 10, section 8.2) that the part of the joint probability of the velocity (with zero time delay) associated with the energy-bearing eddies is approximately normal, at least insofar as the velocities at two points are concerned. This approximation is better for some purposes than for others. For example, this approximation gives reasonably accurate predictions about the relation between the second- and fourth-order correlations (ref. 10, p. 176). This relation is found to be (ref. 10, eq. 8.3.11)

$$\overline{u'_1 u'_j u'_k u'_l} = \overline{u'_1 u'_j} \overline{u'_k u'_l} + \overline{u'_1 u'_k} \overline{u'_j u'_l} + \overline{u'_1 u'_l} \overline{u'_j u'_k} \quad \text{at } \tau = 0 \quad (37)$$

But by extending the reasoning used by Batchelor in section 8.2, we can argue that, when the velocity correlations are separated in time as well as in space, their correlation will be subject to even more random influences from the neighboring flow than when they occur at the same time. These influences will, according to the central limit theorem, tend to make the joint probability distribution more normal. Hence, we expect equation (37) to be even more nearly valid when $\tau \neq 0$. Then in view of equations (33) and (34) we can now write

$$\tilde{R}_{ijkl}(\vec{y}, \vec{\xi}, \tau) = \tilde{R}_{ik} \tilde{R}_{jl} + \tilde{R}_{il} \tilde{R}_{jk} \quad (38)$$

Inserting this into equation (36) and changing the dummy indices gives

$$\begin{aligned} I_{\omega}(\vec{x} | \vec{y}) = & \frac{\rho_0}{\pi c_0} \Re e \left[G_{ij}(\vec{y}) \int_{-\infty}^{\infty} e^{-i\omega\tau} G_{kl}^*(\vec{y} + \vec{U}_c \tau) \int \tilde{R}_{ik} \tilde{R}_{jl} d\vec{\xi} d\tau \right] \\ & + \frac{2\rho_0}{\pi c_0} U \Re e \left[G_{1j}(\vec{y}) \int_{-\infty}^{\infty} e^{-i\omega\tau} G_{1l}^*(\vec{y} + \vec{U}_c \tau) \int U' U'' \tilde{R}_{jl} d\vec{\xi} d\tau \right] \quad (39) \end{aligned}$$

where $U' \equiv U\left(y_2 - \frac{\xi_2}{2}\right)$ and $U'' \equiv U\left(y_2 + \frac{\xi_2}{2}\right)$.

AXISYMMETRIC TURBULENCE - QUADRUPOLE CORRELATIONS

It can be seen from the measurements presented in references 11 and 12 that, at least for jet mixing regions, it is reasonable to assume that the moving-axis correlation tensor $\tilde{R}_{ij}(\vec{y}, \vec{\xi}, \tau)$ is a symmetric function of τ . Thus, figure 27 of reference 11 shows that $\tilde{R}_{11}(\vec{y}, \hat{i}\xi_1, \tau)$ peaks at $\tau = 0$, and figure 13 of reference 12 shows that this function is fairly symmetrical about $\tau = 0$. (Notice that in this figure the lines $\xi_1 = \text{constant}$ are parallel to the dashed line.) Hence, we assume that \tilde{R}_{ij} is an even function of τ . We shall also assume that the turbulence is axisymmetric about the direction of mean flow. Then it is shown in reference 4 that \tilde{R}_{ij} is an axisymmetric tensor of the form

$$\tilde{R}_{ij}(\vec{y}, \vec{\xi}, \tau) = A\xi_i\xi_j + B\delta_{ij} + C\delta_{1i}\delta_{1j} + D(\delta_{1i}\xi_j + \delta_{1j}\xi_i) \quad (40)$$

where the coefficients A , B , and C are functions of \vec{y} , τ , and $\xi \equiv \sqrt{\xi_1^2 + \xi_2^2 + \xi_3^2}$ and are even functions of ξ_1 ; and where D is a function of \vec{y} , τ , and η and an odd function of ξ_1 .

In order to evaluate the first term on the right side of equation (39), observe that

$$\begin{aligned} \int \tilde{R}_{ik} \tilde{R}_{jl} d\vec{\xi} &= \int \left[A\xi_i\xi_k + B\delta_{ik} + C\delta_{1i}\delta_{1k} + D(\delta_{1i}\xi_k + \delta_{1k}\xi_i) \right] \\ &\quad \times \left[A\xi_j\xi_l + B\delta_{jl} + C\delta_{1j}\delta_{1l} + D(\delta_{1j}\xi_l + \delta_{1l}\xi_j) \right] d\vec{\xi} \end{aligned} \quad (41)$$

All the products of the coefficients A , B , etc. which occur in the integrand are even functions of ξ_2 and ξ_3 and either even or odd functions of ξ_1 . (In fact, they are all even except those terms which consist of products of D with either A , B , or C .) But since any integral of an odd function of ξ_i for $i = 1, 2, 3$ is equal to zero, it can be seen by inspection that only terms which have two pairs of equal indices can contribute to the integral. Hence, the integrals must be of the form

$$\int \tilde{R}_{ik} \tilde{R}_{jl} d\vec{\xi} = a_{ik}\delta_{ij}\delta_{kl} + b_{ij}\delta_{ik}\delta_{jl} + c_{ij}\delta_{il}\delta_{jk} \quad (\text{no sum on } i, j, k, \text{ or } l) \quad (42)$$

Therefore, upon noting that $G_{ij} = G_{ji}$ and interchanging names of dummy indices we find that

$$G_{ij}(\vec{y})G_{kl}^*(\vec{y} + \vec{U}_c\tau) \int \tilde{R}_{ik}\tilde{R}_{jl} d\vec{\xi} = a_{ik}G_{ii}(\vec{y})G_{kk}^*(\vec{y} + \vec{U}_c\tau) + (b_{ij} + c_{ij})G_{ij}(\vec{y})G_{ij}^*(\vec{y} + \vec{U}_c\tau) \quad (43)$$

It is convenient to define

$$G_{ij}^T(\vec{y}) \equiv G_{ij}^*(\vec{y} + \vec{U}_c\tau) \quad (44)$$

This shows that the coefficient a_{ik} of $G_{ii}G_{kk}^T$ is the sum of all terms in $\int \tilde{R}_{ik}\tilde{R}_{jl} d\vec{\xi}$ with $i = j$ and $k = l$. Similarly, the coefficient $b_{ij} + c_{ij}$ of $G_{ij}G_{ij}^T$ is the sum of all terms in $\int \tilde{R}_{ik}\tilde{R}_{jl} d\vec{\xi}$ with k and l equal to either i or j . There is a certain ambiguity in the definition of a_{ik} and $b_{ij} + c_{ij}$ since those terms in $\int \tilde{R}_{ik}\tilde{R}_{jl} d\vec{\xi}$ with all four indices equal can be included in either of these terms. But once a_{ik} is defined, $b_{ij} + c_{ij}$ is unique. These results are used in appendix A to show that

$$\begin{aligned} G_{ij}G_{kl}^T \int \tilde{R}_{ik}\tilde{R}_{jl} d\vec{\xi} &= G_{ii}G_{jj}^T \int \tilde{R}_{12}^2 d\vec{\xi} \\ &+ (G_{22}G_{33}^T + G_{33}G_{22}^T) \int (\tilde{R}_{23}^2 - \tilde{R}_{12}^2) d\vec{\xi} + G_{11}G_{11}^T \int (\tilde{R}_{11}^2 - \tilde{R}_{12}^2) d\vec{\xi} \\ &+ 2(G_{12}G_{12}^T + G_{13}G_{13}^T) \int (\tilde{R}_{12}^2 + \tilde{R}_{11}\tilde{R}_{22}) d\vec{\xi} \\ &+ (G_{22}G_{22}^T + G_{33}G_{33}^T) \int (\tilde{R}_{22}^2 - \tilde{R}_{12}^2) d\vec{\xi} \\ &+ 2G_{23}G_{23}^T \int (\tilde{R}_{22}^2 - \tilde{R}_{23}^2) d\vec{\xi} \end{aligned}$$

Applying the reciprocity principle to (11a) shows that for $\vec{x} \neq \vec{y}$

$$G_{ii} = -k^2 G$$

Hence, the first term in equation (39) can be expressed in terms of the relation

$$G_{ij}G_{kl}^T \int \tilde{R}_{ik}\tilde{R}_{jl} d\vec{\xi} = k^4 GG^T S - (G_{22}G_{33}^T + G_{33}G_{22}^T)(Q_{23} - Q_{22}) + G_{ij}G_{ij}^T Q_{ij} \quad (45)$$

where

$$Q_{ij} = Q_{ji} \quad (46)$$

and

$$\left. \begin{aligned} Q_{11} &= \int (\tilde{R}_{11}^2 - \tilde{R}_{12}^2) d\vec{\xi} \\ Q_{12} &= Q_{13} = \int (\tilde{R}_{12}^2 + \tilde{R}_{11}\tilde{R}_{22}) d\vec{\xi} \\ Q_{22} &= Q_{33} = \int (\tilde{R}_{22}^2 - \tilde{R}_{12}^2) d\vec{\xi} \\ Q_{23} &= \int (\tilde{R}_{22}^2 - \tilde{R}_{23}^2) d\vec{\xi} \end{aligned} \right\} \quad (47)$$

$$S = \int \tilde{R}_{12}^2 d\vec{\xi} \quad (48)$$

These five integrals depend on the four correlations \tilde{R}_{11} , \tilde{R}_{22} , \tilde{R}_{12} , and \tilde{R}_{23} .

Turning to the second integral in equation (39), we find from equation (40) that

$$\begin{aligned} G_{1j}(\vec{y})G_{1l}^*(\vec{y} + \vec{U}_c\tau) \int U'U''\tilde{R}_{jl} d\vec{\xi} &= G_{1j}G_{1l}^T \int U'U''[A\xi_j\xi_l + B\delta_{jl} + C\delta_{1j}\delta_{1l} \\ &\quad + D(\xi_j\delta_{1l} + \xi_l\delta_{1j})] d\vec{\xi} \end{aligned} \quad (49)$$

It is shown in appendix B that this equation can be simplified to obtain

$$G_{1j}G_{1l}^T \int U'U''\tilde{R}_{jl} d\vec{\xi} = G_{1j}G_{1j}^T \int U'U''\tilde{R}_{jj} d\vec{\xi} \quad (50)$$

It now follows from equations (39), (45), and (50) that

$$I_{\omega}(\vec{x}|\vec{y}) = I_{\omega}(\vec{x}|\vec{y})_{se} + I_{\omega}(\vec{x}|\vec{y})_{sh} \quad (51)$$

where the self-noise term is

$$\begin{aligned} I_{\omega}(\vec{x}|\vec{y})_{se} = & \frac{\rho_0}{\pi c_0} \text{Re} \left[k^4 G \int_{-\infty}^{\infty} e^{-i\omega\tau} G^T S \, d\tau \right. \\ & - \int_{-\infty}^{\infty} (G_{22} G_{33}^T + G_{33} G_{22}^T)(Q_{23} - Q_{22}) e^{-i\omega\tau} \, d\tau \\ & \left. + G_{ij} \int_{-\infty}^{\infty} e^{-i\omega\tau} G_{ij}^T Q_{ij} \, d\tau \right] \quad (52) \end{aligned}$$

and the shear-noise term is

$$I_{\omega}(\vec{x}|\vec{y})_{sh} = \frac{2\rho_0}{\pi c_0} \text{Re} G_{1j} \int_{-\infty}^{\infty} e^{-i\omega\tau} G_{1j}^T \int U' U'' \tilde{R}_{jj} \, d\vec{\xi} \, d\tau \quad (53)$$

The last term in the self-noise term (52) is a sum of the intensities from independent quadrupoles. The first term is the emission from a monopole source (weighted according to wave number), and the second term is a coupling term between the two longitudinal quadrupoles transverse to the mean flow. The shear-noise term just consists of the sum of three independent quadrupoles.

Equations (47) and (48) show that the self noise depends on the four correlation functions \tilde{R}_{11} , \tilde{R}_{22} , \tilde{R}_{12} , and \tilde{R}_{23} . And equation (53) shows that the shear noise depends on the three correlation functions \tilde{R}_{11} , \tilde{R}_{22} , and \tilde{R}_{33} . However, it follows from equation (40) that

$$2 \int \tilde{R}_{23}^2 \, d\vec{\xi} = \int (\tilde{R}_{22}^2 - \tilde{R}_{22} \tilde{R}_{33}) \, d\vec{\xi} \quad (54)$$

Hence, the noise is completely determined in terms of four correlations of the turbulence.

ISOTROPIC TURBULENCE

The expression for the sound intensity can be further simplified if we assume that the turbulence is locally isotropic in the moving reference frame. That is, we assume that \tilde{R}_{ij} is an isotropic tensor.¹ In this case, the correlation tensor (40) reduces to

$$\tilde{R}_{ij}(\vec{y}, \vec{\xi}, \tau) = A \xi_i \xi_j + B \delta_{ij} \quad (55)$$

where A and B are functions only of ξ and τ (see ref. 10).

Upon defining the correlation-length scale $L(\vec{y}, \tau)$ by

$$L(\vec{y}, \tau) \equiv \frac{1}{(\overline{u^2})^2} \int \tilde{R}_{11}^2 d\vec{\xi} \quad (56)$$

where $\sqrt{\overline{u^2}}$ is the rms turbulent velocity at \vec{y} , we find from the results obtained in appendix C that

$$Q_{ij} = \frac{7}{8} (\overline{u^2})^2 L \quad \text{for } i, j = 1, 2, 3$$

and

$$S = \frac{1}{8} (\overline{u^2})^2 L \quad (57)$$

Equation (52) now becomes

$$I_{\omega}(\vec{x} | \vec{y})_{se} = \frac{7\rho_o}{8\pi c_o} (\overline{u^2})^2 \text{Re} \left[\frac{k^4}{7} G \int_{-\infty}^{\infty} e^{-i\omega\tau} G^T L d\tau + G_{ij} \int_{-\infty}^{\infty} e^{-i\omega\tau} G_{ij}^T L d\tau \right] \quad (58)$$

¹It is shown in ref. 4 that the correlation tensor for isotropic turbulence must always be an even function of τ . Hence, if we began with isotropic turbulence, it would not be necessary to make any assumption about the time dependence of \tilde{R}_{ij} .

In order to simplify the shear-noise term, we use the results of appendix D, which show that

$$\int U'U''\tilde{R}_{11} d\vec{\xi} = \int U'U''\tilde{R}_{33} d\vec{\xi}$$

and

$$\int U'U''\tilde{R}_{22} d\vec{\xi} = 0$$

If we define the correlation-length scale $\mathcal{L}(\vec{y}, t)$ by

$$\mathcal{L}(\vec{y}, \tau) \equiv \frac{1}{Uu^2} \int U'U''\tilde{R}_{11} d\vec{\xi} \quad (59)$$

where U denotes the velocity at \vec{y} , then equation (53) becomes

$$I_{\omega}(\vec{x}|\vec{y})_{sh} = \frac{4\rho_0 U^2 \overline{u^2}}{c_0} Re \left[G_{11} \int_{-\infty}^{\infty} e^{-i\omega\tau} G_{11}^T \mathcal{L} d\tau + G_{13} \int_{-\infty}^{\infty} e^{-i\omega\tau} G_{13}^T \mathcal{L} d\tau \right] \quad (60)$$

Thus, once the Green's function G of the particular geometry has been found, equations (58) and (60) give the spectral density of the intensity of the sound field due to a unit volume of turbulence located at the point of \vec{y} as a function of the turbulence correlation-length scales L and \mathcal{L} .

CALCULATION OF FAR-FIELD GREEN'S FUNCTION

General Case

Since we are only interested in the Green's function $G(\vec{x}|\vec{y})$ when the observation point \vec{x} is in the far field, considerable labor could be saved in calculating the Green's function if the far-field Green's function were calculated directly instead of the general Green's function being calculated and then expanded for \vec{x} in the far field. This can be accomplished by utilizing the reciprocity principle (ref. 13) which states that the Green's

function with the observation point at \vec{x} and the source point at \vec{y} is equal to the Green's function with the observation point at \vec{y} and the source point at \vec{x} . That is,

$$G(\vec{x}|\vec{y}) = G(\vec{y}|\vec{x}) \quad (61)$$

Hence, it follows from equations (11a) and (11b) that

$$(\nabla^2 + k^2)G = -\delta(\vec{x} - \vec{y}) \quad (62)$$

$$\hat{n} \cdot \nabla G = 0 \quad (\text{on solid boundary}) \quad (63)$$

where $\delta(\vec{x} - \vec{y}) = \delta(\vec{y} - \vec{x})$ and the differentiations are with respect to the variable \vec{y} instead of \vec{x} . We now put

$$G(\vec{x}|\vec{y}) = g(\vec{x}|\vec{y}) + \Psi(\vec{x}|\vec{y}) \quad (64)$$

where

$$g(\vec{x}|\vec{y}) = \frac{1}{4\pi|\vec{x} - \vec{y}|} e^{ik|\vec{x} - \vec{y}|} \quad (65)$$

is the free-space Green's function. Upon substituting this into equations (62) and (63), we obtain

$$(\nabla^2 + k^2) \Psi = 0 \quad (66)$$

$$\hat{n} \cdot \nabla \Psi = -\hat{n} \cdot \nabla g \quad (\text{on solid boundary}) \quad (67)$$

Upon expanding $|\vec{x} - \vec{y}|$ for larger values of $|\vec{x}|$ we obtain

$$|\vec{x} - \vec{y}| = r - \frac{\vec{x} \cdot \vec{y}}{r} + O(r^{-1}) \quad \text{as } r \rightarrow \infty$$

where we have put

$$r = |\vec{x}|$$

It is now convenient to express the location of the source point in terms of the spherical coordinates shown in figure 3. Then

$$\frac{\vec{x} \cdot \vec{y}}{r} = y_1 \sin \theta \cos \psi + y_2 \sin \theta \sin \psi + y_3 \cos \theta$$

and

$$g(\vec{x} | \vec{y}) \sim \frac{1}{4\pi r} e^{ikr} g_o(\theta, \psi | \vec{y}) \quad (68a)$$

where

$$g_o(\theta, \psi | \vec{y}) \equiv \exp[-ik(y_1 \sin \theta \cos \psi + y_2 \sin \theta \sin \psi + y_3 \cos \theta)] \quad (68b)$$

represents a plane wave propagating in the $(-\vec{x})$ -direction. Substituting this into equation (67) gives

$$\hat{n} \cdot \nabla \Psi = -\frac{1}{4\pi r} e^{ikr} \hat{n} \cdot \nabla g_o \quad (\text{on solid boundary}) \quad (69)$$

It can now be seen that equations (66) and (69) possess a solution of the form

$$\Psi(\vec{x} | \vec{y}) = \frac{1}{4\pi r} e^{ikr} \Psi_o(\theta, \psi | \vec{y})$$

where Ψ_o is a solution of the boundary-value problem

$$(\nabla^2 + k^2)\Psi_o = 0 \quad (70)$$

$$\hat{n} \cdot \nabla \Psi_o = -\hat{n} \cdot \nabla g_o \quad (\text{on solid boundary}) \quad (71)$$

and since Ψ represents an outgoing wave at infinity, this is the desired solution to the problem. Hence, we can write

$$G(\vec{x} | \vec{y}) = \frac{1}{4\pi r} e^{ikr} G_o(\theta, \psi | \vec{y}) \quad (72)$$

where

$$G_o(\theta, \psi | \vec{y}) = g_o(\theta, \psi | \vec{y}) + \Psi_o(\theta, \psi | \vec{y}) \quad (73)$$

and g_o is the incident plane wave (68) and Ψ_o is the solution to the boundary-value problem (70) and (71). It follows from this that G_o is the solution to the problem of a plane wave from infinity incident on the solid boundary. By eliminating the dependence on the variable r , the problem has been simplified.

Two-Dimensional Geometries

We shall now consider the case where the solid boundaries do not change their shape in the y_3 -direction. Thus, the unit normal vector \hat{n} lies in the y_1y_2 -plane and

$$\hat{n} \cdot \nabla = n_1 \frac{\partial}{\partial y_1} + n_2 \frac{\partial}{\partial y_2} \quad (74)$$

The general Green's function of this boundary-value problem is still three dimensional. However, the far-field Green's function can be simply expressed in terms of the solution to a two-dimensional boundary-value problem. Thus, it follows from equations (68), (70) to (72), (73), and (74) that G_o takes the form

$$G_o(\theta, \psi | \vec{y}) = e^{-iky_3 \cos \theta} G_1(\psi | y_1, y_2) \quad (75)$$

where

$$G_1(\psi | y_1, y_2) = e^{-ik_o(y_1 \cos \psi + y_2 \sin \psi)} + \varphi_o(\psi | y_1, y_2) \quad (76)$$

$$k_o \equiv k \sin \theta \quad (77)$$

and the function φ_o is determined as the solution to the boundary-value problem

$$\left(\frac{\partial^2}{\partial y_1^2} + \frac{\partial^2}{\partial y_2^2} + k_o^2 \right) \varphi_o = 0 \quad (78)$$

$$\hat{n} \cdot \nabla \varphi_0 = -\hat{n} \cdot \nabla e^{-ik_0(y_1 \cos \psi + y_2 \sin \psi)} \quad (\text{on solid boundary}) \quad (79)$$

It can be seen from equations (76) to (79) that G_1 is the solution to the problem of a plane wave from infinity incident on the solid boundary. The wave propagates parallel to the $y_1 y_2$ -plane and has a wave number k_0 .

SUMMARY OF GENERAL EQUATIONS

Before using these results to work out a particular example, we shall summarize the general equations obtained so far.

The spectral density of the intensity of sound at the far-field point \vec{x} emitted from a unit volume at the point \vec{y} can be written as

$$I_\omega(\vec{x}|\vec{y}) = \underbrace{I_\omega(\vec{x}|\vec{y})_{\text{se}}}_{\text{self noise}} + \underbrace{I_\omega(\vec{x}|\vec{y})_{\text{sh}}}_{\text{shear noise}} \quad (51)$$

Axisymmetric Turbulence

Self noise:

$$I_\omega(\vec{x}|\vec{y})_{\text{se}} = \frac{\rho_0}{\pi c_0} \text{Re} \left[k^4 G \int_{-\infty}^{\infty} e^{-i\omega\tau} G^T S \, d\tau \right. \\ \left. - \int_{-\infty}^{\infty} (G_{22} G_{33}^T + G_{33} G_{22}^T)(Q_{23} - Q_{22}) e^{-i\omega\tau} \, d\tau \right. \\ \left. + G_{ij} \int_{-\infty}^{\infty} e^{-i\omega\tau} G_{ij}^T Q_{ij} \, d\tau \right] \quad (52)$$

Shear noise:

$$I_\omega(\vec{x}|\vec{y})_{\text{sh}} = \frac{2\rho_0}{\pi c_0} \text{Re} G_{1j} \int_{-\infty}^{\infty} e^{-i\omega\tau} G_{1j}^T \int U' U'' \tilde{R}_{jj} \, d\vec{\xi} \, d\tau \quad (53)$$

Isotropic Turbulence

Self noise:

$$I_{\omega}(\vec{x} | \vec{y})_{se} = \frac{7\rho_o(\overline{u^2})^2}{8\pi c_o} Re \left[\frac{k^4}{7} G \int_{-\infty}^{\infty} e^{-i\omega\tau} G^{TL} d\tau + G_{ij} \int_{-\infty}^{\infty} e^{-i\omega\tau} G_{ij}^{TL} d\tau \right] \quad (58)$$

Shear noise:

$$I_{\omega}(\vec{x} | \vec{y})_{sh} = \frac{2\rho_o U^2 \overline{u^2}}{\pi c_o} Re \left[G_{11} \int_{-\infty}^{\infty} e^{-i\omega\tau} G_{11}^T \ell d\tau + G_{13} \int_{-\infty}^{\infty} e^{-i\omega\tau} G_{13}^T \ell d\tau \right] \quad (60)$$

where

$$G_{ij} \equiv \frac{\partial^2 G_{\omega}(\vec{x} | \vec{y})}{\partial y_i \partial y_j}$$

and the far-field Green's function G is determined in terms of the incident plane wave problems by

General case:

$$G(\vec{x} | \vec{y}) = \frac{1}{4\pi r} e^{ikr} \left[g_o(\theta, \psi | \vec{y}) + \Psi_o(\theta, \psi | \vec{y}) \right] \quad (80)$$

$$g_o \equiv \exp \left[-ik(y_1 \sin \theta \cos \psi + y_2 \sin \theta \sin \psi + y_3 \cos \theta) \right] \quad (68b)$$

$$(\nabla^2 + k^2)\Psi_o = 0 \quad (70)$$

$$\hat{n} \cdot \nabla \Psi_o = -\hat{n} \cdot \nabla g_o \quad (\text{on solid boundary}) \quad (71)$$

Two-dimensional geometries:

$$\hat{n} \cdot \nabla = n_1 \frac{\partial}{\partial y_1} + n_2 \frac{\partial}{\partial y_2} \quad (74)$$

$$G(\vec{x} | \vec{y}) = \frac{1}{4\pi r} e^{ik(r-y_3 \cos \theta)} \left[e^{-ik_o(y_1 \cos \psi + y_2 \sin \psi)} + \varphi_o(\psi | y_1, y_2) \right] \quad (81)$$

$$k_o = k \sin \theta \quad (77)$$

$$\left(\frac{\partial^2}{\partial y_1^2} + \frac{\partial^2}{\partial y_2^2} + k_o^2 \right) \varphi_o = 0 \quad (78)$$

$$\hat{n} \cdot \nabla \varphi_o = -\hat{n} \cdot \nabla e^{-ik_o(y_1 \cos \psi + y_2 \sin \psi)} \quad (\text{on solid boundary}) \quad (79)$$

For both axisymmetric and isotropic turbulence, the shear-noise term is the sum of contributions from independent quadrupoles with no coupling between them. The self-noise term, however, has this property only in the case of isotropic turbulence since the second term in the expression for the intensity for axisymmetric turbulence is a coupling term between the two longitudinal quadrupoles transverse to the flow. However, in the case where the geometry is two dimensional, it is possible to express this term also as a sum of independent quadrupoles. For in this case, equation (81) and the definition of G_{ij} show that

$$G_{33} = -k^2 \cos^2 \theta G$$

and the differential equation (78) shows that

$$G_{11} + G_{22} + k_o^2 G = 0$$

Hence,

$$G_{11} = \tan^2 \theta G_{33} - G_{22} \quad (82)$$

If this is multiplied by the complex conjugate of the corresponding equation for the time-displaced G_{11} , we find that

$$G_{33}G_{22}^T + G_{22}G_{33}^T = \tan^2 \theta G_{33}G_{33}^T + \frac{1}{\tan^2 \theta} (G_{22}G_{22}^T - G_{11}G_{11}^T)$$

And this shows that the coupling term in equation (52) can be expressed in terms of independent quadrupoles.

A PARTICULAR EXAMPLE

We shall now apply the results obtained in the preceding sections to calculate the spectral density of the intensity of the sound emitted from isotropic convected turbulence confined between the two semi-infinite parallel plates shown in figure 4. In this case the boundary condition (79) becomes

$$\frac{\partial \varphi_0}{\partial y_2} = ik_0 \sin \psi e^{-ik_0 y_1 \cos \psi + ik_0 b \sin \psi} \quad \text{at } y_2 = \pm b \quad (83)$$

The problem of a plane wave incident on two semi-infinite parallel planes subject to the boundary condition (83) has been solved by using the Wiener-Hopf technique and is presented in reference 14. It is shown there that for $|y_2| \leq b$ (see eq. 3.25a in ref. 14)

$$\varphi_0 = \frac{-1}{\sqrt{2\pi}} \int_{-\infty + i\beta}^{\infty + i\beta} (S_- \cosh \gamma y_2 + D_- \sinh \gamma y_2) e^{-\gamma b - i\alpha y_1} d\alpha \quad (84)$$

where the contour integral in the complex $\alpha = \sigma + i\beta$ plane is carried out along any line parallel to the σ -axis with β in the range

$$-\text{Im } k_0 < \beta < \cos \psi \text{Im } k_0 \quad (85)$$

and it is assumed for purposes of obtaining the solution that k_0 has been extended into the complex plane so that it has a positive imaginary part. At the end of the calculation the imaginary part can be set equal to zero. In equation (84),

$$\gamma(\alpha) = \sqrt{\alpha^2 - k_0^2} \quad (86)$$

where the branch cuts are chosen as indicated in figure 1.1 of reference 14. Also,

$$D_- = - \frac{k_o \sin \psi \cos(k_o b \sin \psi)}{\sqrt{2\pi} (k_o + k_o \cos \psi)^{1/2} K_+(k_o \cos \psi)(\alpha - k_o)^{1/2} K_-(\alpha)(\alpha - k_o \cos \psi)} \quad (87)$$

$$S_- = \frac{ik_o \sin \psi \sin(k_o b \sin \psi)}{\sqrt{2\pi} b(k_o + k_o \cos \psi) L_+(k_o \cos \psi)(\alpha - k_o) L_-(\alpha)(\alpha - k_o \cos \psi)} \quad (88)$$

$$K_{\pm}(\alpha) = e^{\mp \chi_1(\alpha) - T_{\pm}(\alpha)} \prod_{n=1}^{\infty} \left\{ \left[1 - k_o^2 b_n^2 \right]^{1/2} \mp i \alpha b_{n-(1/2)} \right\} e^{\pm i \alpha b_{n-(1/2)}} \quad (89)$$

$$L_{\pm}(\alpha) = e^{\mp \chi_2(\alpha) - T_{\pm}(\alpha)} \prod_{n=1}^{\infty} \left[\left(1 - k_o^2 b_n^2 \right)^{1/2} \mp i \alpha b_n \right] e^{\pm i \alpha b_n} \quad (90)$$

$$b_n = \frac{b}{n\pi}$$

$$b_{n-(1/2)} = \frac{b}{\left(n - \frac{1}{2} \right) \pi}$$

$$T_{\pm}(\alpha) = \frac{ib}{\pi} \gamma \ln \left(\frac{\gamma \pm \alpha}{k_o} \right)$$

where the imaginary part of the logarithm lies between $-\pi$ and π .

$$\chi_1(\alpha) = - \frac{ib\alpha}{\pi} \left(1 - C_o + \ln \frac{\pi}{2bk_o} \right) + \frac{1}{2} \alpha b$$

$$\chi_2(\alpha) = - \frac{ib\alpha}{\pi} \left(1 - C_o + \ln \frac{2\pi}{bk_o} \right) + \frac{1}{2} \alpha b$$

and $C_0 = 0.5772 \dots$ is Euler's constant. In addition, K_{\pm} and L_{\pm} satisfy the relations

$$\left. \begin{aligned} K_+(\alpha)K_-(\alpha) &= e^{-\gamma b} \cosh \gamma b \\ L_+(\alpha)L_-(\alpha) &= (\gamma b)^{-1} e^{-\gamma b} \sinh \gamma b \end{aligned} \right\} \quad (91)$$

at least within the strip (85) of the complex $\alpha = \sigma + i\beta$ plane. Using equation (86) with the appropriate branch cuts shows that

$$\gamma(k_0 \cos \psi) = -ik_0 \sin \psi \quad (92)$$

Introducing this relation in equation (91) yields

$$\left. \begin{aligned} K_+(k_0 \cos \psi)K_-(k_0 \cos \psi) &= e^{ik_0 b \sin \psi} \cos(k_0 b \sin \psi) \\ L_+(k_0 \cos \psi)L_-(k_0 \cos \psi) &= \frac{e^{ik_0 b \sin \psi}}{k_0 b \sin \psi} \sin(k_0 b \sin \psi) \end{aligned} \right\} \quad (93)$$

Upon substituting equations (88) and (89) into equation (84) and using equations (92) and (93) to simplify the results, we obtain

$$\begin{aligned} \varphi_0 = e^{-ik_0 b \sin \psi} & \left[\frac{1}{2\pi i} \int_{-\infty+i\beta}^{\infty+i\beta} \frac{L_-(k_0 \cos \psi)(k_0 - k_0 \cos \psi)}{L_-(\alpha)(\alpha - k_0)(\alpha - k_0 \cos \psi)} e^{-\gamma b - i\alpha y_1} \cosh \gamma y_2 d\alpha \right. \\ & \left. + \frac{1}{2\pi} \int_{-\infty+i\beta}^{\infty+i\beta} \frac{K_-(k_0 \cos \psi)(k_0 - k_0 \cos \psi)^{1/2} e^{-\gamma b - i\alpha y_1}}{K_-(\alpha)(\alpha - k_0)^{1/2}(\alpha - k_0 \cos \psi)} \sinh \gamma y_2 d\alpha \right] \quad (94) \end{aligned}$$

Now we are interested in the situation where the source point \vec{y} is within the channel. This corresponds to $y_1 < 0$. In this case, the contour integral can be closed in the upper half plane. It can be seen by inspection that the branch cuts in the integrand cancel and that the integrand has only poles in the upper half plane. Hence, it can be evaluated by the method of residues to obtain

$$\begin{aligned}
\varphi_0 = & -e^{-ik_0(y_1 \cos \psi + y_2 \sin \psi)} + e^{-ik_0 b \sin \psi} \left[e^{-ik_0 y_1} \frac{L_-(k_0 \cos \psi)}{L_-(k_0)} \right. \\
& + \frac{1}{i} \sum_{n=1}^{\infty} \frac{L_-(k_0 \cos \psi)(k_0 - k_0 \cos \psi) e^{in\pi} e^{i\beta_n(b_n - y_1)}}{L'_-(\beta_n) b_n (\beta_n - k_0)(\beta_n - k_0 \cos \psi)} \cos \frac{y_2}{b_n} \\
& \left. + \frac{1}{i} \sum_{n=1}^{\infty} \frac{K_-(k_0 \cos \psi)(k_0 - k_0 \cos \psi)^{1/2} e^{i[n-(1/2)]\pi} e^{i\beta_{n-(1/2)}[b_{n-(1/2)} - y_1]}}{K'_-[\beta_{n-(1/2)}] b_{n-(1/2)} [\beta_{n-(1/2)} - k_0]^{1/2} [\beta_{n-(1/2)} - k_0 \cos \psi]} \sin \frac{y_2}{b_{n-(1/2)}} \right]
\end{aligned}$$

where

$$\beta_v = \begin{cases} i \sqrt{\frac{\pi^2 v^2}{b^2} - k_0^2} & \text{for } v \geq \frac{k_0 b}{\pi} \\ \sqrt{k_0^2 - \frac{\pi^2 v^2}{b^2}} & \text{for } v \leq \frac{k_0 b}{\pi} \end{cases} \quad \begin{matrix} v = n \text{ or } v = n - \frac{1}{2} \\ n = 1, 2, 3, \dots \end{matrix}$$

and k_0 can now be taken as real. The terms $K'_-[\beta_{n-(1/2)}]$ and $L'_-(\beta_n)$ denote $K_-[\beta_{n-(1/2)}]$ and $L_-(\beta_n)$, respectively, with the factor $n = v$ omitted in the infinite product:

$$K'_-[\beta_{n-(1/2)}] = \left[\frac{1}{ib_{n-(1/2)}} e^{i\alpha b_{n-(1/2)}} \frac{K_-(\alpha)}{\alpha - \beta_{n-(1/2)}} \right] \bigg|_{\alpha=\beta_{n-(1/2)}}$$

$$L'_-(\beta_n) = \left[\frac{1}{ib_n} e^{i\alpha b_n} \frac{L_-(\alpha)}{\alpha - \beta_n} \right] \bigg|_{\alpha=\beta_n}$$

Upon using these results in equation (81), we find that the far-field Green's function becomes

$$G(\vec{x}|\vec{y}) = \frac{1}{4\pi r} e^{ik(r-y_3 \cos \theta - b \sin \theta \sin \psi)} \mathcal{G}(\psi, \theta | y_1, y_2) \quad \left. \begin{array}{l} \text{where we have put} \\ \mathcal{G}(\psi, \theta | y_1, y_2) = e^{-ik_0 y_1} M_-(\psi) + S_1^{(0)} \\ M_-(\psi) = \frac{L_-(k_0 \cos \psi)}{L_-(k_0)} \end{array} \right\} \quad (95)$$

$$S_1^{(j)} = \frac{1}{i} \sum_{n=1}^{\infty} (-i\beta_n)^j J_n \cos \frac{y_2}{b_n} - \sum_{n=1}^{\infty} [-i\beta_{n-(1/2)}]^j I_n \sin \frac{y_2}{b_{n-(1/2)}} \quad \text{for } j = 0, 1, 2 \quad (96)$$

where $S_1^{(j)}$ is the j^{th} derivative of $S_1^{(0)}$ with respect to y_1 and

$$I_n = \frac{(-1)^n K_-(k_0 \cos \psi) (k_0 - k_0 \cos \psi)^{1/2} e^{i\beta_{n-(1/2)} [b_{n-(1/2)} - y_1]}}{K_-'[\beta_{n-(1/2)}] b_{n-(1/2)} [\beta_{n-(1/2)} - k_0]^{1/2} [\beta_{n-(1/2)} - k_0 \cos \psi]} \quad \left. \begin{array}{l} \\ J_n = \frac{(-1)^n L_-(k_0 \cos \psi) (k_0 - k_0 \cos \psi) e^{i\beta_n (b_n - y_1)}}{L_-'(\beta_n) b_n (\beta_n - k_0) (\beta_n - k_0 \cos \psi)} \end{array} \right\} \quad (97)$$

These results can now be used to calculate the various quadrupole source terms which appear in equations (52), (53), (58), and (59). Thus,

$$G_{ij}(\vec{x}|\vec{y}) = \frac{1}{4\pi r} e^{ik(r-y_3 \cos \theta - b \sin \theta \sin \psi)} \mathcal{G}_{ij}(\psi, \theta | y_1, y_2) \quad (98)$$

where $G_{ij} = G_{ji}$, and in view of equation (82)

$$\left. \begin{aligned} G &= M_- e^{-ik_o y_1} + S_1^{(0)} \\ G_{11} &= -k_o^2 M_- e^{-ik_o y_1} + S_1^{(2)} \\ G_{12} &= S_2^{(1)} \\ G_{13} &= -ik \cos \theta \left[-ik_o M_- e^{-ik_o y_1} + S_1^{(1)} \right] \\ G_{22} &= \tan^2 \theta G_{33} - G_{11} \\ G_{23} &= -ik \cos \theta S_2^{(0)} \\ G_{33} &= -k^2 \cos^2 \theta \left[M_- e^{-ik_o y_1} + S_1^{(0)} \right] \end{aligned} \right\} \quad (99)$$

and we have put

$$S_2^{(j)} \equiv -\frac{1}{i} \sum_{n=1}^{\infty} \frac{(-i\beta_n)^j}{b_n} J_n \sin \frac{y_2}{b_n} - \sum_{n=1}^{\infty} \frac{[-i\beta_{n-(1/2)}]^j}{b_{n-(1/2)}} I_n \cos \frac{y_2}{b_{n-(1/2)}} \quad \text{for } j = 0, 1 \quad (100)$$

We shall now restrict our attention to isotropic turbulence. In order to evaluate the integrals in equations (58) and (59) to predict the self and shear noise, it is necessary to know the dependence on τ of the turbulence correlation lengths L and \mathcal{L} . Chu (ref. 11) has shown that for the mixing region of a jet $\partial^4 L / \partial \tau^4$ and $\partial^4 \mathcal{L} / \partial \tau^4$ could be fit fairly well with functions of the form $c_1 \operatorname{sech} c_2 \tau \cos c_3 \tau$ (see fig. 37 in ref. 11). We shall, for lack of better information about the turbulence, assume that relations of this form also hold for the turbulence between the plates.² Thus, following Chu we put

²Actually, it turns out that the final results are quite insensitive to the details of the models used for L and \mathcal{L} .

$$\left. \begin{aligned} \frac{\partial^4 \mathbf{L}}{\partial \tau^4} &= \mathbf{L}_0^{(\text{IV})} \operatorname{sech} \omega_f^{(2)} \tau \cos \omega_*^{(2)} \tau \\ \frac{\partial^4 \mathcal{L}}{\partial \tau^4} &= \mathcal{L}_0^{(\text{IV})} \operatorname{sech} \omega_f^{(1)} \tau \cos \omega_*^{(1)} \tau \end{aligned} \right\} \quad (101)$$

where

$$\mathbf{L}_0^{(\text{IV})} = \left(\frac{\partial^4 \mathbf{L}}{\partial \tau^4} \right)_{\tau=0}$$

$$\mathcal{L}_0^{(\text{IV})} = \left(\frac{\partial^4 \mathcal{L}}{\partial \tau^4} \right)_{\tau=0}$$

The time dependence in \mathbf{G} and the \mathbf{G}_{ij} is associated with the variable y_1 , which only occurs in exponentials. Hence, the integrals over τ which must be performed in equations (58) and (60) can be found by specializing the constant a in the relation

$$\begin{aligned} \int_{-\infty}^{\infty} e^{i(\omega - U_c a)\tau} \mathbf{L} \, d\tau &= \frac{1}{(\omega - U_c a)^4} \int_{-\infty}^{\infty} e^{i(\omega - U_c a)\tau} \frac{\partial^4 \mathbf{L}}{\partial \tau^4} \, d\tau \\ &= \frac{\mathbf{L}_0^{(\text{IV})}}{(\omega - U_c a)^4} \int_{-\infty}^{\infty} e^{i(\omega - U_c a)\tau} \operatorname{sech} \omega_f^{(2)} \tau \cos \omega_*^{(2)} \tau \, d\tau \\ &= \frac{\pi \mathbf{L}_0^{(\text{IV})}}{2\omega_f^{(2)}(\omega - U_c a)^4} \left\{ \operatorname{sech} \frac{\pi[\omega - U_c a + \omega_*^{(2)}]}{2\omega_f^{(2)}} + \operatorname{sech} \frac{\pi[\omega - U_c a - \omega_*^{(2)}]}{2\omega_f^{(2)}} \right\} \end{aligned}$$

and in a similar relation for \mathcal{L} .

We shall now suppose that the turbulent eddy is far enough from the end of the duct so that the contribution to the integrals in equations (58) and (59) are principally from the parts of the Green's function for the interior of the duct. Thus, for the case where the eddy is moving toward the end of the duct, we suppose that the point \bar{y} is far enough

from the end so that the eddy at \vec{y} will decay before it reaches the end of the duct. Using values of the eddy lifetime typical of jets, we estimate that this will occur if the center of the eddy is about 1/2 to 1/4 of the duct width from the end. When these results together with equations (44) and (95) to (100) are used in equations (58) and (59), we find

$$I_{\omega}(\vec{x}|\vec{y})_{se} = \frac{7\rho_o(\overline{u^2})^2}{8\pi c_o^6(4\pi r)^2} L_o^{(IV)} Re \left\{ \frac{k^4}{7} \mathcal{G}[\mathcal{G}^{(2)}]^* + \mathcal{G}_{ij}[\mathcal{G}_{ij}^{(2)}]^* \right\} \quad (102)$$

$$I_{\omega}(\vec{x}|\vec{y})_{sh} = \frac{2\rho_o U^2 \overline{u^2}}{\pi c_o^6(4\pi r)^2} L_o^{(IV)} Re \left\{ \mathcal{G}_{11}[\mathcal{G}_{11}^{(1)}]^* + \mathcal{G}_{13}[\mathcal{G}_{13}^{(1)}]^* \right\} \quad (103)$$

where $\mathcal{G}_{ij}^{(m)} = \mathcal{G}_{ji}^{(m)}$ for $m = 1, 2$ and

$$\left. \begin{aligned} \mathcal{G}^{(2)} &= M_- D^{(2)} e^{-ik_o y_1} + {}^{(2)}S_1^{(0)} \\ \mathcal{G}_{11}^{(m)} &= -k_o^2 M_- D^{(m)} e^{-ik_o y_1} + {}^{(m)}S_1^{(2)} \quad \text{for } m = 1, 2 \\ \mathcal{G}_{12}^{(2)} &= {}^{(2)}S_2^{(1)} \\ \mathcal{G}_{13}^{(m)} &= -ik \cos \theta \left[-ik_o M_- D^{(m)} e^{-ik_o y_1} + {}^{(m)}S_1^{(1)} \right] \quad \text{for } m = 1, 2 \\ \mathcal{G}_{22}^{(2)} &= \tan^2 \theta {}^{(2)}\mathcal{G}_{33} - {}^{(2)}\mathcal{G}_{11} \\ \mathcal{G}_{23}^{(2)} &= -ik \cos \theta {}^{(2)}S_2^{(0)} \\ \mathcal{G}_{33}^{(2)} &= -k^2 \cos^2 \theta \mathcal{G}^{(2)} \end{aligned} \right\} \quad (104)$$

$$\left. \begin{aligned} {}^{(m)}S_1^{(j)} &= \frac{1}{i} \sum_{n=1}^{\infty} (-i\beta_n)^j J_n A_n^{(m)} \cos \frac{y_2}{b_n} - \sum_{n=1}^{\infty} \left[-i\beta_{n-(1/2)} \right]^j I_n A_{n-(1/2)}^{(m)} \sin \frac{y_2}{b_{n-(1/2)}} \quad \text{where } \begin{cases} j = 1, 2 & \text{for } m = 1 \\ j = 0, 1, 2 & \text{for } m = 2 \end{cases} \\ {}^{(2)}S_2^{(j)} &= \frac{1}{i} \sum_{n=1}^{\infty} \frac{(-i\beta_n)^j}{b_n} J_n A_n^{(2)} \sin \frac{y_2}{b_n} - \sum_{n=1}^{\infty} \frac{[-i\beta_{n-(1/2)}]^j}{b_{n-(1/2)}} I_n A_{n-(1/2)}^{(2)} \cos \frac{y_2}{b_{n-(1/2)}} \quad \text{for } j = 0, 1 \end{aligned} \right\} \quad (105)$$

$$\left. \begin{aligned} D^{(m)} &= \frac{\pi}{2k_f^{(m)}(1 - M_c \sin \theta)^4 k^4} \left(\operatorname{sech} \left\{ \frac{\pi}{2k_f^{(m)}} \left[k(1 - M_c \sin \theta) + k_*^{(m)} \right] \right\} + \operatorname{sech} \left\{ \frac{\pi}{2k_f^{(m)}} \left[k(1 - M_c \sin \theta) - k_*^{(m)} \right] \right\} \right) \quad \text{for } m = 1, 2 \\ A_v^{(m)} &= \frac{\pi}{2k_f^{(m)}(k - M_c \beta_v)^4} \left(\operatorname{sech} \left\{ \frac{\pi}{2k_f^{(m)}} \left[k - M_c \beta_v + k_*^{(m)} \right] \right\} + \operatorname{sech} \left\{ \frac{\pi}{2k_f^{(m)}} \left[k - M_c \beta_v - k_*^{(m)} \right] \right\} \right) \quad \text{for } m = 1, 2 \end{aligned} \right\} \quad (106)$$

and

$$v = \begin{cases} n & \text{for } n = 1, 2, 3, \dots \\ n - \frac{1}{2} & \end{cases}$$

Here we have put

$$k_f^{(m)} \equiv \frac{\omega_f^{(m)}}{c_o}$$

$$k_*^{(m)} \equiv \frac{\omega_*^{(m)}}{c_o}$$

and

$$M_c \equiv \frac{U_c}{c_o} \quad (107)$$

is the convection Mach number of the eddy.

The spectral density of the intensity of the self and shear noise can now be computed by substituting equations (89), (90), (95) to (100), and (104) to (106) into equations (102) and (103).

The expressions for $I_\omega(\vec{x}|\vec{y})_{se}$ and $I_\omega(\vec{x}|\vec{y})_{sh}$ become particularly simple when

$\psi = 0$ (i.e., in the plane of the duct). Thus, it follows from equation (97) that $I_n = J_n = 0$. Equations (95), (96), (100), and (105), therefore, show that all the $S_v^{(j)}$ and $^{(m)}S_k^{(j)}$ are equal to zero and $M_- = 1$. It can now be seen from equations (77), (99) and (102) to (104) that

$$I_\omega(\vec{x}|\vec{y})_{se} = \frac{\rho_o \left(\overline{u^2}\right)^2 L_o^{(IV)} k^4 D^{(2)}}{\pi c_o^6 (4\pi r)^2} \quad \text{at } \psi = 0 \quad (108)$$

and

$$I_\omega(\vec{x}|\vec{y})_{sh} = \frac{2\rho_o U^2 \overline{u^2} \rho_o^{(IV)}}{\pi c_o^6 (4\pi r)^2} k^4 D^{(1)} \sin^2 \theta \quad \text{at } \psi = 0 \quad (109)$$

DISCUSSION

Emission of Sound From Monopole Source of Unit Strength

Before considering the sound emission from a region of turbulence within the duct, it is useful to consider the sound emission from a monopole source placed in various locations within the channel. It is shown in reference 15 (ch. 7) that the intensity of sound in the far field from a harmonic monopole source of unit strength can be expressed in terms of the far-field Green's function G by

$$I_{mon} = \frac{k^2 \rho_o c_o |G|^2}{2\pi}$$

For the two-dimensional channel shown in figure 4, the far-field Green's function is given by equations (95), (89), (90), (96), and (97). It can be seen from these equations that $|G|$ depends on θ and k only in the combination

$$k_o = k \sin \theta$$

Hence, the number of curves necessary for presenting the results can be minimized by plotting

$$\frac{b^2 \sin^2 \theta I_{\text{mon}}}{\rho_0 c_0} = (k_0 b)^2 |G|^2$$

as a function of ψ for various values of the wavelength parameter

$$\frac{\lambda}{b \sin \theta} = \frac{2\pi}{kb \sin \theta}$$

and various values of the source location y_1/b and y_2/b . The geometrical relation of the angles θ and ψ to the duct walls is illustrated in figure 5. Holding θ and r fixed and varying ψ corresponds to traversing the circle C in the observation plane p parallel to the $y_1 y_2$ -plane. When $\theta = \pi/2$, the plane p is the $y_1 y_2$ -plane.

The directivity patterns are shown in figures 6 to 8. These figures are polar plots of $(4\pi r b)^2 \sin^2 \theta I_{\text{mon}} / \rho c_0$ as a function of the angle ψ for various positions of the source within the duct. In order to keep the scales of these figures reasonable, the figures are divided into three groups. The first group, figures 6(a) to (g), presents the curves for wavelength parameters of 8, 6, and 4. The second group, figures 7(a) to (m), corresponds to wavelength parameters of 2, 3/2, and 1. And the third set of curves, figures 8(a) to (h), are for wavelength parameters of 3/4 and 1/2. The reason that the intensities at $\psi = \pi$ and $\psi = -\pi$ are not equal is that the duct walls extend to minus infinity and thereby separate these points.

It can be seen from figure 6 that for the long wavelengths the patterns are fairly symmetrical, with the sound being radiated fairly uniformly in all directions. The patterns become more uniform as the wavelength increases. However, it can be seen from equation (95) that only the first term makes any contribution to the far-field Green's function G for very long wavelengths because the infinite sum $S_1^{(0)}$ becomes very small. But this term is the solution for the far-field radiation pattern of a plane wave traveling down the duct from $y_1 = -\infty$ (ref. 14). Notice also that this term is independent of the vertical location y_2 of the source within the channel, and the intensity I_{mon} is independent of the coordinate y_1 . Hence, the far-field radiation pattern is independent of the source location within the duct for long wavelengths.

The terms in the infinite sum $S_1^{(0)}$ represent different modes which can propagate within the duct. The first sum in equation (96) represents symmetric modes, and the second sum represents antisymmetric modes. As λ decreases (i.e., k_0 increases), the exponentials which enter these terms through equation (97) change from real to complex (by means of β_v) for successively higher order terms in the sums. This corresponds to successively higher order modes propagating within the duct. Thus, as the wavelength becomes shorter, more modes can propagate and, as shown in the figures,

the radiation pattern becomes more nonuniform. As each new mode comes into play, the pattern changes markedly.

It can be seen from figure 6, that the first mode in the sum $S_1^{(0)}$ becomes significant when $\lambda/(b \sin \theta) \approx 4$ if the source is off axis ($y_2 \neq 0$). However, if the source is on axis, it does not become significant until $\lambda/(b \sin \theta)$ has decreased approximately to 2. This is caused by the fact that only the symmetrical modes can propagate when the source is on axis and these modes switch on at shorter wavelengths than the antisymmetrical modes. This effect also causes the radiation pattern to be more complex when the source is off axis ($y_2 \neq 0$). Thus, as shown in figures 7 and 8, large lobes develop as the source is moved from the axis towards the wall. It can be seen that as the wavelength becomes shorter, the pattern becomes more complicated. However, the basic outlines of these patterns tend to follow the line of sight from the source as the geometric acoustics limit ($\lambda \ll b$) is approached. Actually, the wavelengths considered here are too long to evidence strong geometric acoustics effects.

Emission of Sound From a Unit Volume of Turbulence Located at a Point Within the Duct and Proposed Experiment

In the preceding subsection the emission from a monopole source within a duct was discussed. In this section we shall discuss the results for the sound emission for convected locally isotropic turbulence within the rectangular duct. This configuration was chosen because of its resemblance to the augmentor wing ejector flap shown in figure 1. However, it must be emphasized that the results given in this subsection do not by any means represent the total noise emitted from an augmentor wing. They give only the sound emitted from a unit volume of turbulence located in the mixing region within the augmentor ejector. In order to find the complete noise pattern, it is necessary to integrate these results over the entire interior of the flap. In addition to this, there are other possible noise sources which can contribute to the noise pattern.

However, it is possible to propose an experiment which corresponds closely to the present analysis. This experiment consists of placing a small intense jet at various locations within a large wide duct and measuring the narrow-band intensity spectra in the far field. Although it is anticipated that the lobes of the observed directivity patterns will not be nearly as sharp as those predicted by the present analysis (due to the fact that the source is not localized and that the microphones do not measure a narrow enough frequency range), it is still felt that reasonable agreement should be obtained.

Discussion of equations. - It has been shown that the spectral density of the intensity of the sound in the far field emitted from a point \bar{y} within the duct can be ex-

pressed as the sum of two terms. The first of these, $I_{\omega}(\vec{x}|\vec{y})_{se}$, is called the self noise and represents the noise emitted by the action of the turbulent eddies with themselves. This term is given by equation (102). It is proportional to the sum of the intensities of all six independent quadrupoles corrected for convection effects by the mean flow. (Notice that the first term is really a simple source, but it is by virtue of equation (99) proportional to the longitudinal quadrupole with axis in the y_3 -direction.) As in the case of jet noise, this term is also proportional to the fourth-order two-point turbulence velocity correlations which are accounted for by the factor $L_o^{(IV)}$.

The second term contributing to the far-field intensity is the shear noise $I_{\omega}(\vec{x}|\vec{y})_{sh}$, which represents the sound due to the action of the turbulence on the mean shear. It is given by equation (103). It can be seen that it is proportional to the two longitudinal quadrupoles suitably modified by convection effects in the directions perpendicular to the velocity gradient (y_1 and y_3 directions). This term is also proportional to the second-order two-point turbulence velocity correlations, as well as the mean-square velocity. The turbulence velocity correlations are accounted for by the term $L_o^{(IV)}$.

In the plane $\theta = \pi/2$ (shown in fig. 5), a number of the quadrupoles make no contribution to either the shear or self noise. The reason is the $\cos \theta$ dependence of these quadrupoles, as shown in equations (99) and (104). Thus, the shear noise is simply proportional to the longitudinal y_1 -direction quadrupole. An inspection of the equations for $\theta = \pi/2$ shows that this quadrupole also tends to dominate the self noise at low frequencies.

It is also of interest to have expressions for the intensities in the y_1y_3 -plane, which is perpendicular to $\theta = \pi/2$ -plane, as shown in figure 9. This corresponds to setting ψ equal to 0 and letting θ vary. The expressions for $I_{\omega}(\vec{x}|\vec{y})_{se}$ and $I_{\omega}(\vec{x}|\vec{y})_{sh}$ for the case where $\psi = 0$ are given by equations (108) and (109), respectively. These equations take on particularly simple forms. The directivity behavior of the self noise is strictly through the term $D^{(2)}$, whereas the directivity of the shear noise is through the terms $D^{(1)}\sin^2\theta$. The terms $D^{(1)}$ and $D^{(2)}$ are given by the first of equations (106). They contain the same convective amplification factor $(1 - M_c \sin \theta)^{-4}$ that appears in jet noise (ref. 7). In fact, the angular dependence of the terms $D^{(1)}$ and $D^{(2)}$ is caused strictly by the convection of the sound source. The results can also be shown to be consistent with those obtained by Ffowcs Williams in reference 3.

Organization of plots and choice of parameters. - The shear- and self-noise terms

$$\frac{I_{\omega}(\vec{x}|\vec{y})_{se} 8\pi c_o^6 (4\pi r)^2}{7\rho_o \left(\overline{u^2}\right)^2 L_o^{(IV)}}$$

and

$$\frac{I_{\omega}(\vec{x}|\vec{y})_{\text{sh}} \pi c_0^6 (4\pi r)^2}{2\rho_0 U^2 \bar{u}^2 \rho_0^{(IV)}}$$

are plotted as a function of the azimuthal angle ψ for $\theta = \pi/2$ in figures 10 to 16 and for $\theta = \pi/4$ in figure 17. They are plotted as a function of θ for $\psi = 0$ in figures 18 to 22. These variations correspond to varying the observation point in the far field in the three planes shown in figures 5 and 9. These directivity patterns are influenced by the wave numbers of the turbulence which emits the sound. In the present model the turbulence spectra are characterized by the parameters $k_f^{(m)}$ and $k_*^{(m)}$ for $m = 1$ or 2 (compare eq. (101) where the corresponding frequencies are defined). For the self-noise m equals 2 , whereas for the shear noise m equals 1 .

In reference 11, it is found that the turbulence data for round jets were best fitted by taking

$$b_0 k_f^{(1)} \approx M_*$$

$$b_0 k_f^{(2)} \approx 2.3 M_*$$

$$b_0 k_*^{(1)} \approx 2 M_*$$

$$b_0 k_*^{(2)} \approx 5.4 M_*$$

where M_* is the jet-exit Mach number and b_0 is the jet radius. For lack of better information, these relations will also be used in the present case. We shall suppose that M_* is the exit Mach number of the flow into the duct. For example, for the augmentor wing shown in figure 1, M_* might correspond to the velocity of the jet entering the augmentor flap at point 1. Again, as in a jet, we shall relate the eddy convection Mach number to M_* by assuming that

$$|M_c| \approx \frac{1}{2} M_*$$

Figures 1 and 4 show that it is appropriate to take M_c as positive for modeling the sound coming from the rear of the augmentor wing exit, whereas it is appropriate to take M_c as negative for modeling the sound coming from the opening in the front of the flap (entrance). Therefore, results for both these cases are presented. For the sound from the front of the flap, it would seem appropriate to choose b_o equal to the width of the passage at point 1, which is approximately $1/4 b$. For the sound coming from the rear of the flap, a value closer to b would seem appropriate. Therefore, results are presented for both the cases $b_o/b = 1/4$ and $b_o/b = 1$.

Discussion of results. - Results are presented for the $\theta = \pi/2$, $\theta = \pi/4$, and $\psi = 0$ planes.

$\theta = \pi/2$ plane: Figures 10 to 16 are plots of the far-field self and shear noise in the $\theta = \pi/2$ plane. The first two parts of these figures are polar plots of the self noise in two different frequency ranges, and the last two are polar plots of the shear noise for two different frequency ranges. Comparing the first and last parts of these figures shows that the shear noise is always elongated in the direction of the duct axis (y_1 -direction), whereas the self noise tends to radiate uniformly or laterally. This downstream beaming of the shear noise is caused by the fact that, in the $\theta = \pi/2$ plane, only the longitudinal quadrupole in the y_1 -direction makes any contributions, whereas the self noise is composed of this plus a number of other longitudinal and lateral quadrupoles. These figures also show that at any given frequency, the shear-noise curves have much fewer lobes than the self-noise curves. This can also be attributed to the longitudinal quadrupole nature of the shear noise since the high directivity of this quadrupole in the downstream direction allows it to be beamed out of the duct without interacting with the walls. There is, therefore, much less interference due to reflections and diffraction by the duct than in the more uniformly directed self noise.

Figures 10 and 11 are identical except that the direction of the convection velocities M_c is reversed. The self-noise curves with M_c in the positive direction have much weaker lobes than those with M_c in the negative direction. The reason for this is that the convective effects tend to beam the self noise in the direction of motion. Thus, when M_c is in the positive direction, the sound is beamed out of the duct. This beamed pattern will then interact to a lesser extent with the channel walls than when M_c is negative. However, the already highly directional shear-noise patterns show no significant additional beaming due to convection, and their directivity patterns are therefore quite similar. Figures 12 and 13 show the effect of decreasing the Mach number M_* from 0.8 to 0.3 (with a corresponding decrease in M_c). Comparing figure 12 with figure 10 shows that increasing the magnitude of the convection velocity in the negative direction causes a marked decrease in intensity with no significant change in the shape of the directivity patterns. Comparing figure 13 with figure 11 shows that increasing the convection velocity in the positive direction causes a slight decrease in intensity with no

significant change in the shape of the directivity patterns.

Most of the curves are drawn for the case where $b_o/b = 1/4$. Figure 14 shows the effect of putting $b_o/b = 1$. A comparison of figures 11 and 14 shows that the curves for $b_o/b = 1$ exhibit less interference effects than those for $b_o/b = 1/4$.

Figure 15 shows the effect of moving the turbulent source region away from the center of the duct toward the upper wall ($y_2 > 0$). Comparing this figure with figure 10 shows that this has little more effect on the shear noise than beaming it in a downward direction. However, the self noise exhibits a complex change in the interference effects as the source is moved toward the wall. This is probably related to the fact that the antisymmetric mode can propagate within the duct when the source is off center.

Figure 16 shows the effect of moving the turbulent source point farther into the duct. Comparing figures 10 and 16 shows that (for both self and shear noise) this causes very little change in either the directivity pattern or the magnitude of the intensity.

$\theta = \pi/4$ plane: Figure 17 is a plot of the far-field intensities for the $\theta = \pi/4$ plane. This plane is (as shown in fig. 5) parallel to the $\theta = \pi/2$ plane but shifted over from the centerline of the duct. Upon comparing figures 10 and 17, we see that the shear-noise curves on these two planes are similar. However, the figures show that the self-noise intensity patterns exhibit weaker interference effects in the $\theta = \pi/4$ plane than in the $\theta = \pi/2$ plane.

$\psi = 0$ plane: Figures 18 to 22 are plots of the far-field, self and shear noise in the $\psi = 0$ plane, which corresponds to the y_1y_3 -plane shown in figure 9. These plots are arranged in the same way as those for the $\theta = \pi/2$ plane. Thus, the first two parts of these figures are polar plots of the self noise in two different frequency ranges, and the last two are polar plots of the shear noise for two different frequency ranges. They also correspond to the same values of M_c and M_* as those for the $\theta = \pi/2$ planes. These figures are essentially plots of equations (108) and (109). It can be seen from these equations that the far-field intensities are independent of the source location within the duct. Hence, unlike the previous cases, these coordinates no longer appear as parameters in the plots. In addition, the quadrupoles in this plane take on a simple form and, hence, cannot exhibit the interference effects which occurred in all other planes. Thus, the curves in figures 18 to 22 are much smoother than those in the previous figures.

These figures also show that the self noise is more intense in the y_1 -direction (i.e., the direction along the duct axis) than in the direction perpendicular to this when the convective Mach number M_c is positive, and that it is less intense along the y_1 -direction than in the perpendicular direction when M_c is negative. The first two parts of figures 19 and 21 show that this elongation is much more pronounced at high convective Mach numbers than at low Mach numbers. This is essentially the downstream beaming effect caused by convective amplification, which occurs in jets. In fact, the order of magnitude of the effect is about the same in the present case as it is for jets (ref. 8). On the other hand, figures 10 to 16 show that the shapes of the directivity patterns in the

$\theta = \pi/2$ plane are much more dominated by diffraction effects than by convection. Thus, the far-field intensity pattern behaves in much the same way as for jet noise in the plane of the duct and behaves in a much different fashion in the plane perpendicular to the duct.

The variation of the intensity with frequency in the $\psi = 0$ plane is much the same as in the $\theta = \pi/2$ plane. This is not surprising since the points at $\theta = \pi/2$ in figures 18 and 21 correspond to the points with $\psi = 0$ (from the same values of M_c , M_* , and frequency) in the figures for the $\theta = \pi/2$ plane. As in the case of jet noise, the results for $\theta = 0$ are independent of M_c (ref. 8).

SUMMARY OF RESULTS

A theoretical description has been given of the sound emitted from a nearly parallel turbulent shear flow confined to a region near solid boundaries. The analysis leads to formulas which can be used to calculate the directivity of the spectra of the sound emitted from a unit volume of turbulence located at an arbitrary point within the flow. In order to use these results to calculate the sound emitted from any finite region of turbulence, it is necessary to integrate the formulas over the region of turbulence. This requires a knowledge of certain turbulence-correlation-length scales at each point within the flow.

The results are applied to obtain the sound emitted from a unit volume of turbulence located at an arbitrary point in a turbulent flow confined to the interior of an open-ended semi-infinite duct. Numerical results for the spectral density of the far-field intensity of the self and shear noise are obtained for this case. It is shown that the directivity patterns in the plane of the duct are much the same as for jet noise; whereas those in the plane perpendicular to this are considerably different, being dominated more by diffraction effects than by convection effects. This is especially true at the higher frequencies. The shear noise in the plane perpendicular to the duct is dominated by the longitudinal quadrupole with its axis along the duct.

Lewis Research Center,
National Aeronautics and Space Administration,
Cleveland, Ohio, August 11, 1972,
501-04.

APPENDIX A

REDUCTION OF SELF-NOISE CORRELATION INTEGRALS FOR AXISYMMETRIC TURBULENCE

It follows from equation (41) that

$$\begin{aligned}
 \int \tilde{R}_{ik} \tilde{R}_{jl} d\vec{\xi} = \int & \left[A^2 \xi_i \xi_j \xi_k \xi_l + AB(\delta_{ik} \xi_j \xi_l + \delta_{jl} \xi_i \xi_k) + AC(\delta_{1j} \delta_{1l} \xi_i \xi_k + \delta_{1i} \delta_{1k} \xi_j \xi_l) \right. \\
 & + AD(\delta_{1j} \xi_i \xi_k \xi_l + \delta_{1l} \xi_i \xi_k \xi_j + \delta_{1i} \xi_j \xi_k \xi_l + \delta_{1k} \xi_i \xi_j \xi_l) + D^2(\delta_{1i} \delta_{1j} \xi_k \xi_l \\
 & + \delta_{1k} \delta_{1l} \xi_i \xi_j + \delta_{1i} \delta_{1l} \xi_k \xi_j + \delta_{1k} \delta_{1j} \xi_i \xi_l) + B^2 \delta_{ik} \delta_{jl} + BC(\delta_{ik} \delta_{1j} \delta_{1l} \\
 & + \delta_{jl} \delta_{1i} \delta_{1k}) + BD(\delta_{ik} \delta_{1j} \xi_l + \delta_{ik} \delta_{1l} \xi_j + \delta_{jl} \delta_{1i} \xi_k + \delta_{jl} \delta_{1k} \xi_i) \\
 & + C^2 \delta_{1i} \delta_{1j} \delta_{1k} \delta_{1l} + CD(\delta_{1i} \delta_{1k} \delta_{1j} \xi_l + \delta_{1i} \delta_{1l} \delta_{1k} \xi_j + \delta_{1i} \delta_{1j} \delta_{1l} \xi_k \\
 & \left. + \delta_{1j} \delta_{1k} \delta_{1l} \xi_i) \right] d\vec{\xi} \tag{A1}
 \end{aligned}$$

It can be seen by inspection of this equation that a suitable choice for the coefficient a_{ik} in equation (42) is

$$a_{ik} = \int A^2 \xi_i^2 \xi_k^2 d\vec{\xi} + \int (2AD\xi_1 + D^2) (\delta_{1i} \xi_k^2 + \delta_{1k} \xi_i^2) d\vec{\xi} \tag{A2}$$

It follows from this equation that

$$a_{ik} = a_{ki} \tag{A3}$$

$$a_{13} = a_{12} \tag{A4}$$

But upon using equations (A3) and (A4) we get

$$\begin{aligned}
G_{ii}G_{kk}^T a_{ik} &= a_{11}G_{11}G_{11}^T + a_{22}G_{22}G_{22}^T + a_{33}G_{33}G_{33}^T + a_{12}(G_{11}G_{22}^T + G_{22}G_{11}^T + G_{11}G_{33}^T + G_{33}G_{11}^T) + a_{23}(G_{22}G_{33}^T + G_{33}G_{22}^T) \\
&= a_{11}G_{11}G_{11}^T + a_{22}G_{22}G_{22}^T + a_{33}G_{33}G_{33}^T + a_{12}(G_{11}G_{22}^T + G_{22}G_{11}^T + G_{11}G_{33}^T + G_{33}G_{11}^T + G_{22}G_{33}^T + G_{33}G_{22}^T) + (a_{23} - a_{12})(G_{22}G_{33}^T + G_{33}G_{22}^T) \\
&= a_{11}G_{11}G_{11}^T + a_{22}G_{22}G_{22}^T + a_{33}G_{33}G_{33}^T + a_{12}(G_{ii}G_{jj}^T - G_{11}G_{11}^T - G_{22}G_{22}^T - G_{33}G_{33}^T) + (a_{23} - a_{12})(G_{22}G_{33}^T + G_{33}G_{22}^T) \\
&= (a_{11} - a_{12})G_{11}G_{11}^T + (a_{22} - a_{12})G_{22}G_{22}^T + (a_{33} - a_{12})G_{33}G_{33}^T + a_{12}G_{ii}G_{jj}^T + (a_{23} - a_{12})(G_{22}G_{33}^T + G_{33}G_{22}^T)
\end{aligned} \tag{A5}$$

By using equations (43) and (A5) and the remarks following equation (44), it can now be seen by inspection of equation (A1) that

$$\begin{aligned}
G_{ij}G_{kl}^T \int \tilde{R}_{ik}\tilde{R}_{jl} d\bar{\xi} &= a_{12}G_{ii}G_{jj}^T + (a_{23} - a_{12})(G_{22}G_{33}^T + G_{33}G_{22}^T) \\
&+ G_{11}G_{11}^T \left[a_{11} - a_{12} + \int (2AB\xi_1^2 + 2AC\xi_1^2 + 2D^2\xi_1^2 + B^2 + 2BC + 4BD\xi_1 + C^2 + 4CD\xi_1) d\bar{\xi} \right] \\
&+ G_{12}G_{12}^T \int (4A^2\xi_1^2\xi_2^2 + 2AB\xi_2^2 + 2AB\xi_1^2 + 2AC\xi_2^2 + 2D^2\xi_2^2 + 8AD\xi_1\xi_2^2 + 2B^2 + 2BC + 4BD\xi_1) d\bar{\xi} \\
&+ G_{13}G_{13}^T \int (4A^2\xi_1^2\xi_3^2 + 2AB\xi_3^2 + 2AB\xi_1^2 + 2AC\xi_3^2 + 2D^2\xi_3^2 + 8AD\xi_1\xi_3^2 + 2B^2 + 2BC + 4BD\xi_1) d\bar{\xi} \\
&+ G_{22}G_{22}^T \left[a_{22} - a_{12} + \int (2AB\xi_2^2 + B^2) d\bar{\xi} \right] + G_{33}G_{33}^T \left[a_{33} - a_{12} + \int (2AB\xi_3^2 + B^2) d\bar{\xi} \right] \\
&+ G_{23}G_{23}^T \int (4A^2\xi_2^2\xi_3^2 + 2AB\xi_2^2 + 2AB\xi_3^2 + 2B^2) d\bar{\xi}
\end{aligned}$$

By carrying out the integrations in polar coordinates, it can be verified that the coefficients of $G_{12}G_{12}^T$ and $G_{13}G_{13}^T$ are equal and that the coefficients of $G_{22}G_{22}^T$ and $G_{33}G_{33}^T$ are equal (see eq. (A2) and recall that $\int_0^{2\pi} \cos^2\psi d\psi = \int_0^{2\pi} \sin^2\psi d\psi$).

Hence, it follows from equation (A2) that

$$\begin{aligned}
G_{ij}G_{kl}^T \int \tilde{R}_{ik}\tilde{R}_{jl} \, d\tilde{\xi} &= a_{12}G_{ii}G_{jj}^T + (a_{23} - a_{12})(G_{22}G_{33}^T + G_{33}G_{22}^T) \\
&+ G_{11}G_{11}^T \left[\int (A^2\xi_1^4 + 4AD\xi_1^3 + 4D^2\xi_1^2 + 2AB\xi_1^2 + 2AC\xi_1^2 + B^2 + 2BC + 4BD\xi_1 + C^2 + 4CD\xi_1) \, d\tilde{\xi} - a_{12} \right] \\
&+ (G_{12}G_{12}^T + G_{13}G_{13}^T) \int (4A^2\xi_1^2\xi_2^2 + 2AB\xi_2^2 + 2AB\xi_1^2 + 2AC\xi_2^2 + 2D^2\xi_2^2 + 8AD\xi_1\xi_2^2 + 2B^2 + 2BC + 4BD\xi_1) \, d\tilde{\xi} \\
&+ (G_{22}G_{22}^T + G_{33}G_{33}^T) \left[\int (A^2\xi_2^4 + 2AB\xi_2^2 + B^2) \, d\tilde{\xi} - a_{12} \right] \\
&+ G_{23}G_{23}^T \int (4A^2\xi_2^2\xi_3^2 + 2AB\xi_2^2 + 2AB\xi_3^2 + 2B^2) \, d\tilde{\xi}
\end{aligned} \tag{A6}$$

Now it follows from equation (40) that

$$\tilde{R}_{11}^2 = A^2\xi_1^4 + 2AB\xi_1^2 + 2AC\xi_1^2 + 4AD\xi_1^3 + B^2 + 2BC + 4BD\xi_1 + C^2 + 4CD\xi_1 + 4D^2\xi_1^2$$

$$\tilde{R}_{12}^2 = A^2\xi_1^2\xi_2^2 + 2AD\xi_1\xi_2^2 + D^2\xi_2^2$$

$$\begin{aligned}
2(\tilde{R}_{12}^2 + \tilde{R}_{11}\tilde{R}_{22}) &= 4A^2\xi_1^2\xi_2^2 + 8AD\xi_1\xi_2^2 + 2D^2\xi_2^2 + 2AB\xi_2^2 \\
&+ 2AC\xi_2^2 + 2AB\xi_1^2 + 2B^2 + 2BC + 4BD\xi_1
\end{aligned}$$

$$\tilde{R}_{22}^2 = A^2\xi_2^4 + 2AB\xi_2^2 + B^2$$

$$\tilde{R}_{23}^2 = A^2\xi_2^2\xi_3^2$$

Hence, it follows from these relations and equation (A2) that equation (A6) can be written as

$$\begin{aligned}
G_{ij}G_{kl}^T \int \tilde{R}_{ik}\tilde{R}_{jl} d\tilde{\xi} &= G_{ii}G_{jj}^T \int \tilde{R}_{12}^2 d\tilde{\xi} + \left(G_{22}G_{33}^T + G_{33}G_{22}^T\right) \int \left(\tilde{R}_{23}^2 - \tilde{R}_{12}^2\right) d\tilde{\xi} \\
&+ G_{11}G_{11}^T \int \left(\tilde{R}_{11}^2 - \tilde{R}_{12}^2\right) d\tilde{\xi} + 2\left(G_{12}G_{12}^T + G_{13}G_{13}^T\right) \int \left(\tilde{R}_{12}^2 + \tilde{R}_{11}\tilde{R}_{22}\right) d\tilde{\xi} \\
&+ \left(G_{22}G_{22}^T + G_{33}G_{33}^T\right) \int \left(\tilde{R}_{22}^2 - \tilde{R}_{12}^2\right) d\tilde{\xi} + 2G_{23}G_{23}^T \int \left(\tilde{R}_{22}^2 - \tilde{R}_{23}^2\right) d\tilde{\xi}
\end{aligned}$$

The particular form of the last integral has been obtained by introducing polar coordinates and carrying out the integration over the angle variable.

APPENDIX B

REDUCTION OF SHEAR-NOISE CORRELATION INTEGRALS FOR AXISYMMETRIC TURBULENCE

It follows from interchanging names of dummy indices in equation (49) that

$$\begin{aligned}
 G_{1j}G_{1l}^T \int U'U''\tilde{R}_{jl} d\vec{\xi} &= G_{1j}G_{1l}^T \int U'U''A\xi_j\xi_l d\vec{\xi} + G_{1i}G_{1i}^T \int U'U''B d\vec{\xi} \\
 &+ (G_{1j}G_{11}^T + G_{11}G_{1j}^T) \int U'U''D\xi_j d\vec{\xi} + G_{11}G_{11}^T \int U'U''C d\vec{\xi}
 \end{aligned} \tag{B1}$$

Upon noting that A is an even function of ξ_i for $i = 1, 2, 3$; that U' and U'' are functions only of ξ_2 ; and that any integral of an odd function of ξ_i for $i = 1, 2, 3$ is zero, we find that

$$G_{1j}G_{1l}^T \int U'U''A\xi_j\xi_l d\vec{\xi} = G_{1j}G_{1j}^T \int U'U''A\xi_j^2 d\vec{\xi}$$

And since D is an even function of ξ_2 and ξ_3 and an odd function of ξ_1

$$(G_{1j}G_{11}^T + G_{11}G_{1j}^T) \int U'U''D\xi_j d\vec{\xi} = 2G_{11}G_{11}^T \int U'U''D\xi_1 d\vec{\xi}$$

Hence, equation (B1) becomes

$$\begin{aligned}
 G_{1j}G_{1l}^T \int U'U''\tilde{R}_{jl} d\vec{\xi} &= G_{11}G_{11}^T \int U'U''(A\xi_1^2 + B + C + 2D\xi_1) d\vec{\xi} \\
 &+ G_{12}G_{12}^T \int U'U''(A\xi_2^2 + B) d\vec{\xi} + G_{13}G_{13}^T \int U'U''(A\xi_3^2 + B) d\vec{\xi}
 \end{aligned}$$

We can therefore write from equation (40) that

$$G_{1j} G_{1l}^T \int U' U'' \tilde{R}_{jl} \, d\bar{\xi} = G_{1j} G_{1j}^T \int U' U'' \tilde{R}_{jj} \, d\bar{\xi}$$

APPENDIX C

REDUCTION OF SELF-NOISE CORRELATION INTEGRALS FOR ISOTROPIC TURBULENCE

It is shown in reference 4 that the requirements of continuity dictate that

$$4A + \xi \frac{\partial A}{\partial \xi} + \frac{1}{\xi} \frac{\partial B}{\partial \xi} = 0$$

where $\xi = |\vec{\xi}|$ and that this in turn implies that (see ref. 10) there exists a function F such that

$$A = - \frac{1}{2\xi} \frac{\partial F}{\partial \xi} \tag{C1}$$

$$B = F + \frac{1}{2} \xi \frac{\partial F}{\partial \xi}$$

Substituting these results into equation (55) shows that

$$\begin{aligned} \int \tilde{R}_{ik} \tilde{R}_{jl} d\vec{\xi} &= \int \left[\left(F + \frac{1}{2} \xi F' \right) \delta_{ik} - \frac{1}{2} \frac{\xi_i \xi_k}{\xi} F' \right] \left[\left(F + \frac{1}{2} \xi F' \right) \delta_{jl} - \frac{1}{2} \frac{\xi_j \xi_l}{\xi} F' \right] d\vec{\xi} \\ &= \delta_{ik} \delta_{jl} \int \left(F + \frac{1}{2} \xi F' \right)^2 d\vec{\xi} - \frac{1}{2} \int \left(F + \frac{1}{2} \xi F' \right) F' \left(\frac{\xi_i \xi_k}{\xi} \delta_{jl} + \frac{\xi_j \xi_l}{\xi} \delta_{ik} \right) d\vec{\xi} \\ &\quad + \frac{1}{4} \int F'^2 \frac{\xi_i \xi_j \xi_k \xi_l}{\xi^2} d\vec{\xi} \end{aligned}$$

where we have put

$$F' \equiv \frac{\partial F}{\partial \xi}$$

Upon introducing spherical coordinates and carrying out the integrations over the angle variables, this becomes

$$\begin{aligned} \int \tilde{R}_{ik} \tilde{R}_{jl} d\vec{\xi} &= 4\pi \delta_{ik} \delta_{jl} \int_0^\infty \xi^2 \left(F + \frac{1}{2} \xi F' \right) \left(F + \frac{1}{6} \xi F' \right) d\xi \\ &\quad + \frac{\pi}{15} (\delta_{ij} \delta_{kl} + \delta_{ik} \delta_{jl} + \delta_{il} \delta_{kj}) \int_0^\infty \xi^2 (\xi F')^2 d\xi \end{aligned}$$

But

$$\begin{aligned} \int_0^\infty \xi^2 \left(F + \frac{1}{2} \xi F' \right) \left(F + \frac{1}{6} \xi F' \right) d\xi &= \int_0^\infty \xi^2 \left[F^2 + \frac{2}{3} \xi F F' + \frac{1}{12} (\xi F')^2 \right] d\xi \\ &= \frac{F^2 \xi^3}{3} \Big|_0^\infty + \int_0^\infty \left(\frac{2}{3} \xi F F' - \frac{2}{3} \xi F F' \right) \xi^2 d\xi + \frac{1}{12} \int_0^\infty \xi^2 (\xi F')^2 d\xi \end{aligned} \quad (C2)$$

Now we must require that the integral $\int \tilde{R}_{ij} d\vec{\xi}$ remain finite. Hence, it follows from equations (55) and (C1) that this implies that $\int_0^\infty F \xi^2 d\xi$ remain finite. Hence, F must approach zero faster than ξ^{-3} as $\xi \rightarrow \infty$. This shows that the integrated term in equation (C2) vanishes and we obtain

$$\int \tilde{R}_{ik} \tilde{R}_{jl} d\vec{\xi} = \frac{\pi}{3} \left[\delta_{ik} \delta_{jl} + \frac{1}{5} (\delta_{ij} \delta_{kl} + \delta_{ik} \delta_{jl} + \delta_{il} \delta_{kj}) \right] \int_0^\infty \xi^2 (\xi F')^2 d\xi$$

and since, in particular,

$$\int \tilde{R}_{11}^2 d\vec{\xi} = \frac{8\pi}{15} \int_0^\infty \xi^2 (\xi F')^2 d\xi$$

it follows that

$$\int \tilde{R}_{ik} \tilde{R}_{jl} d\vec{\xi} = \frac{1}{8} \left[6\delta_{ik} \delta_{jl} + \delta_{ij} \delta_{kl} + \delta_{il} \delta_{kj} \right] \int \tilde{R}_{11}^2 d\vec{\xi}$$

It now follows from equations (47) and (48) that

$$Q_{ij} = \frac{7}{8} \int \tilde{R}_{11}^2 d\vec{\xi} \quad \text{for } i, j = 1, 2, 3$$

and

$$S = \frac{1}{8} \int \tilde{R}_{11}^2 d\vec{\xi}$$

APPENDIX D

REDUCTION OF SHEAR-NOISE CORRELATION INTEGRALS FOR ISOTROPIC TURBULENCE

Substituting equation (56) into equation (55) shows that

$$\int U'U''\tilde{R}_{jj} d\vec{\xi} = \int U'U'' \left(F + \frac{1}{2} \xi F' - \frac{1}{2} \frac{\xi_j^2}{\xi} F' \right) d\vec{\xi} \quad (\text{no sum on } j)$$

Upon introducing cylindrical coordinates with the axial direction along the ξ_2 -axis and $\mu^2 = \xi_1^2 + \xi_3^2$, we find that

$$\int U'U''\tilde{R}_{11} d\vec{\xi} = \int U'U''\tilde{R}_{33} d\vec{\xi}$$

and

$$\int U'U''\tilde{R}_{22} d\vec{\xi} = 2\pi \int_{-\infty}^{\infty} U\left(y_2 - \frac{\xi_2}{2}\right) \int_0^{\infty} \left[F + \frac{1}{2} \xi F' \left(1 - \frac{\xi_2^2}{\xi^2} \right) \right] \mu d\mu d\xi_2$$

But since $\xi^2 = \mu^2 + \xi_2^2$

$$\begin{aligned} \int_0^{\infty} \left[F(\xi) + \frac{1}{2} \xi F'(\xi) \left(1 - \frac{\xi_2^2}{\xi^2} \right) \right] \mu d\mu &= \int_{|\xi_2|}^{\infty} \left[F(\xi) + \frac{1}{2} \xi F'(\xi) \left(1 - \frac{\xi_2^2}{\xi^2} \right) \right] \xi d\xi \\ &= \int_{|\xi_2|}^{\infty} F(\xi) \xi d\xi + \frac{1}{2} F(\xi) (\xi^2 - \xi_2^2) \Big|_{|\xi_2|}^{\infty} - \int_{|\xi_2|}^{\infty} F(\xi) \xi d\xi = 0 \end{aligned}$$

where the dependence of \mathbf{F} on τ has been suppressed. Hence,

$$\int \mathbf{U}' \mathbf{U}'' \tilde{\mathbf{R}}_{22} \, d\vec{\xi} = 0$$

APPENDIX E

SYMBOLS

A	coefficient in tensor R_{ij}
$A_v^{(m)}$	defined by eq. (106)
a	constant
a_{ik}	coefficient in eq. (42)
B	coefficient in tensor R_{ij}
b	one-half of distance separating semi-infinite parallel plates
b_{ij}	coefficient first appearing in eq. (42)
b_o	jet radius
b_n	$b/n\pi$, $n = 1, 2, 3, \dots$
$b_{n-(1/2)}$	$\frac{b}{\left(n - \frac{1}{2}\right)\pi}$, $n = 1, 2, 3, \dots$
C	coefficient in tensor R_{ij}
C_o	Euler's constant, 0.5772 . . .
c_{ij}	coefficient in eq. (42)
c_o	speed of sound in medium of density ρ_o and pressure p_o
c_1, c_2, c_3	constants
D	coefficient in tensor \tilde{R}_{ij}
$D^{(m)}$	defined by eq. (106)
D_-	defined by eq. (87)
F	defined by eq. (C1)
$G(\vec{x} \vec{y})$	Green's function at \vec{x} due to point source at \vec{y}
$G_{ij}(\vec{x} \vec{y})$	$\partial^2 G(\vec{x} \vec{y})/\partial y_i \partial y_i$
$G_{ij}(\vec{y})$	$G_{ij}(\vec{x} \vec{y})$, where \vec{x} dependence has been suppressed
$G_{ij}^T(\vec{y})$	$G_{ij}^*(\vec{y} + \vec{U}_c \tau)$
$G_\omega(\vec{x} \vec{y})$	spectral density of Green's function
$G_0(\theta, \psi \vec{y})$	defined by eqs. (72) and (73)

$G_1(\psi y_1, y_2)$	defined by eqs. (75) and (76)
G	defined by eq. (95)
G_{ij}	defined by eq. (98)
$G_{ij}^{(m)}$	defined by eqs. (103) and (104), $m = 1, 2$
$g(\vec{x} \vec{y})$	free-space Green's function
$g_0(\theta, \psi \vec{y})$	wave function for plane wave (eq. (68))
h	typical length associated with distances between boundaries
$I_\omega(\vec{x})$	spectral density of far-field intensity at \vec{x}
$I_\omega(\vec{x} \vec{y})$	spectral density of far-field intensity at \vec{x} due to unit volume of source located at \vec{y}
I_{mon}	far-field intensity from a monopole source of unit strength
I_n	defined by eq. (97)
\hat{i}	unit vector in y_1 -direction
J_n	defined by eq. (97)
$K_\pm(\alpha)$	defined by eq. (89)
$K'_-[\beta_{v-(1/2)}]$	$K_-[\beta_{v-(1/2)}]$ with factor corresponding to $n = v$ omitted
k	wave number
$k_f^{(m)}$	$\omega_f^{(m)}/c_0$
k_o	$k \sin \theta$
$k_*^{(m)}$	$\omega_*^{(m)}/c_0$
L	turbulence correlation length defined by eq. (57)
$L_\pm(\alpha)$	defined by eq. (90)
$L'_-(\beta_v)$	$L_-[\beta_v]$ with factor corresponding to $n = v$ omitted
$L_o^{(IV)}$	fourth time derivative of L evaluated at $\tau = 0$
\mathcal{L}	turbulence correlation length defined by eq. (60)
$\mathcal{L}_o^{(IV)}$	fourth time derivative of \mathcal{L} evaluated at $\tau = 0$
l	typical correlation length associated with turbulent eddies
M_c	convection Mach number of eddy
M_e	Mach number characteristic of turbulence

M_*	jet-exit Mach number
$M_-(\psi)$	defined by eq. (95)
n_i	component of unit normal in i^{th} direction
\hat{n}	unit normal
P	Fourier transform of $p - p_0$
p	pressure
p_{ij}	pressure tensor
p_0	average pressure
Q_{ij}	defined by eq. (47)
R	radius of curvature in direction of flow
$R_{ijkl}^+(\vec{y}, \vec{\xi}, \tau)$	fourth-order moving-axis velocity correlation functions defined in eq. (28)
$R_{ijkl}^c(\vec{y}, \vec{\xi}, \tau)$	
$\tilde{R}_{ij}(\vec{y}, \vec{\xi}, \tau)$	second-order moving-axis velocity correlation function (eq. (34))
$\tilde{R}_{i,jk}$	third-order moving-axis velocity correlation function defined in eq. (35)
$\tilde{R}_{ijkl}(\vec{y}, \vec{\xi}, \tau)$	fourth-order moving-axis velocity correlation function defined by eq. (33)
$\left. \begin{array}{l} R_{ijkl}^{(0)}, R_{ijkl}^{(1)} \\ R_{ijkl}^{(2)}, R_{ijkl}^+ \\ R_{ijkl}^c \end{array} \right\}$	fourth-order velocity correlation functions (eqs. (17) to (20) and eq. (24))
r	distance of observation point from origin
S	defined by eq. (48)
S_-	defined by eq. (88)
$S_1^{(j)}$	defined by eq. (96)
$S_2^{(j)}$	defined by eq. (100)
$^{(m)}S_1^{(j)}$	defined by eq. (105)
$^{(2)}S_2^{(j)}$	defined by eq. (105)
\mathcal{S}	surface
T	a large interval of time
T_{ij}	Fourier transform of τ_{ij}

$T_{\pm}(\alpha)$	function of α appearing in expressions for $K_{\pm}(\alpha)$ and $L_{\pm}(\alpha)$
t	time
$U(y_2)$	mean velocity in y_1 -direction
U'	$U\left(y_2 - \frac{\xi_2}{2}\right) = U\left(y_2 - \frac{\eta_2}{2}\right)$
U''	$U\left(y_2 + \frac{\xi_2}{2}\right) = U\left(y_2 + \frac{\eta_2}{2}\right)$
\bar{U}_c	convection velocity of eddy
u_i	component of turbulent velocity in i^{th} direction
u'_i	$u_i(\vec{y}', t)$
u''_i	$u_i(\vec{y}'', t + \tau)$
$\overline{u^2}$	mean-square turbulent velocity
$\mathcal{V}, \mathcal{V}^2$	volumes for source integration
v	magnitude of velocity
v_i	component of velocity in i^{th} direction
v'_i	$v_i(\vec{y}', t)$
v''_i	$v_i(\vec{y}'', t + \tau)$
v_n	normal velocity component
x_1, x_2, x_3	components of \vec{x}
\vec{x}	coordinate of observation point
y_1, y_2, y_3	components of \vec{y}
\vec{y}	coordinate of source point
\vec{y}'	$\vec{y} + \frac{1}{2}(\hat{i}\eta_1 - \vec{\eta})$
\vec{y}''	$\vec{y} + \frac{1}{2}(\hat{i}\eta_1 + \vec{\eta})$
α	complex wave number variable
β	imaginary part of α
β_v	defined by equation immediately preceding eq. (95)
γ	defined by eq. (86)
δ_{ij}	Kronecker delta

$\delta(\vec{x} - \vec{y})$	Dirac delta function with argument $(\vec{x} - \vec{y})$
η	magnitude of $\vec{\eta}$
η_i	component of $\vec{\eta}$ in i^{th} direction
$\vec{\eta}$	$\vec{y}'' - \vec{y}'$
$\vec{\eta}^{(1)}$	$\vec{y}' - \vec{y}''$
θ	polar angle measured from y_3 -direction
λ	wavelength
μ	radial coordinate in cylindrical coordinates
$\vec{\xi}$	$\vec{\eta} - \vec{U}_c \tau$
ρ	density
ρ_0	ambient density
σ	real part of α
τ	time translation
τ_{ij}	stress tensor
$\varphi_0(\psi y_1, y_2)$	solution to boundary-value problem given by eqs. (78) and (79)
$\chi_1(\alpha)$	function appearing in expression for $K_{\pm}(\alpha)$
$\chi_2(\alpha)$	function appearing in expression for $L_{\pm}(\alpha)$
$\Psi(\vec{x} \vec{y})$	component of Green's function (eq. (64))
$\Psi_0(\theta, \psi \vec{y})$	factor occurring in $\Psi(\vec{x} \vec{y})$ which is solution to eqs. (70) and (71)
ψ	azimuthal angle in $y_1 y_2$ -plane measured from y_1 -axis
ω	angular frequency
$\omega_f^{(i)}, \omega_*^{(i)}$	characteristic angular frequencies appearing in time-dependent part of velocity correlation function (eq. (101))

Subscripts:

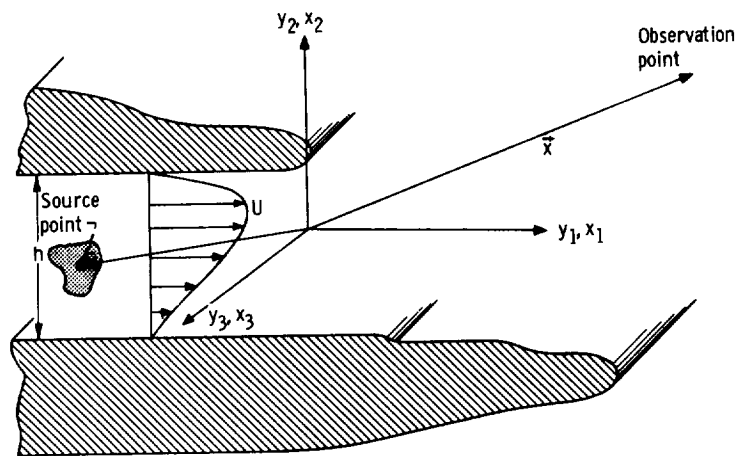
se	self-noise component
sh	shear-noise component

Superscripts:

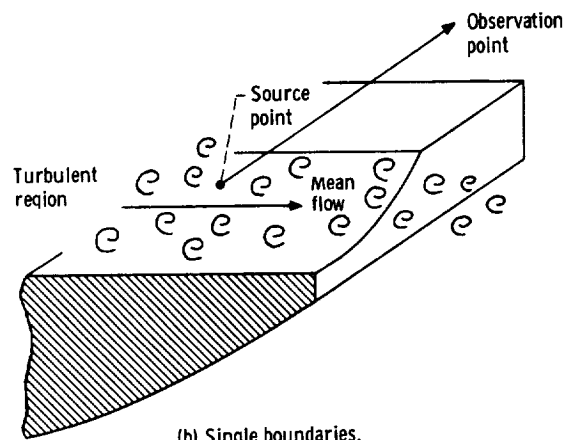
—	time average
*	complex conjugate
1, 2, 3	components of vector

REFERENCES

1. Dorsch, R. G.; Krejsa, E. A.; and Olsen, W. A.: Blown Flap Noise Research. Paper 71-745, AIAA, June 1971.
2. Lighthill, M. J.: On Sound Generated Aerodynamically. I. General Theory. Proc. Roy. Soc. (London), Ser. A, vol. 211, no. 1107, Mar. 20, 1952, pp. 564-587.
3. Ffowcs Williams, J. E.; and Hall, L. H.: Aerodynamic Sound Generation by Turbulent Flow in the Vicinity of a Scattering Half Plane. J. Fluid Mech., vol. 40, pt. 4, Mar. 9, 1970, pp. 657-670.
4. Goldstein, M.; and Rosenbaum, B.: Emission of Sound from Axisymmetric Turbulence Convected by a Mean Flow with Application to Jet Noise. NASA TN-6939, 1972.
5. Ffowcs Williams, J. E.: The Noise from Turbulence Convected at High Speed. Phil. Trans. Roy. Soc., Ser. A, vol. 255, no. 1061, Apr. 18, 1963, pp. 469-503.
6. Lighthill, M. J.: Jet Noise. AIAA J., vol. 1, no. 7, July 1963, pp. 1507-1517.
7. Ribner, H. S.: Quadrupole Correlations Governing the Pattern of Jet Noise. J. Fluid Mech., vol. 38, part 1, Aug. 14, 1969, pp. 1-24.
8. Ribner, H. S.: The Generation of Sound by Turbulent Jets. Advances in Applied Mechanics. Vol. 8. Academic Press, 1964, pp. 104-182.
9. Lilley, G. M.: On the Noise from Air Jets. Rep. ARC-20376, Aeronautical Res. Council, Gt. Britain, Sept. 8, 1958.
10. Batchelor, George K.: The Theory of Homogeneous Turbulence. Cambridge University Press, 1959.
11. Chu, Wing T.: Turbulence Measurements Relevant to Jet Noise. Rep. UTIAS-119, University of Toronto (AD-645322), Nov. 1966.
12. Davies, P. O. A. L.; Fisher, M. J.; and Barratt, M. J.: The Characteristics of the Turbulence in the Mixing Region of a Round Jet. J. Fluid Mech., vol. 15, pt. 3, Mar. 1963, pp. 337-367.
13. Morse, Philip M.; and Feshbach, Herman: Methods of Theoretical Physics. McGraw-Hill Book Co., Inc., 1953.
14. Noble, Benjamin: Methods Based on the Wiener-Hopf Technique for the Solution of Partial Differential Equations. Pergamon Press, 1958.
15. Morse, Philip M.; and Ingard, K. Uno.: Theoretical Acoustics. McGraw-Hill Book Co., Inc., 1968.



(a) Two boundaries.



(b) Single boundaries.

Figure 1. - Configuration of noise source and solid boundaries.

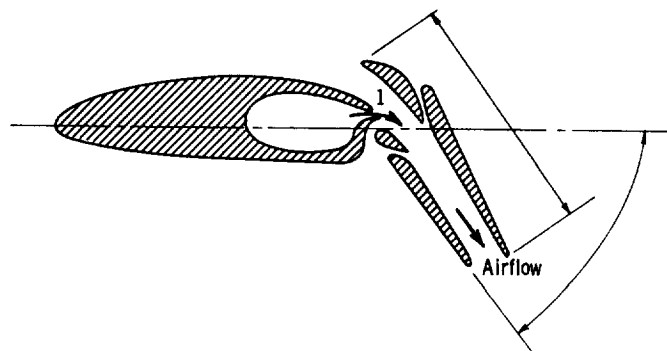


Figure 2. - Augmentor wing ejector flap.

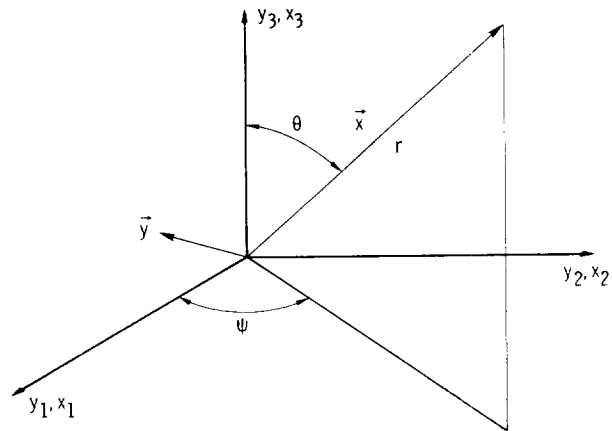


Figure 3. - Spherical polar coordinates.

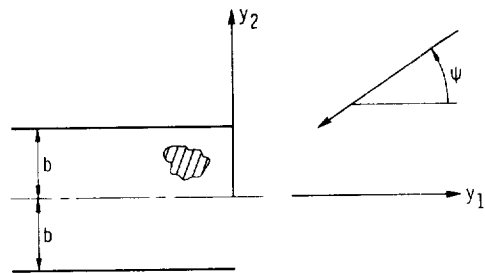


Figure 4. - Configuration of two-dimensional channel.

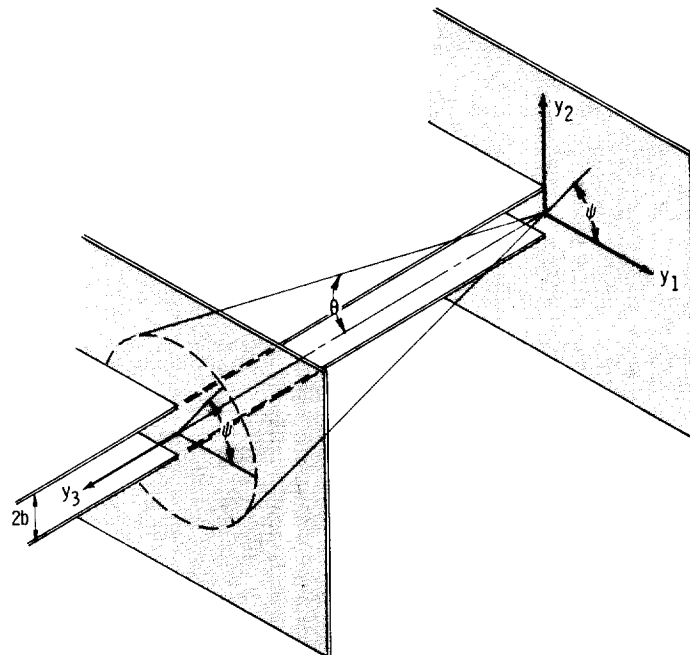


Figure 5. - Location of observation planes.

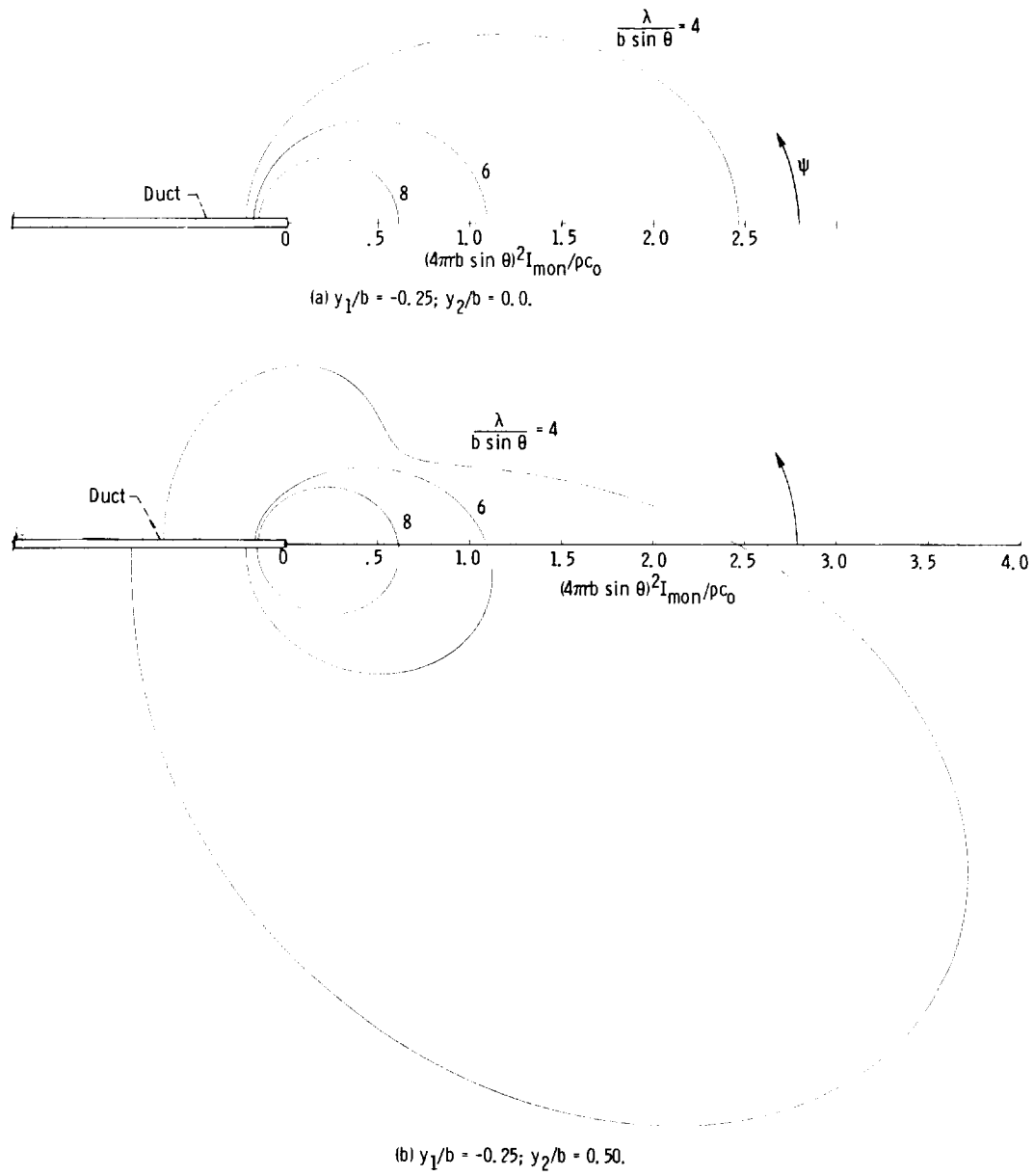
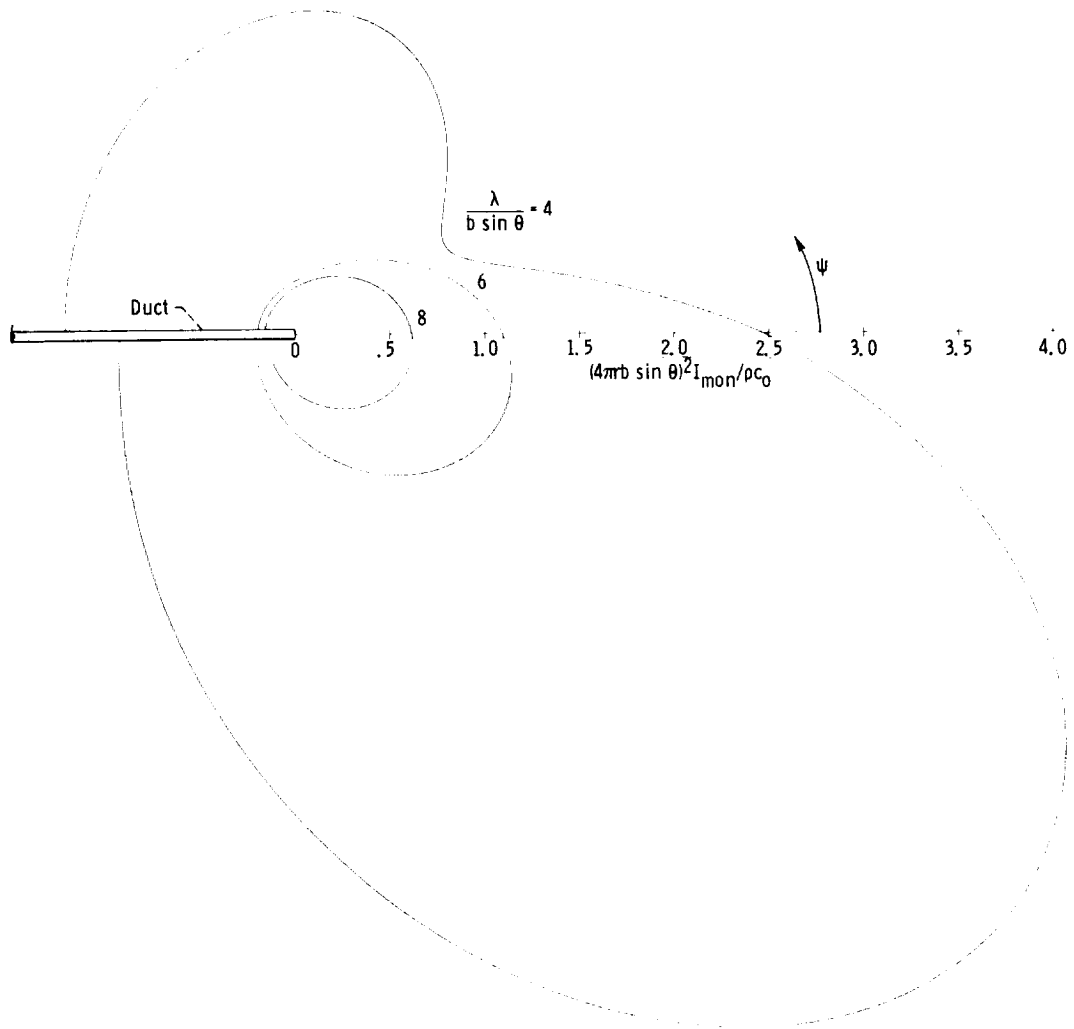
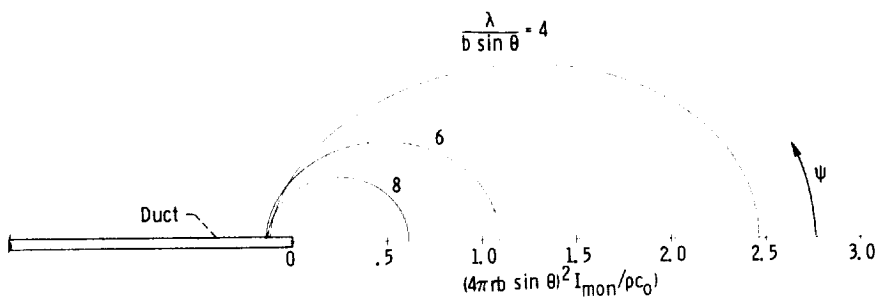


Figure 6. - Polar plot of $(4\pi r b \sin \theta)^2 I_{mon} / \rho c_0$ as function of ψ - low frequency range.

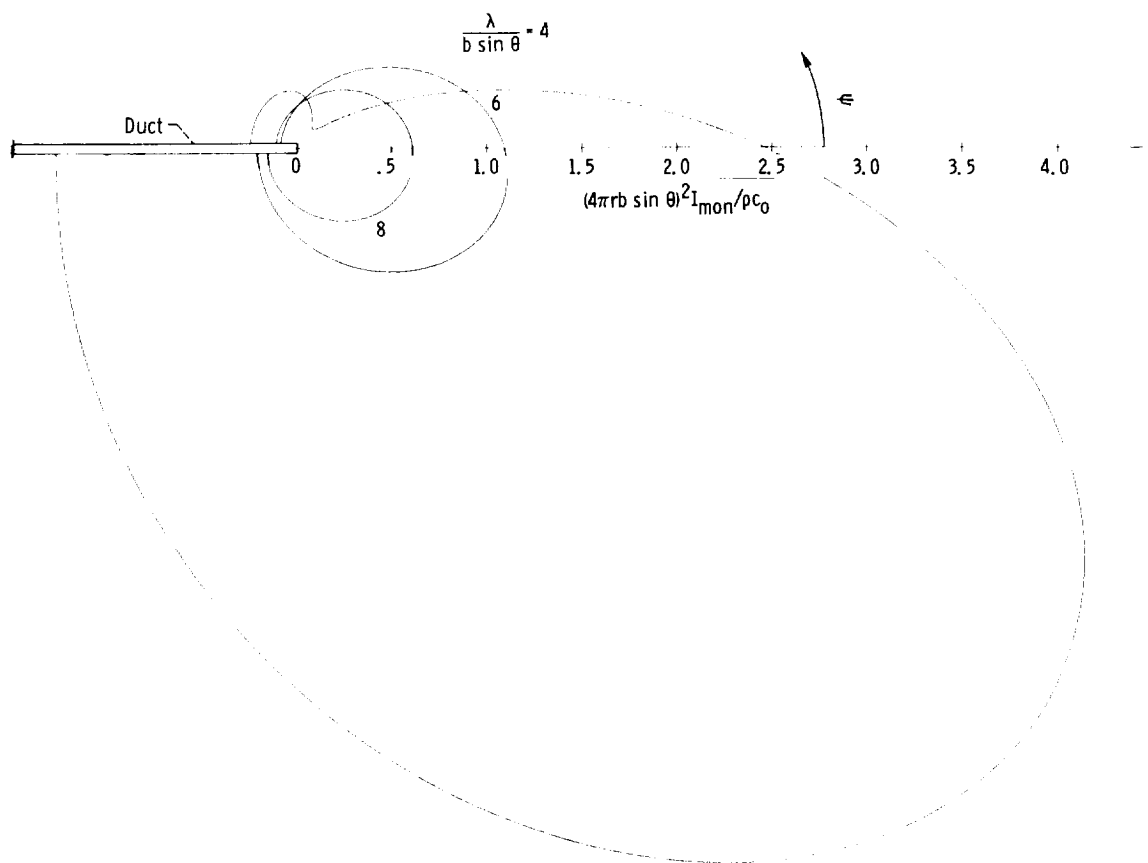


(c) $y_1/b = -0.25$; $y_2/b = 0.75$.

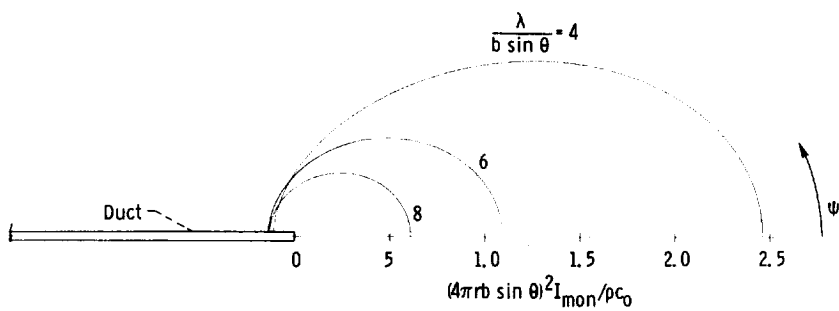


(d) $y_1/b = -1.0$; $y_2/b = 0.0$.

Figure 6. - Continued.

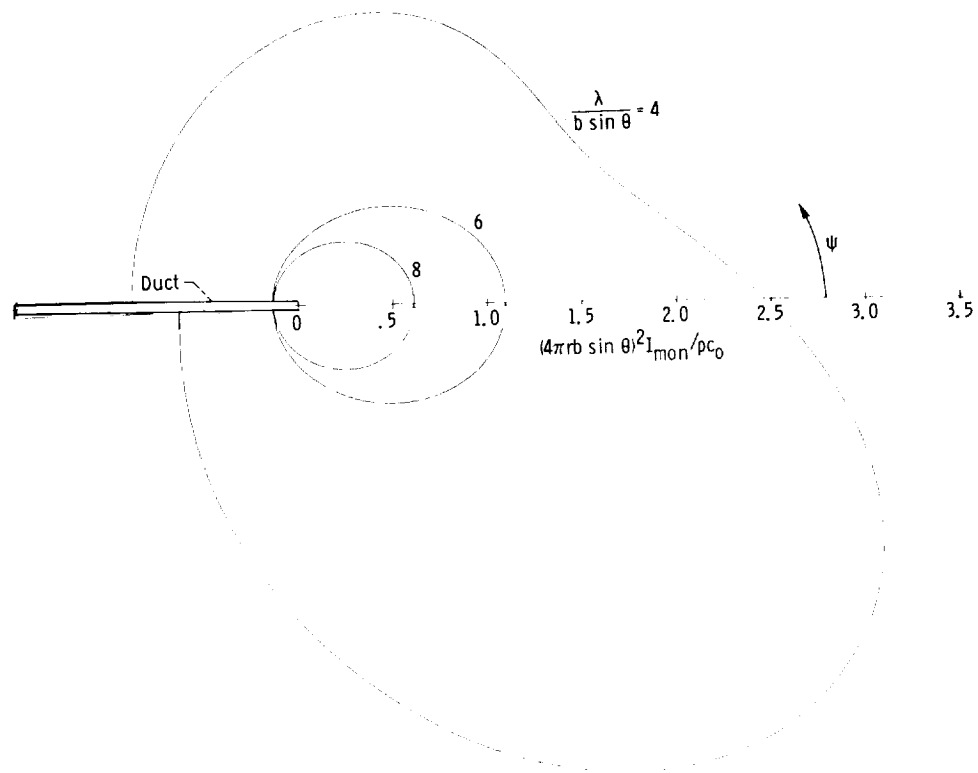


(e) $y_1/b = -1.0$; $y_2/b = 0.5$.



(f) $y_1/b = -16.0$; $y_2/b = 0.0$.

Figure 6. - Continued.



(g) $y_1/b = -16.0$; $y_2/b = 0.5$.

Figure 6. - Concluded.

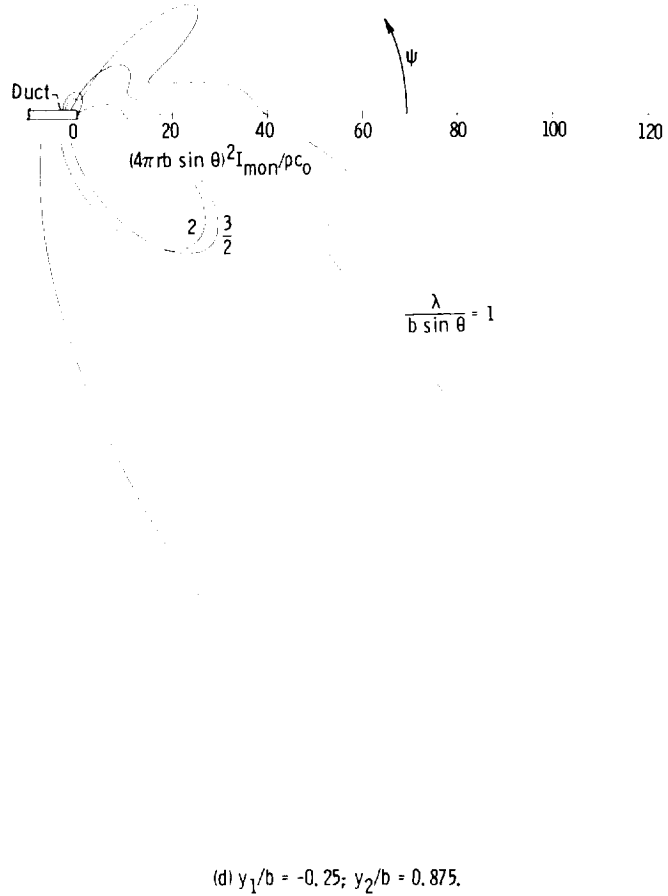
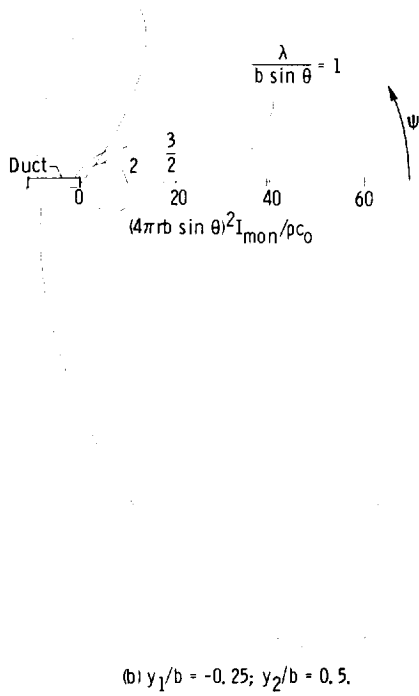
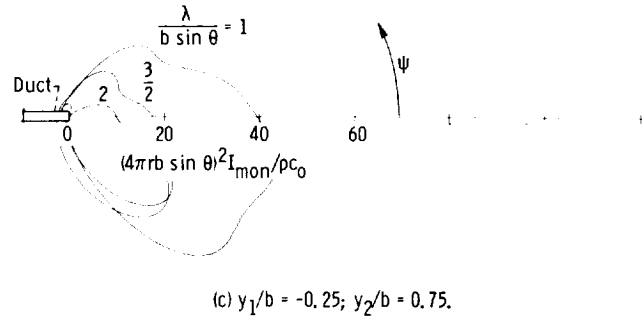
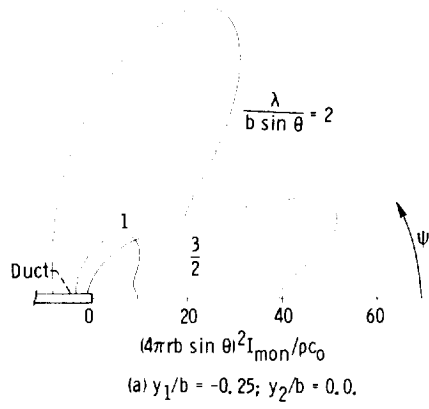


Figure 7. - Polar plot of $(4\pi r b \sin \theta)^2 I_{mon}/\rho c_0$ as a function of ψ - intermediate-frequency range.

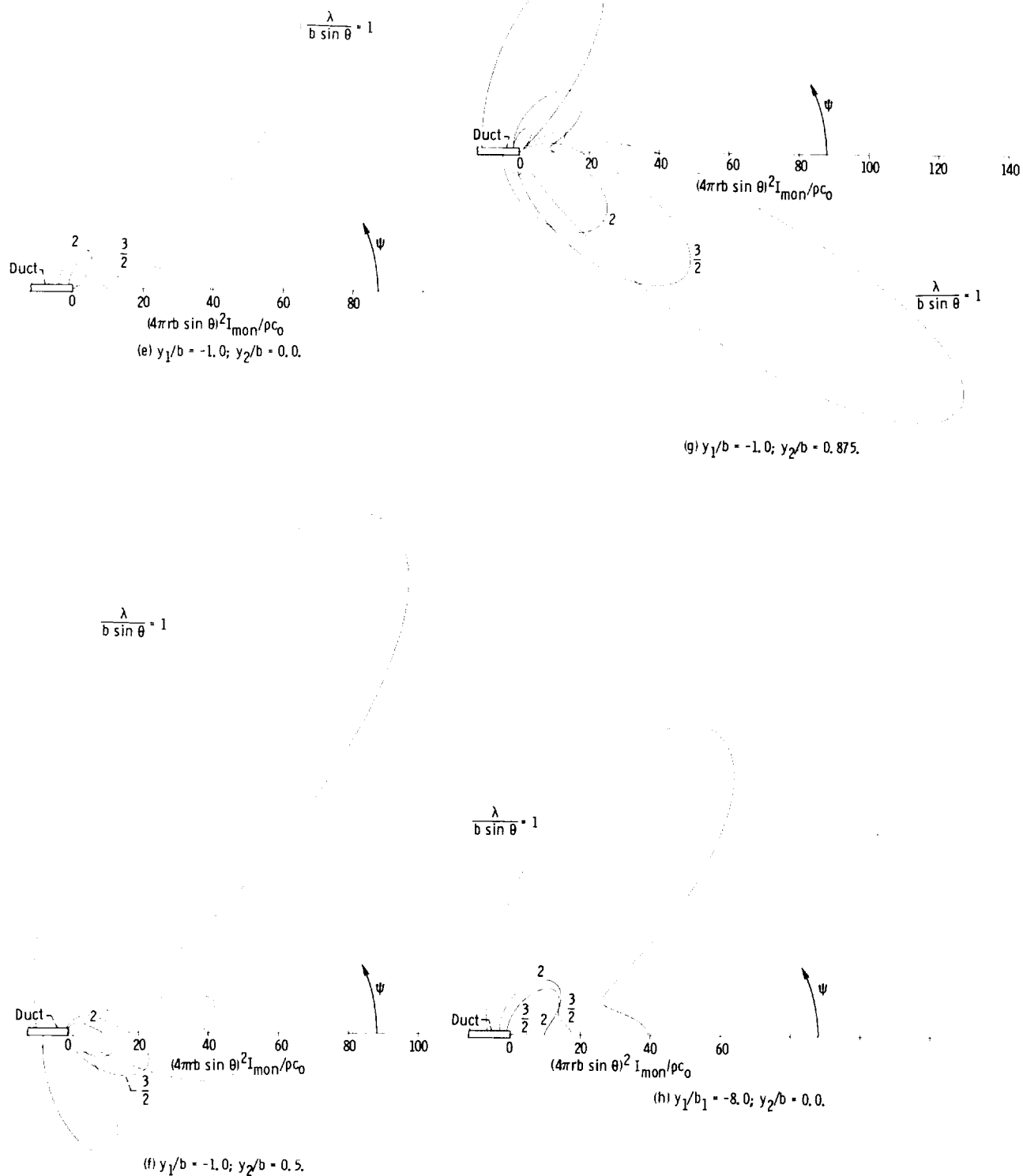


Figure 7. - Continued.

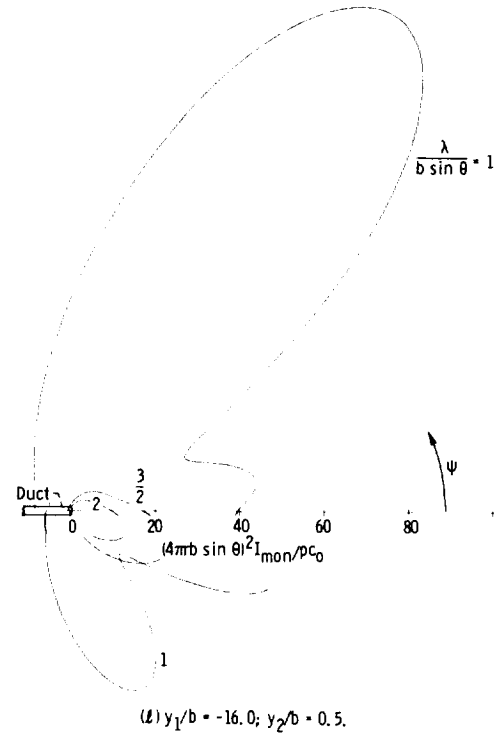
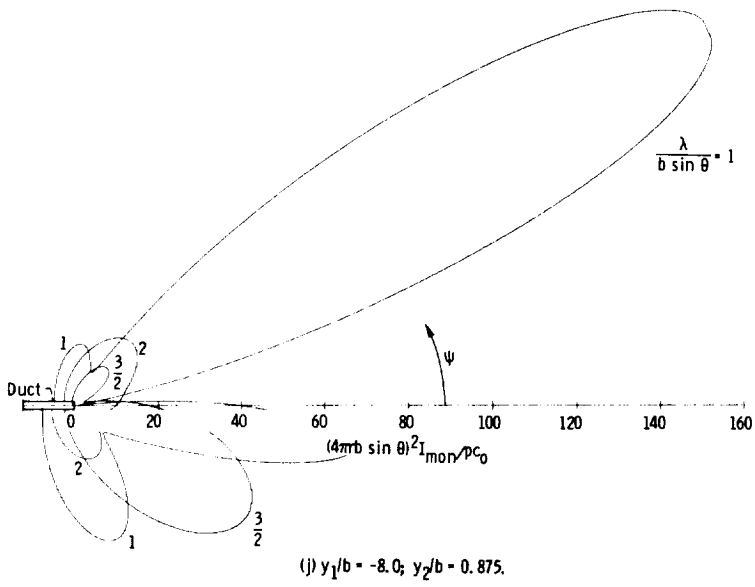
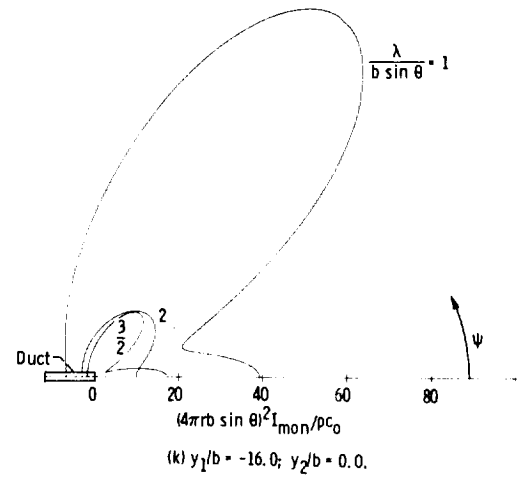
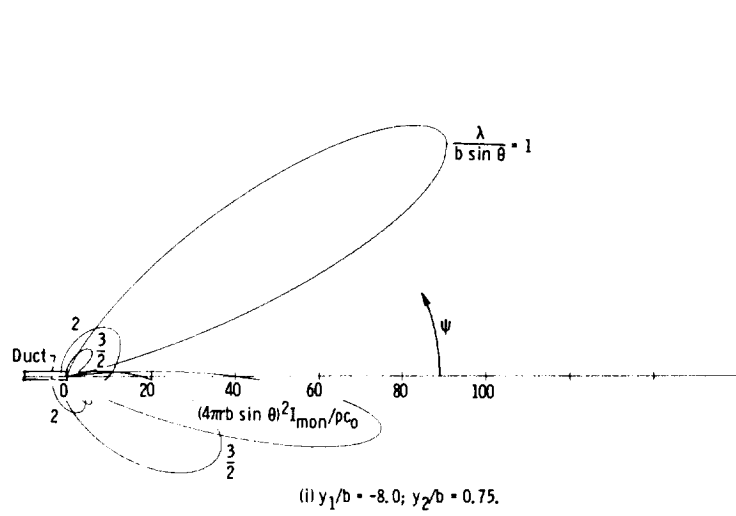


Figure 7. - Continued.

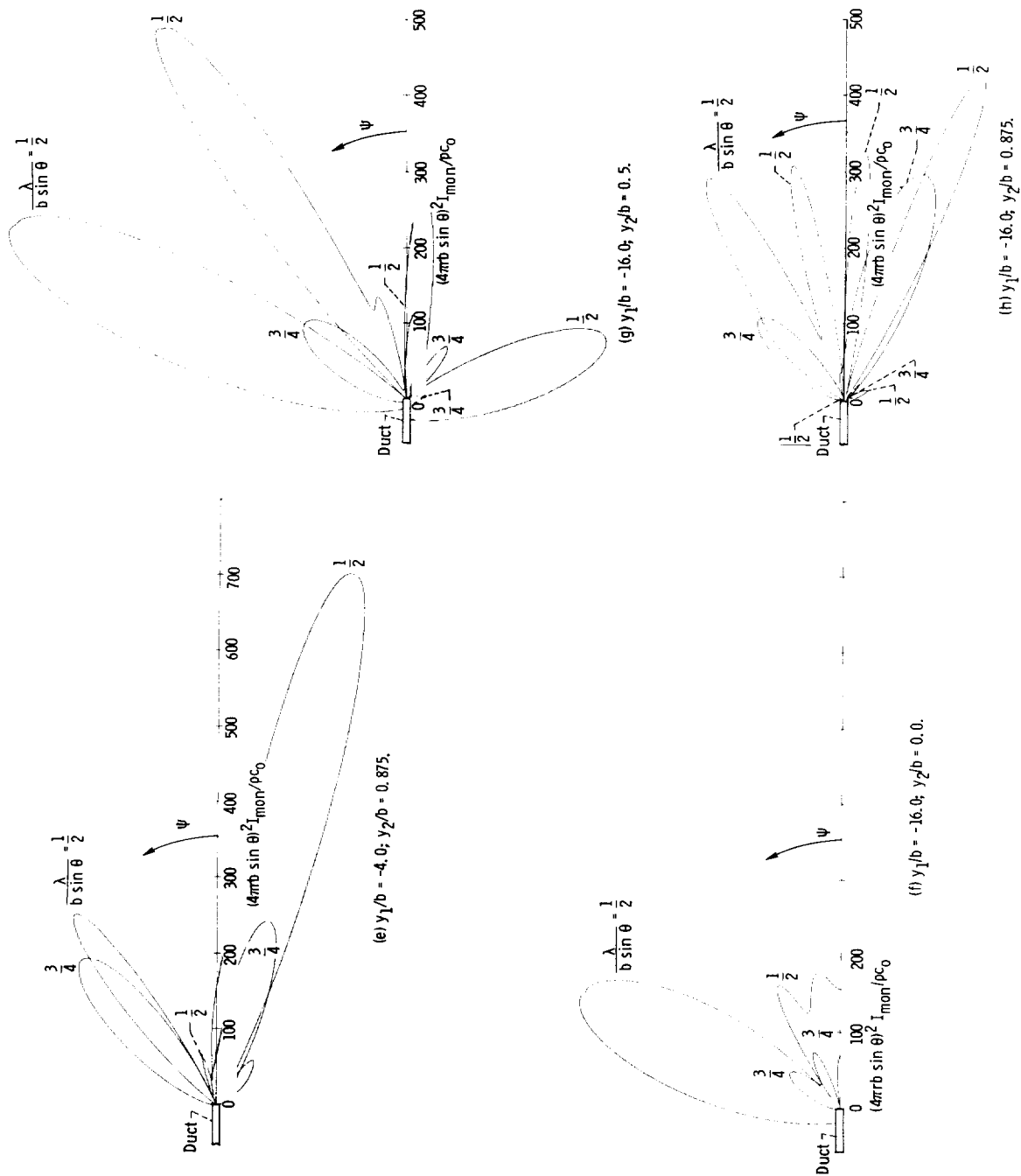


Figure 8. - Concluded.

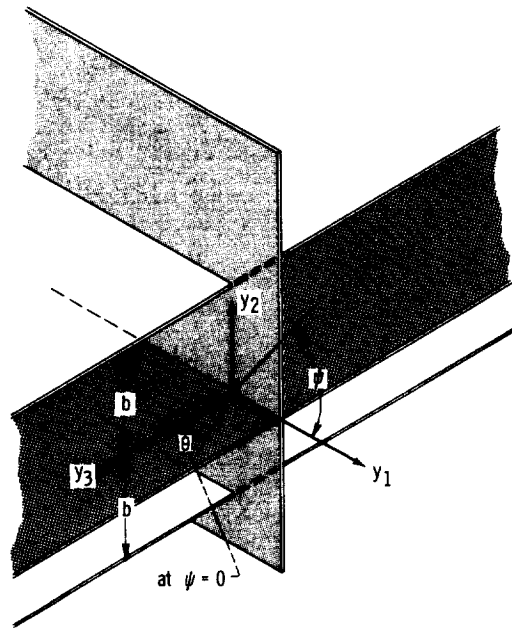


Figure 9. - Observation plane corresponding to $\psi = 0$.

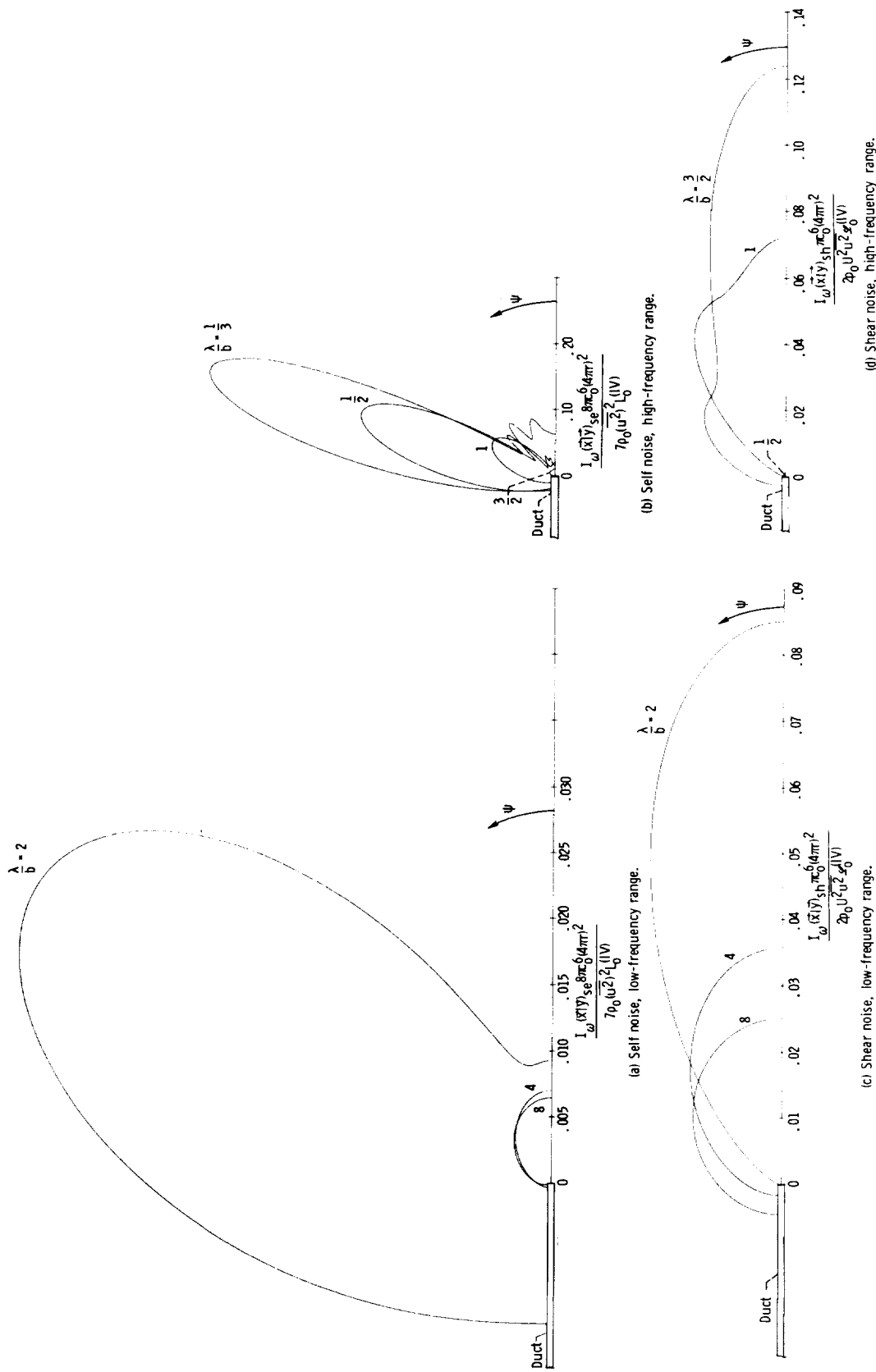


Figure 10. - Polar plot of directivity pattern for spectral density of far-field intensity as function of azimuthal angle ψ in $\theta = \pi/2$ plane for convection Mach number of eddy $M_c = 0.4$; jet-exit Mach number $M_e = 0.8$; $y_1/b = -1$; $y_2/b = 0$; and radius ratio $b_0/b = 1/4$.

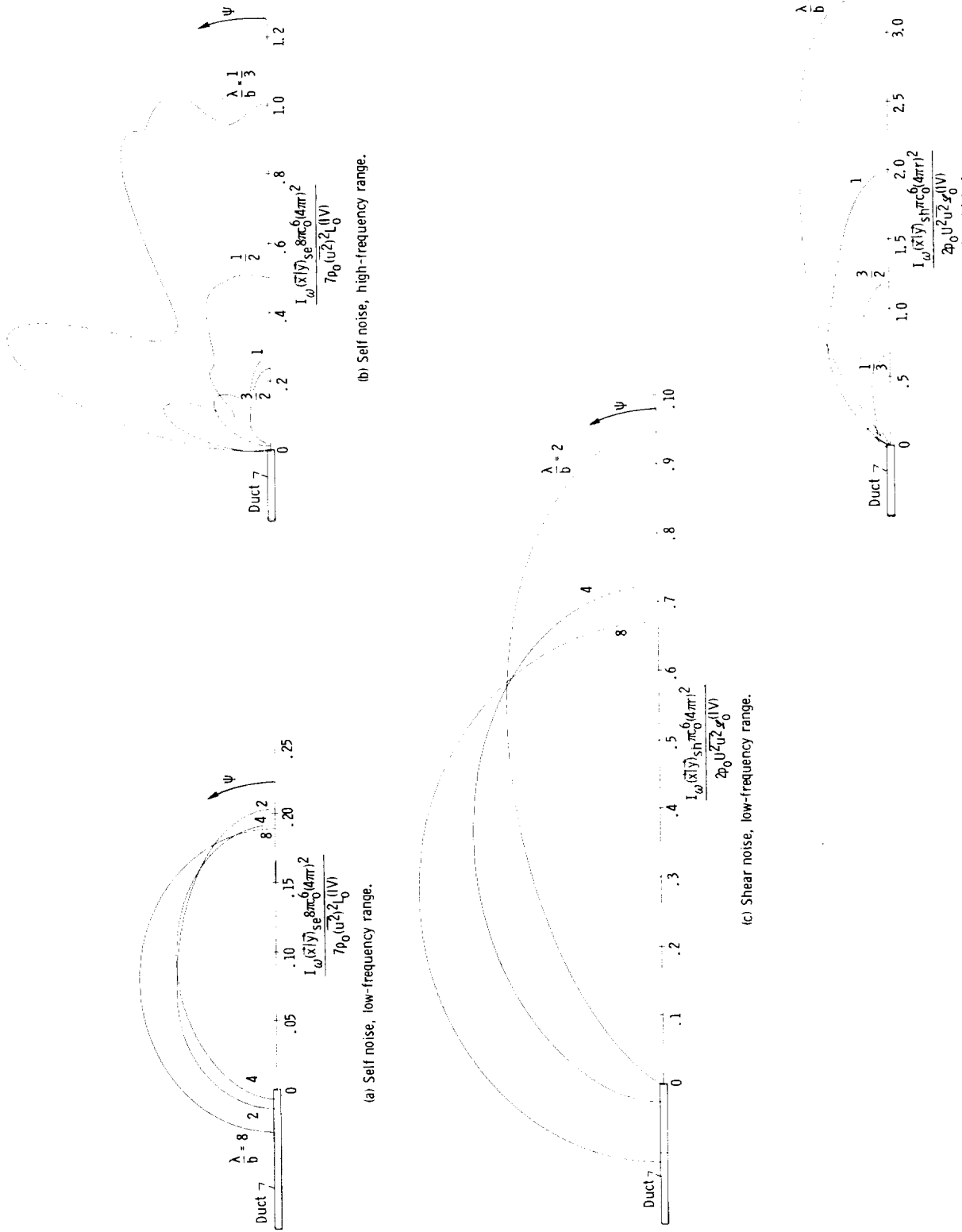


Figure 11. - Polar plot of directivity pattern for spectral density of far-field intensity as function of azimuthal angle ψ in $\theta = \pi/2$ plane for convection Mach number of eddy $M_c = 0.4$; jet-exit Mach number $M_e = 0.8$; $y_1/b = -1$; $y_2/b = 0$; and radius ratio $b_0/b = 1/4$.

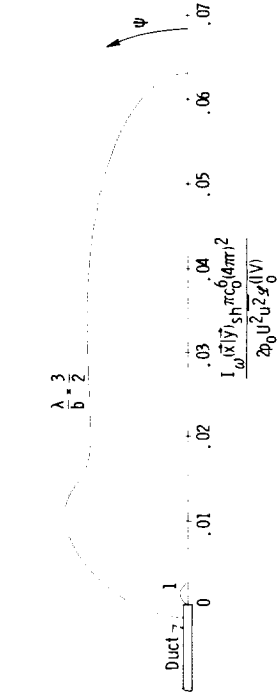
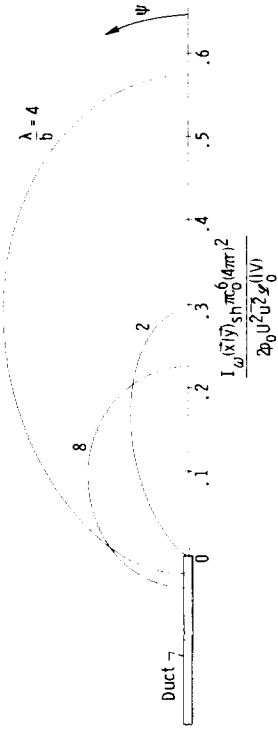
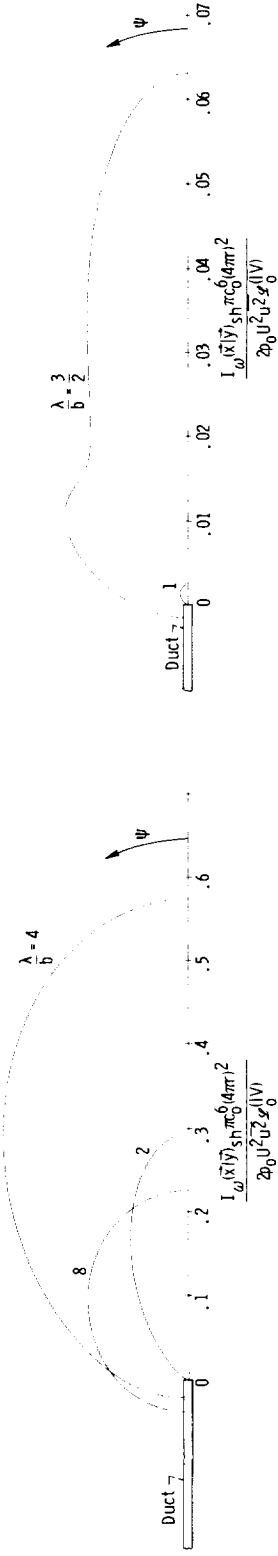
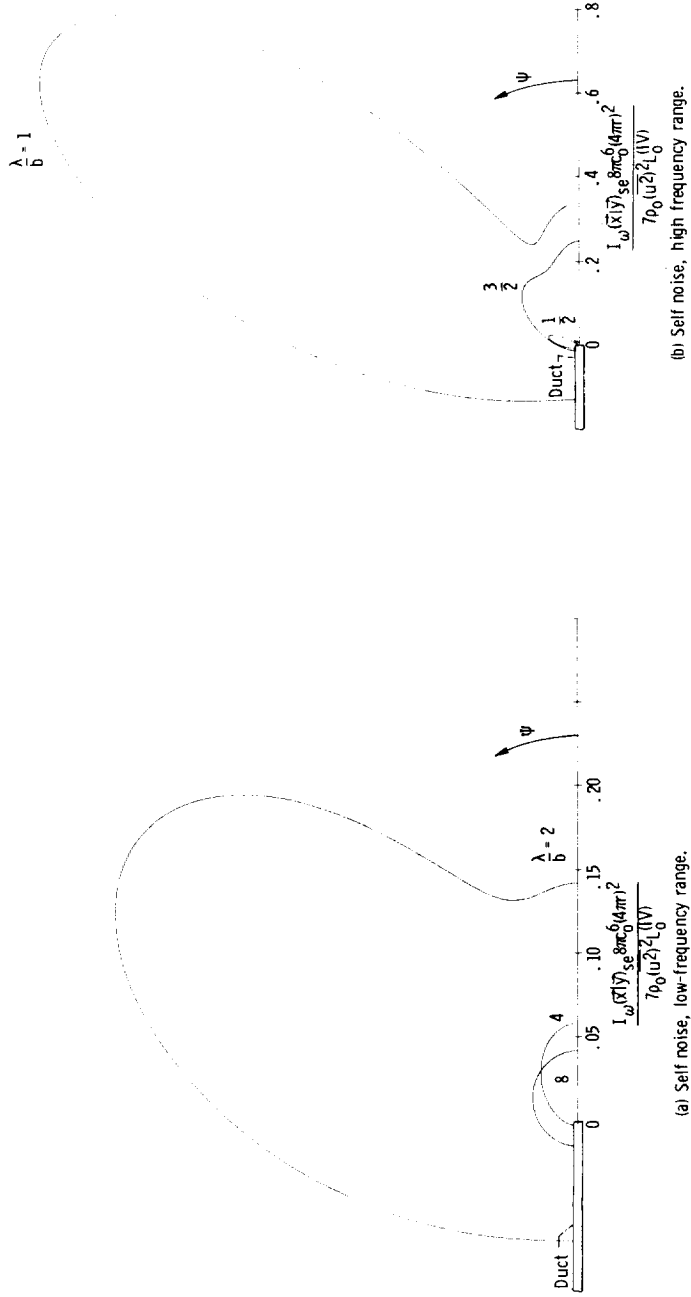


Figure 12. - Polar plot of directivity pattern for spectral density of far-field intensity as a function of azimuthal angle ψ in $\theta = \pi/2$ plane for convection Mach number of eddy $M_c = -0.15$; jet-exit Mach number $M_e = 0.3$; $y_1/b = -1$; $y_2/b = 0$; and radius ratio $b_0/b = 1/4$.

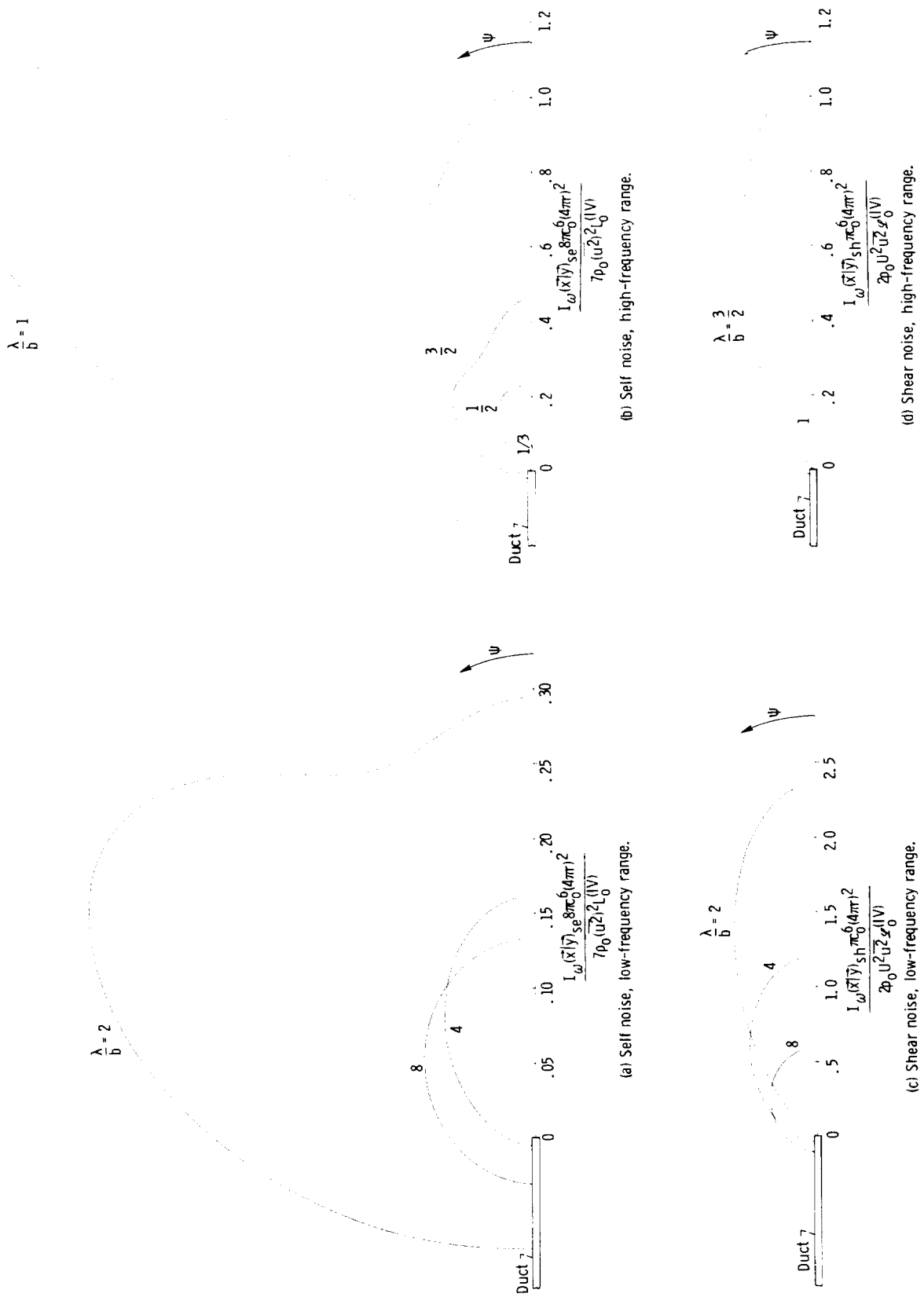


Figure 13. - Polar plot of directivity pattern for spectral density of far-field intensity as a function of azimuthal angle ψ in $\theta = \pi/2$ plane for convection Mach number of eddy $M_c = 0.15$; jet-exit Mach number $M_* = 0.3$; $y_1/b = -1$; $y_2/b = 0$; and radius ratio $b_0/b = 1/4$.

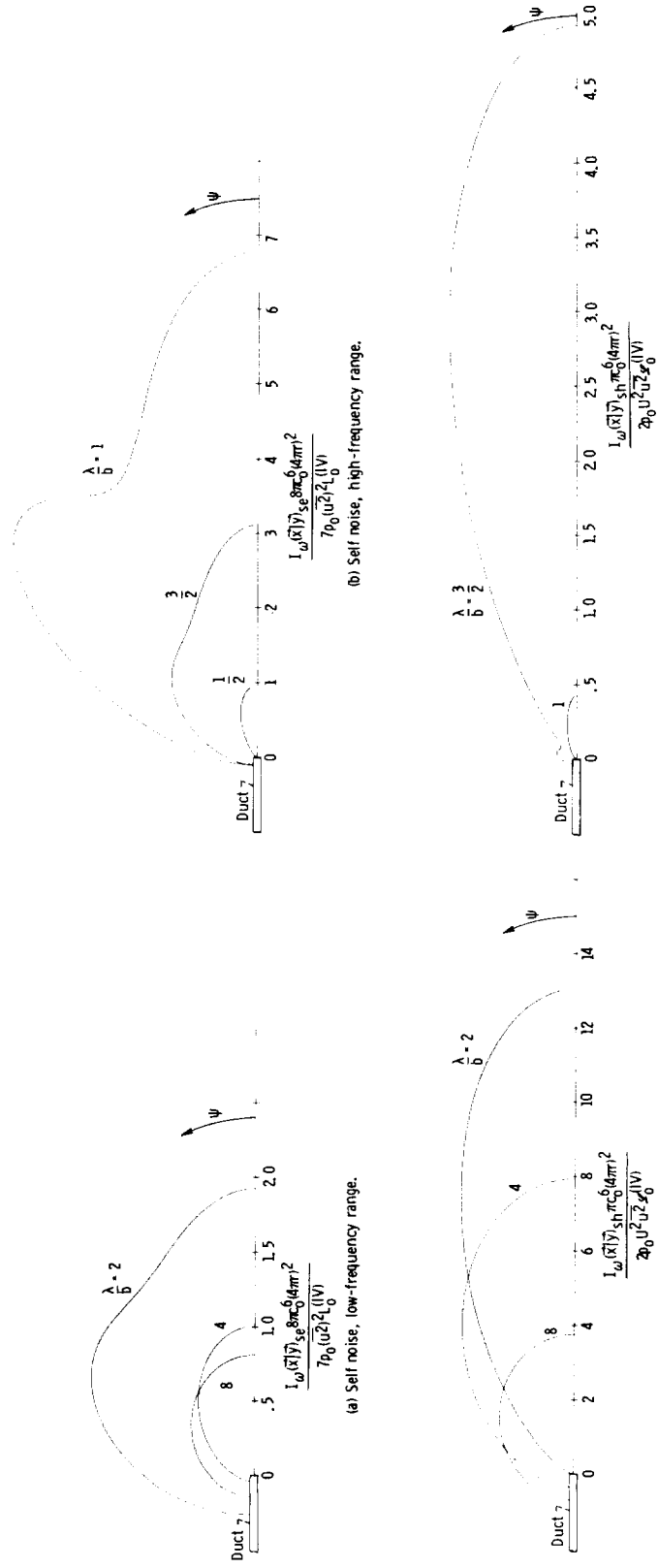
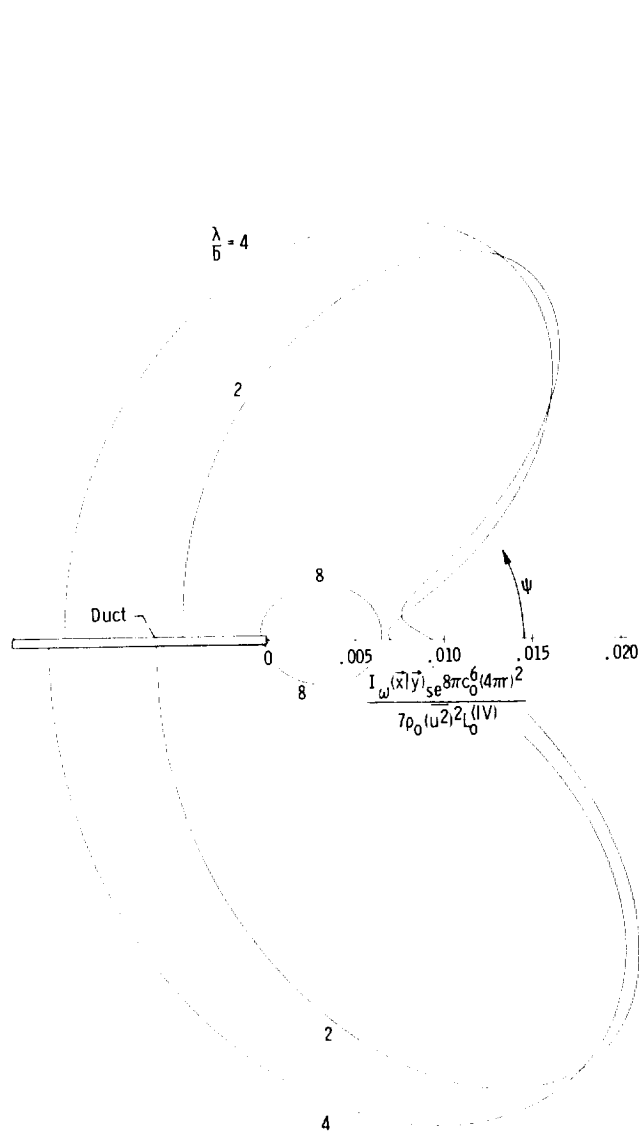
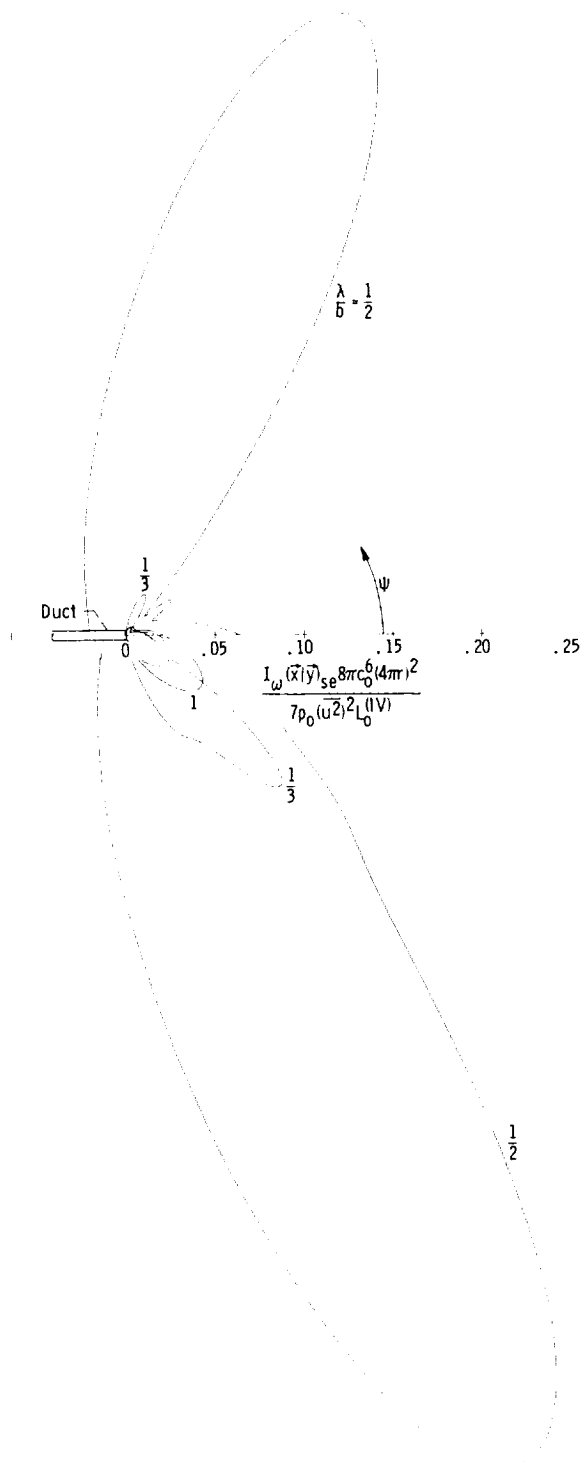


Figure 14. - Polar plot of directivity pattern for spectral density of far-field intensity as a function of azimuthal angle ψ in $\theta = \pi/2$ plane for convection Mach number in eddy $M_c = 0.4$, jet-exit Mach number $M_e = 0.8$, $y/b = -1$, $y/b = 0$, and radius ratio $b_0/b = 1$.

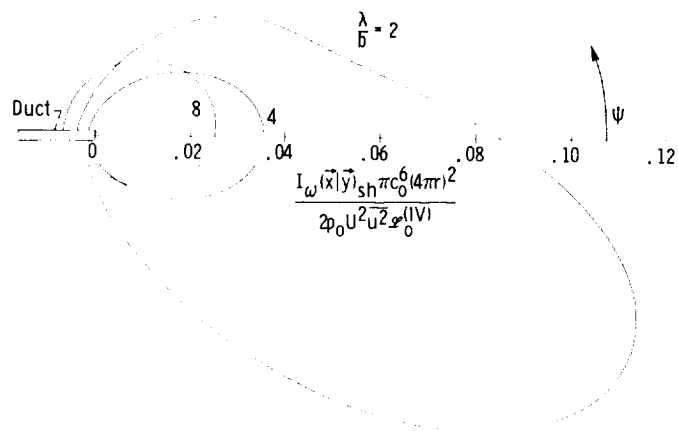


(a) Self noise, low-frequency range.

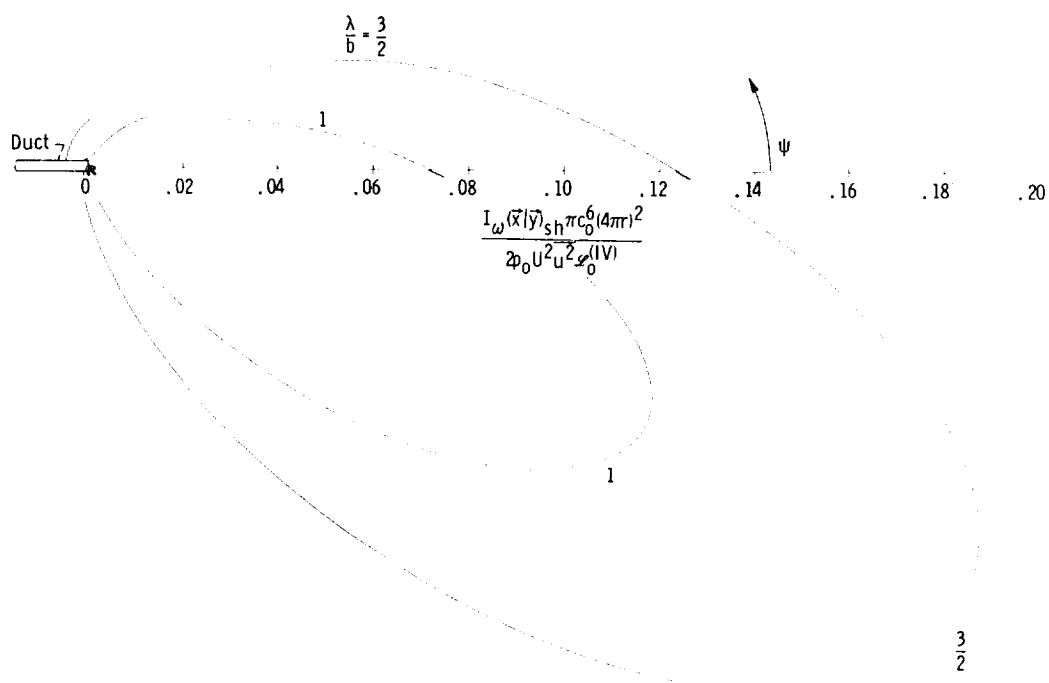


(b) Self noise, high-frequency range.

Figure 15. - Polar plot of directivity pattern for spectral density of far-field intensity as function of azimuthal angle ψ in $\theta = \pi/2$ plane for convection Mach number of eddy $M_c = -0.4$; jet-exit Mach number $M_e = 0.8$; $y_1/b = -1$; $y_2/b = 3/4$; and $b_0/b = 1/4$.



(c) Shear noise, low-frequency range.



(d) Shear noise, high-frequency range.

Figure 15. - Concluded.

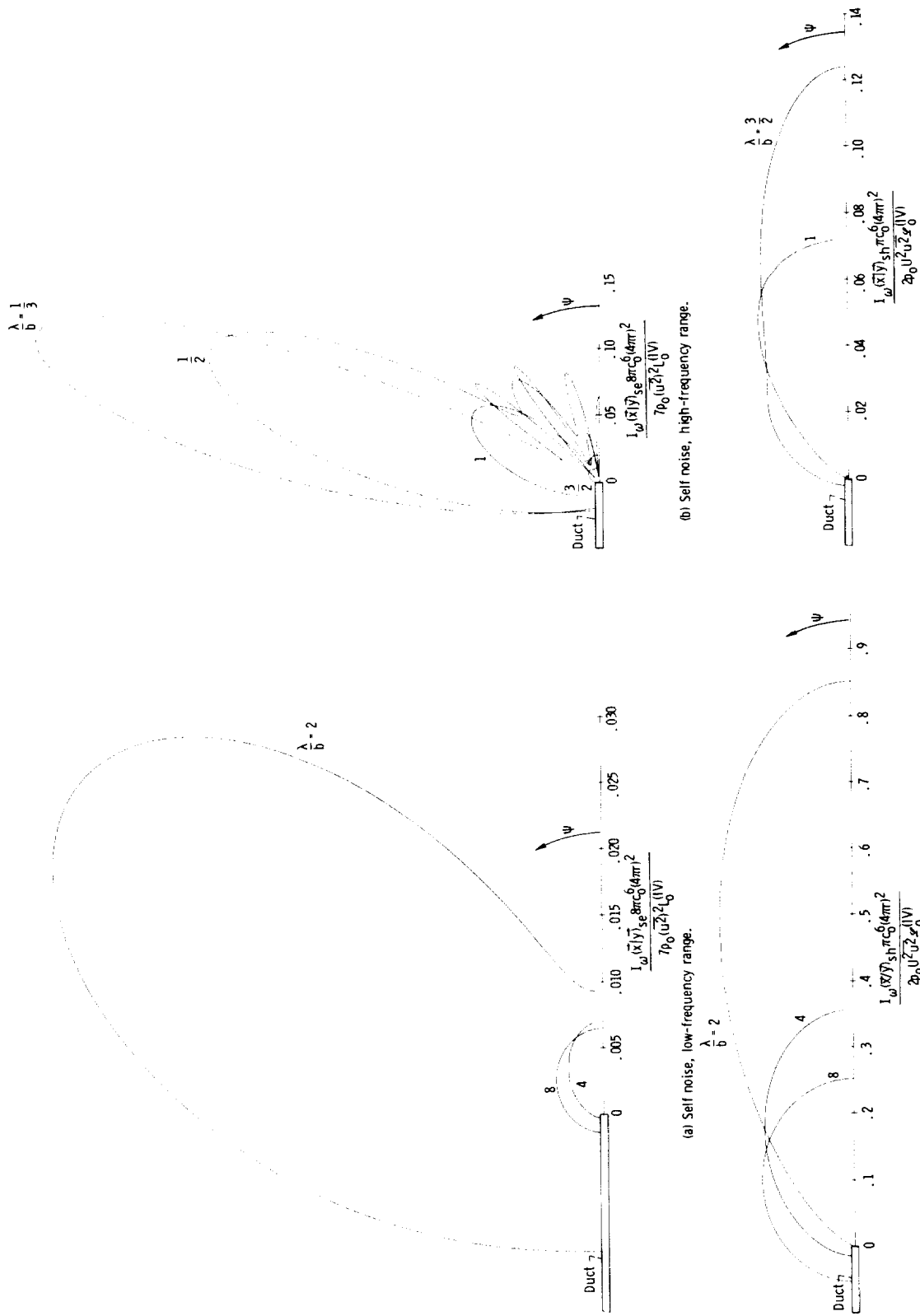


Figure 16. - Polar plot of directivity pattern for spectral density of far-field intensity as a function of azimuthal angle ψ in $\theta = \pi/2$ plane for convection Mach number in eddy $M_c = -0.4$; jet-exit Mach number $M_{je} = 0.8$; $y_1/b = -8$; $y_2/b = 0$; and radius ratio $b_0/b = 1/4$.

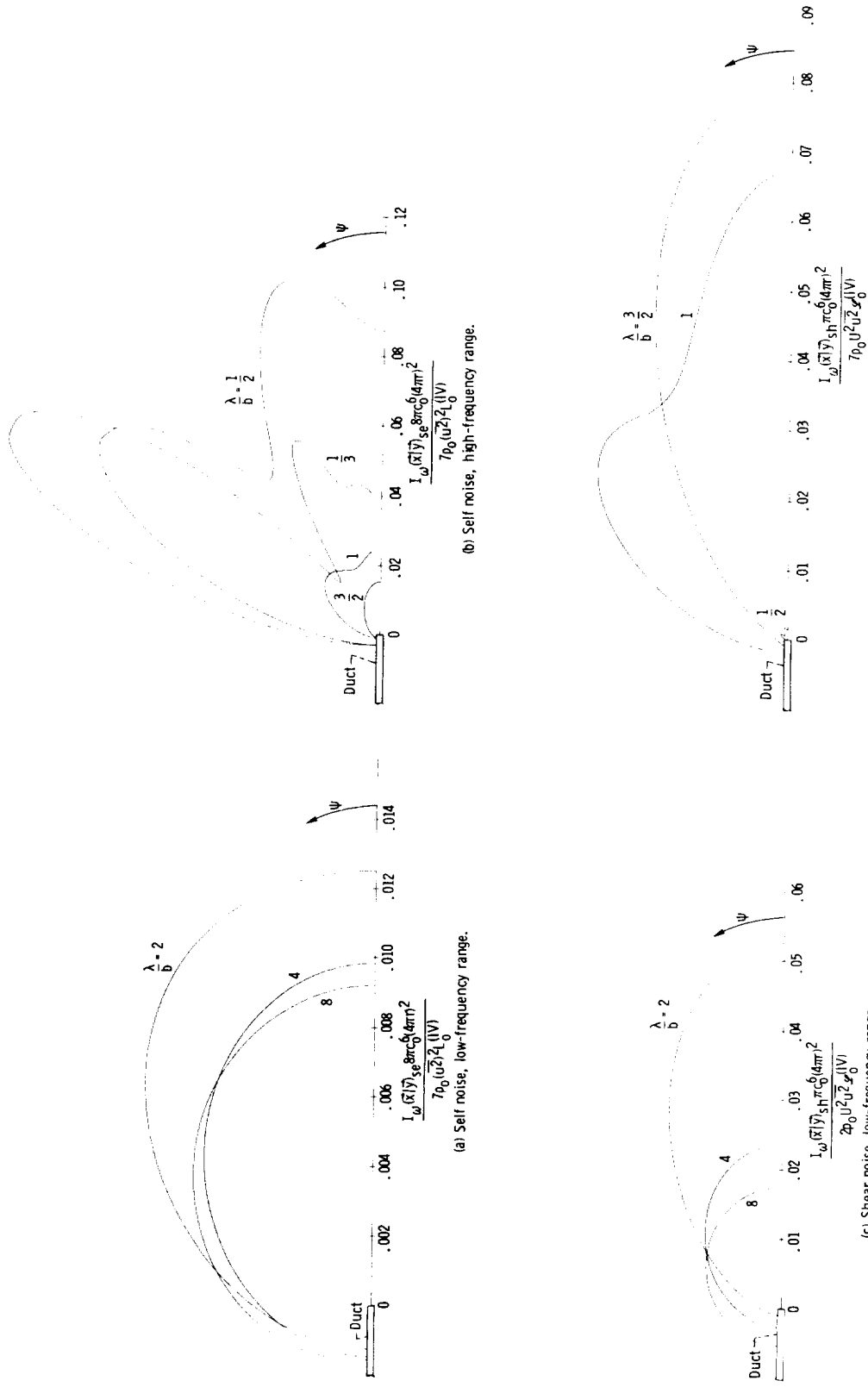


Figure 17. - Polar plot of directivity pattern for spectral density of far-field intensity as function of azimuthal angle ψ in $\theta = \pi/4$ plane for convection Mach number of eddy $M_c = -0.4$, jet-exit Mach number $M_e = 0.8$; $y_1/b = -1$; $y_2/b = 0$; and radius ratio $b_0/b = 1/4$.

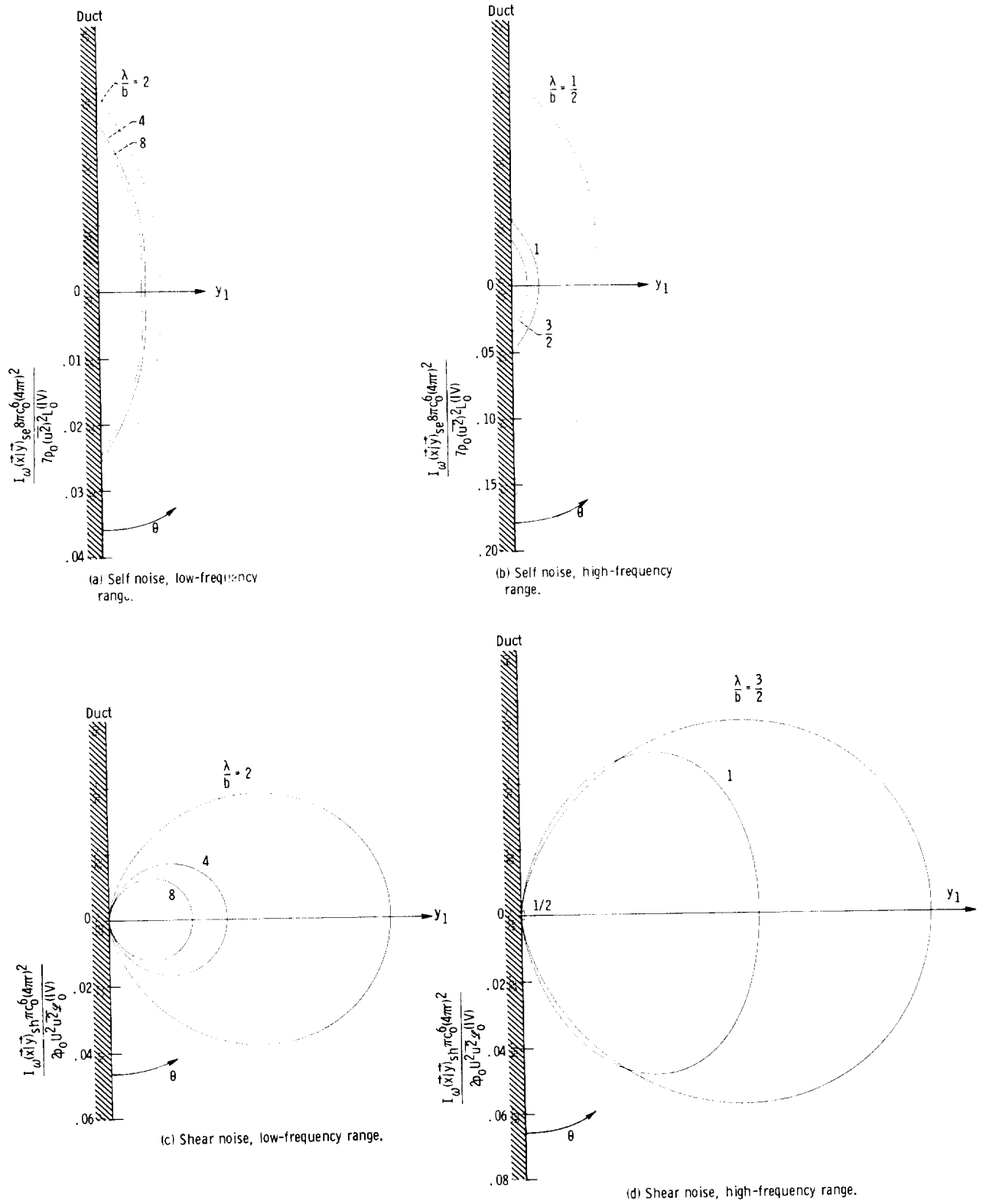


Figure 18. - Polar plot of directivity pattern for spectral density of far-field intensity as function of polar angle θ in $\psi = 0$ plane for convection Mach number of eddy $M_C = -0.4$; jet-exit Mach number $M_e = 0.8$; and radius ratio $b_0/b = 1/4$.

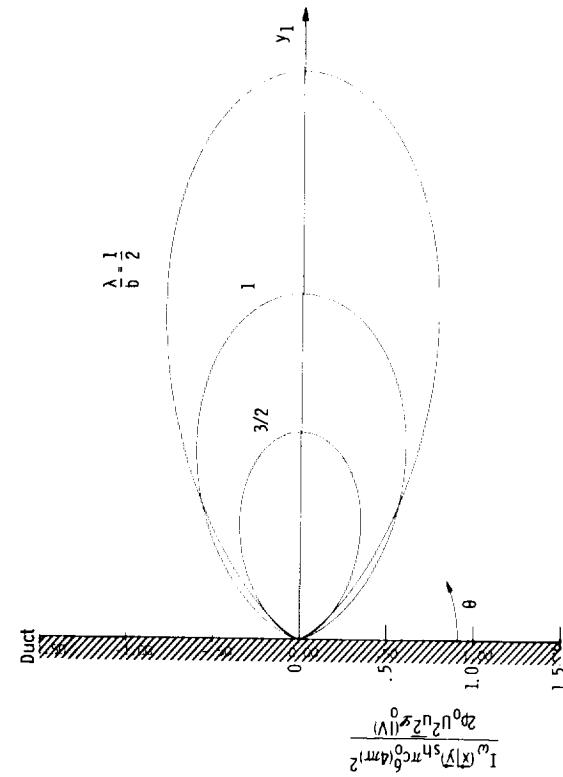
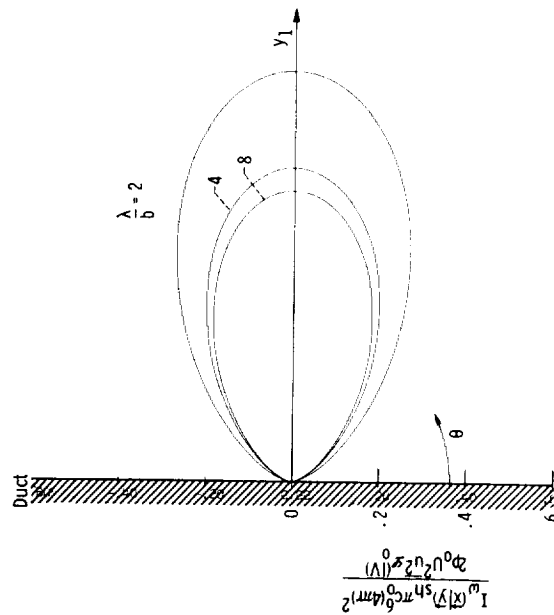
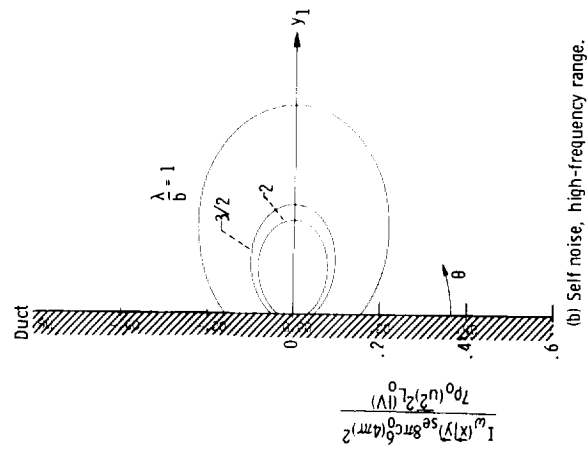
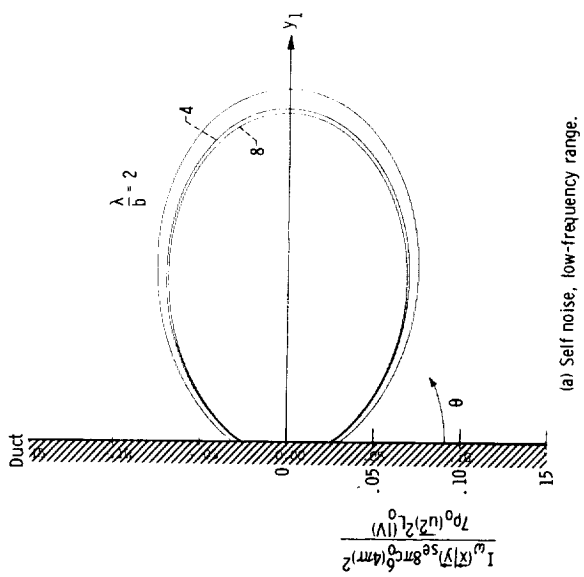


Figure 19. - Polar plot of directivity pattern for spectral density of far-field intensity as function of polar angle θ in $\psi = 0$ plane for convection Mach number of eddy $M_c = 0.4$; jet-exit Mach number $M_e = 0.8$; and radius ratio $b_0/b = 1/4$.

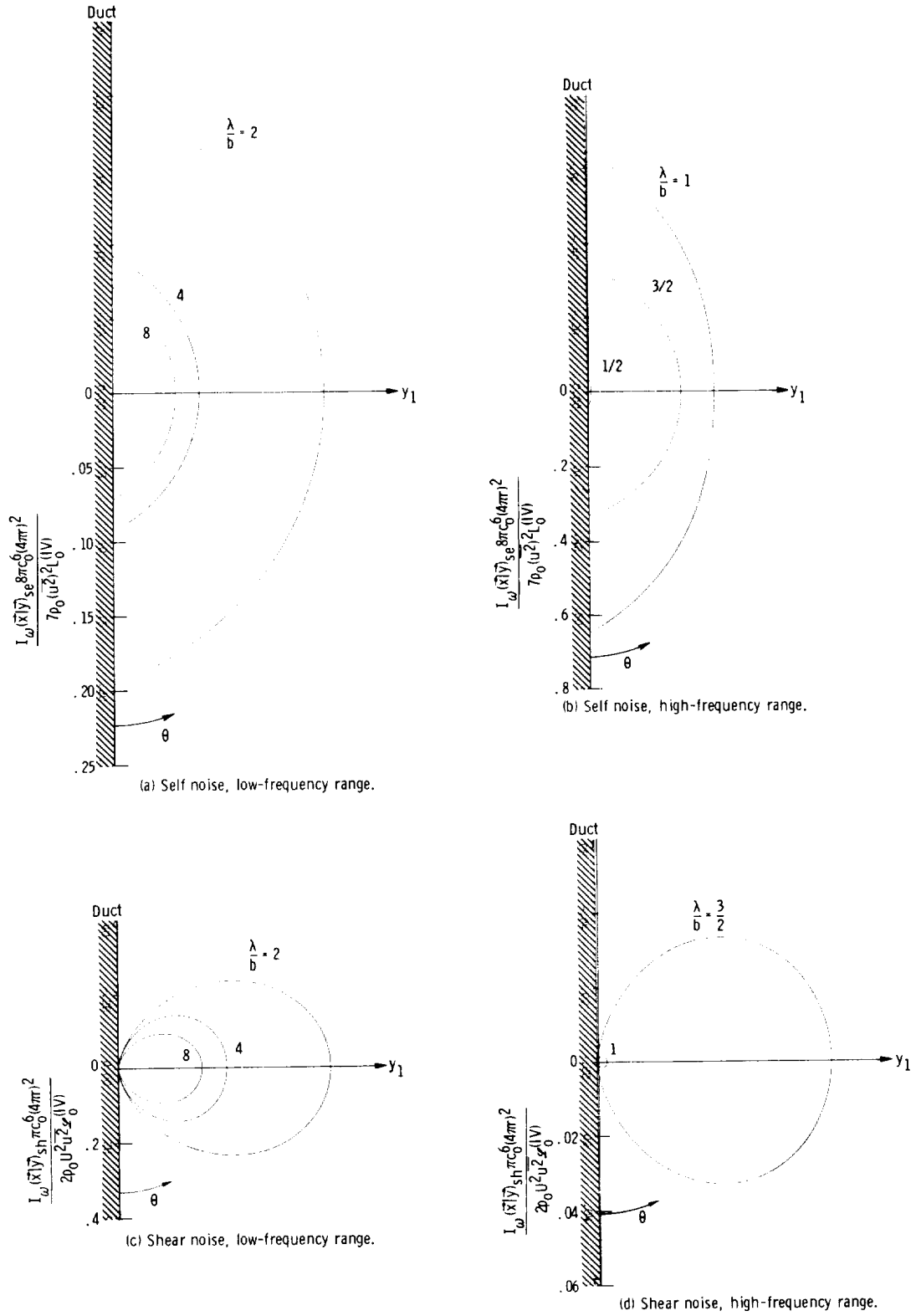
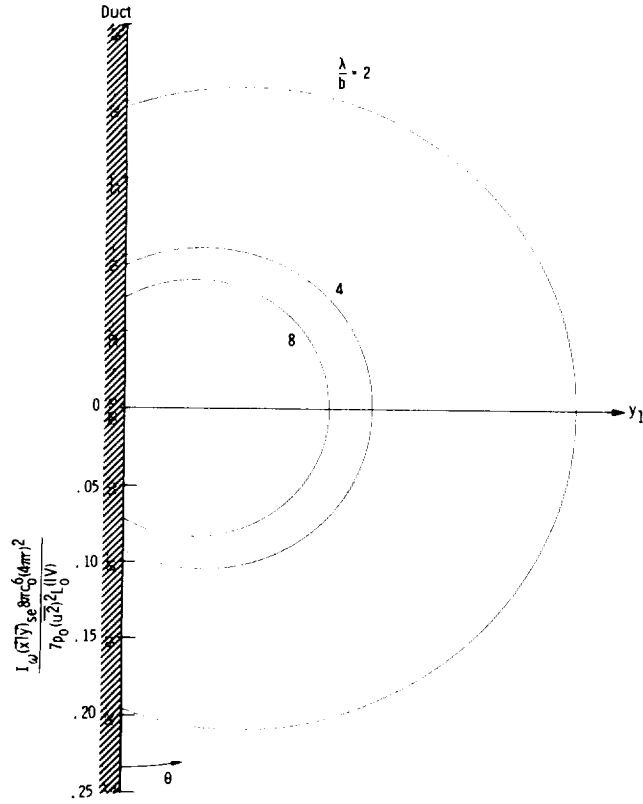
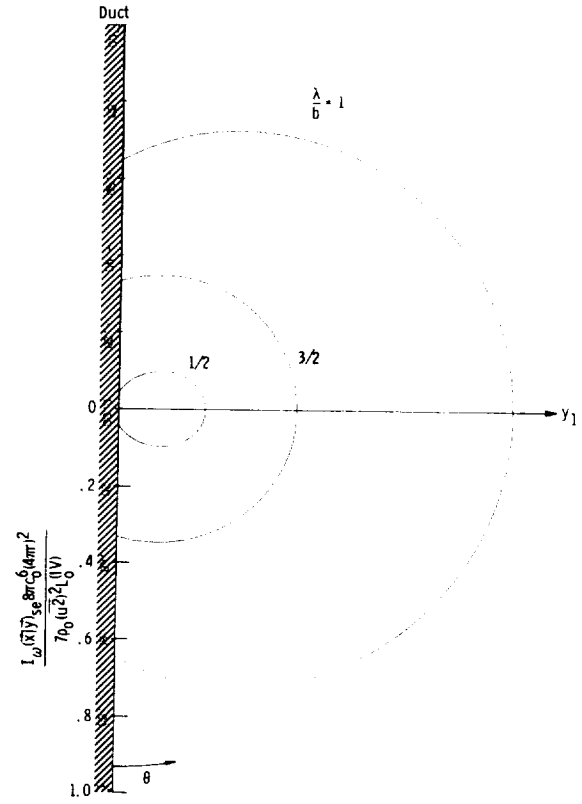


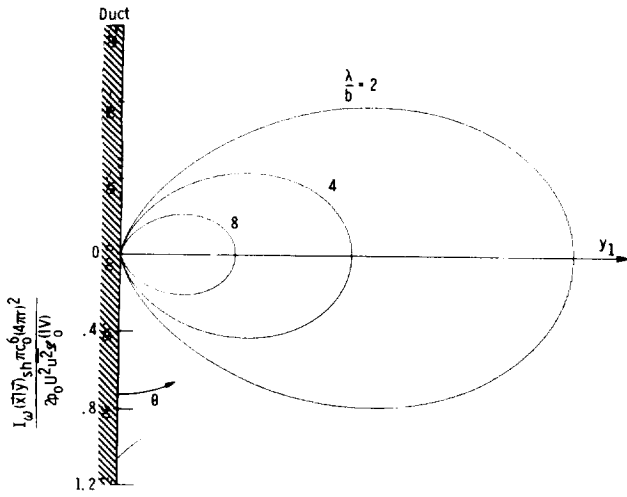
Figure 20. - Polar plot of directivity pattern for spectral density of far-field intensity as function of polar angle θ in $\psi = 0$ plane for convection Mach number of eddy $M_c = -0.15$; jet-exit Mach number $M_e = 0.3$; and radius ratio $b_0/b = 1/4$.



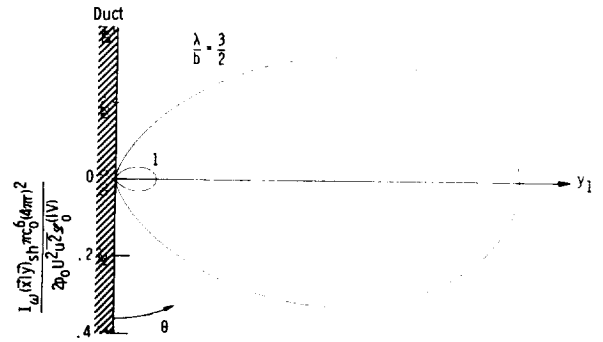
(a) Self noise, low-frequency range.



(b) Self noise, high-frequency range.



(c) Shear noise, low-frequency range.



(d) Shear noise, high-frequency range.

Figure 21. - Polar plot of directivity pattern for spectral density of far-field intensity as function of polar angle θ in $\psi = 0$ plane for convection Mach number of eddy $M_c = 0.15$; jet-exit Mach number $M_a = 0.3$; and radius ratio $b_0/b = 1/4$.

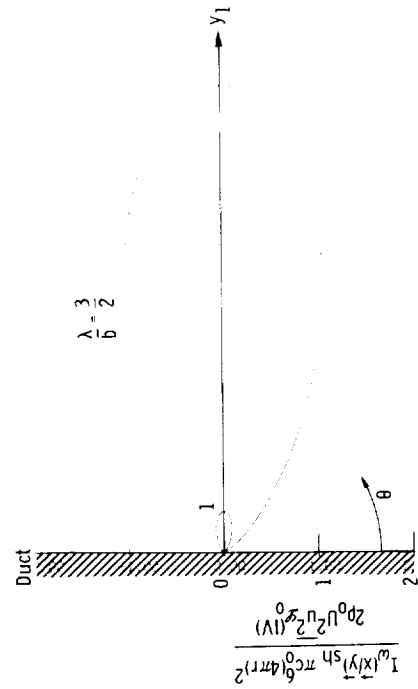
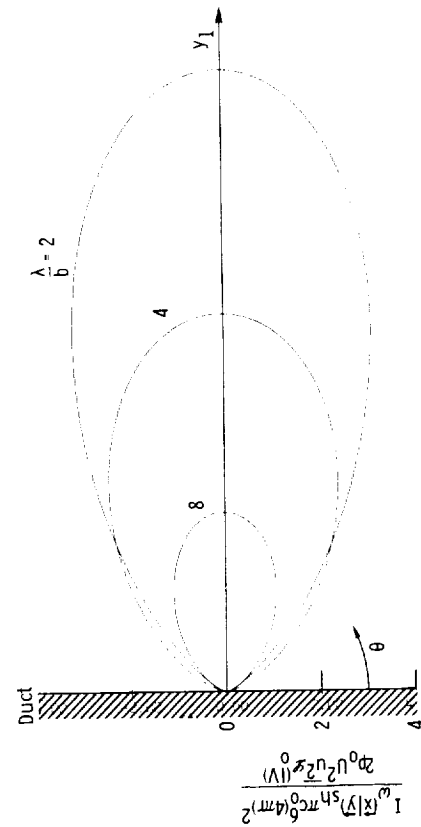
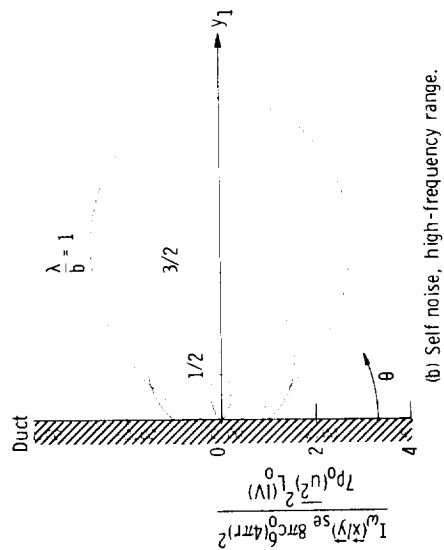
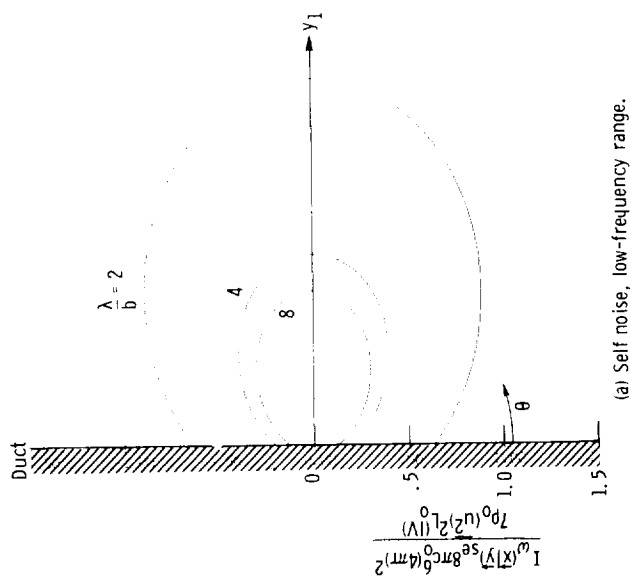


Figure 22. - Polar plot of directivity pattern for spectral density of far-field intensity as function of polar angle θ in $\psi = 0$ plane for convection Mach number in eddy $M_c = 0.4$; jet-exit Mach number $M_e = 0.8$, and radius ratio $b_0/b = 1$.